

https://dspace.org/

Impact of CBD and Tamoxifen treatment on cell death and cell survival in breast cancer in vitro

Mahasha, Mahlatse Fortunate

2024
University of the Witwatersrand, Johannesburg
https://hdl.handle.net/10539/46959

Mahasha, Mahlatse Fortunate . (2024). Impact of CBD and Tamoxifen treatment on cell death and cell survival in breast cancer in vitro [Master`s dissertation, University of the Witwatersrand, Johannesburg]. WIReDSpace.

Downloaded from a DSpace repository. https://dspace.org/

Impact of CBD and Tamoxifen treatment on cell death and cell survival in breast cancer in vitro



UNIVERSITY OF THE
WITWATERSRAND,
JOHANNESBURG

Mahlatse Fortunate Mahasha (Student no.1411488)

A dissertation submitted in fulfilment of the requirements for the Degree of Master of Science in Medicine (MSc. Med)

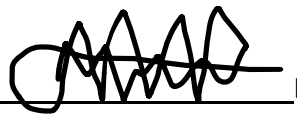
FACULTY OF HEALTH SCIENCES

UNIVERSITY OF THE WITWATERSRAND, JOHANNESBURG

2024

Declaration:

I, Mahlatse Fortunate Mahasha, student number 1411488, declare that this Dissertation titled "**Impact of Cannabidiol and Tamoxifen treatment on cell death and cell survival in breast cancer in vitro** is my own work and that I contributed adequately towards research findings in this dissertation.

Signature of Student  Date: 05/06/2024

Abstract

The main non-psychotropic component of *Cannabis sativa*, Cannabidiol (CBD), alleviates breast cancer treatment-associated side effects but its effects with standard therapy remain unclear. In breast cancer, CBD has been shown to exhibit anti-cancer properties by inducing apoptosis and pro-death autophagy. This study aimed to investigate the effects of combined CBD and Tamoxifen treatment on metabolism, cell death, and cell survival mechanisms in luminal-A breast cancer cell lines MCF7 and T47D. The CBD concentration relative to IC50 was established by testing a range of CBD concentrations: 5 µM, 7 µM, and 10 µM, at 24 h, 48 h, and 72 h using the neutral red cell viability assay. The scratch assay was used to determine the effects of the concentrations on migratory capacity. Two models of treatment were used, single-dose treatment (model 1) and daily-replacement treatment (model 2), and appropriate controls were included. Treatment with 2 µM Tamoxifen and 5 µM CBD for 48 h was determined to be the optimal treatment condition. The MTT assay was performed, and the absorbance ratio indicative of cell proliferation was calculated. The ability of the cells to metabolize the drug components was examined through an assessment of CYP450 reductase (CPR) enzyme activity. The mRNA and protein expression levels of three autophagic markers; *BECN1, LC3B,* and *p62,* were investigated using qPCR and immunocytochemistry, respectively. Friedman's Anova ($p<0.05$) and Kruskal Wallis ($p<0.05$) post hoc tests were used to statistically analyse the data. Combined CBD and Tamoxifen treatment showed the greatest decrease in the proliferation of MCF7 cells and T47D cells compared with all other treatments across both treatment models, with the daily-replacement treatment model (model 2) showing more efficacy thus suggesting that combined treatment may inhibit cell proliferation. CYP450 enzyme reductase activity was higher in T47D cells compared with MCF7 cells in both treatment models suggesting increased metabolic activity and susceptibility to combined treatment. However, in the daily replacement model, MCF7 cell CPR activity could not be ascertained, suggesting either prodrug availability or reduced CPR activity. Further analysis is required in this regard. For immunolocalization, optimization was conducted in late 2021 and all three antibodies showed clear and expected immunolocalization but when the experiments were repeated early 2022, immunofluorescence was reduced (P62 and BECN1), with LC3B not detectable. P62 and BECN1 were expressed in both MCF7 and T47D

cells across both treatment models although BECN1 expression was not sufficient to be quantified and assessed statistically. LC3B protein levels could not be accurately quantified irrespective of the treatment model used. Low amounts of target mRNA in MCF7 cells resulted in undetermined Cq values of *LC3B*, *P62* and *BECN1* genes across both treatment models. In T47D cells, Cq values of target genes were determined across both treatment models and the fold change in gene expression indicated that combined CBD and Tamoxifen treatment effectively upregulates target genes albeit not significantly (*LC3B*, *P62* and *BECN1*) with the single-dose treatment model (model 1) compared with the daily replacement model. Both the immunofluorescence and qPCR experiments would be required to be repeated to ensure conclusive results. The findings of this study nevertheless indicate that combined CBD and Tamoxifen treatment may inhibit tumour growth, but tumour cells may be able to evade cell death pathways resulting in tumour cell survival.

Presentations arising from this work.
Oral presentations

An assessment of CBD and Tamoxifen treatment on cell death and cell survival. MF Mahasha, KR Xulu, TN Augustine. *Faculty of Health Science Research Day and Postgraduate expo, Wits University, Johannesburg, 2022*.

Cannabidiol enhances the effects of tamoxifen in breast cancer cell lines. Kutlwano R. Xulu (PhD), Mahlatse F. Mahasha (BHSc Hons), Tanya N. Augustine (PhD). *Surgical Research Society of Southern Africa, 2022.*

Impact of increasing Cannabidiol concentrations with Tamoxifen in MCF7 breast cancer: Cell viability and cell migration. MF Mahasha, KR Xulu, TN Augustine. *12th Cross-Faculty Postgraduate Symposium, Wits University, Johannesburg, 2021.*

Acknowledgements

Supervisors

Prof Tanya Augustine: I am grateful for the opportunity to work besides you, but most importantly for the values you have instilled in me. Through the highs and lows, you have imparted profound knowledge, skills, and useful life hacks that I believe will forever benefit me in my journey as an academic. Thank you for your support and for leading the lab with so much diligence.

Dr Kutlwano Xulu: Thank you for the support and guidance that you have provide me with throughout my MSc journey. I am profoundly grateful for the knowledge and wisdom you have imparted. It was not an easy journey, but we made it through. Thank you and God bless you.

Funding

I want to thank the following entities for the funding provided for this project:

NRF grant (M121263) awarded to Prof T. Augustine

Faculty Research Council grant awarded to Ms MF. Mahasha (2021)

NRF grant-holder linked student bursary awarded to Prof T. Augustine and used for Ms MF. Mahasha (2020-2021).

NRF extension grant awarded to Ms MF. Mahasha (2022).

Laboratory resources and equipment

I thank the following Schools and Departments within the University of the Witwatersrand for providing resources needed to complete this study:

• The School of Anatomical Sciences for use of laboratory facilities to conduct experiments

• Department of Internal Medicine for the use of Nanodrop to measure mRNA concentrations for qPCR experiments.

• The School of Surgery for use of the cDNA thermocycler

• The Life Sciences Imaging Facility for use of the LSM confocal microscope

Expertise

I thank the following people for expertise and training in various equipment and laboratory techniques: Prof Tanya Augustine, Dr Kutlwano Xulu, Dr Kyrtania Pather, Dr Aurelie Deroubaix, Mrs Hasiena Ali, Mr Bradley Khoza, Dr Ekene Nweke, and Ms Thérèse Dix-Peek.

Special thank you to the following people

Dr Kyrtania Pather (Department of Family Medicine and Primary care, University of the Witwatersrand) for your valuable contribution in this journey. Thank you for the unwavering support, motivation, and training in various laboratory skills.

Prof Raquel Duarte (Department of Internal Medicine, University of the Witwatersrand) for donating MCF7 cells for the experimental part of this study.

Prof Sharon Prince (Department of Human Biology, University of Cape Town) for donating T47D cells used in this study.

Postgraduate students

A huge thank you to the death lab gang (Deruskhka Arnachellen, Thabang Mackade, Simone Gallant, Nastassia Altriche and Lehlogonolo Marakalla), you have all been a great support system.

Family

- My sister (Francina Mahasha) for always believing in me and supporting me in every way possible. Your love carried me through the most difficult research days.
- My parents (Selina Khuwela Mahasha and William Sesepe Mahasha) for your prayers and for always cheering me on.

- My siblings (Charles, Sence, Tshepo, and Lerato Mahasha) for believing in me and motivating me to go on.
- My nieces and nephews, thank you for bringing me so much joy.
- My spiritual leader (Apostle Ignicious Maphuthi Kgomo) and my spiritual home (Revelation Christian Centre) for the prayers and petitions you have made before God concerning my journey. Thank you for the teachings that carried me through the most difficult circumstances in my life.
- A special thank you to the Holy spirit, thank you for being my friend, for listening to my complains and providing me with comfort. Thank you for being a wonderful counsellor (John14:26-27). To God be the glory.

Dedication

I dedicate this work to my mother (Selina Khuwela Mahasha). You are a super mom; you have moved mountains for me to get here.

List of abbreviations and symbols

Abbreviation	Full form
ACTB	Actin beta
ATCC	American Type Culture Collection
ATG	Autophagy related gene
BECN1	Beclin-1
Ca^{2+}	Calcium
CBD	Cannabidiol
CBN	Cannabinol
cDNA	Complementary deoxyribonucleic acid
CK	Cytokeratin
COX	Cyclo-oxygenase
CYP	Cytochrome P450
Mg	Milligram
GPCRs	G-protein coupled recptors
CB	Cannabinoid
CB_1	Cannabinoid receptor 1
CB2	Cannabinoid receptor 2
p53	Tumour protein 53
Ki-67	Kiel-67
ECM	Extracellular matrix
DAPI	4’,6-damidino-2-phenylindole
DC	Diluent control
DMEM	Dulbecco’s Modified Eagles Medium
DMSO	Dimethyl sulfoxide
EBSS	Earle’s Balanced Salt Solution
EDTA	Ethylenediaminetetraacetic acid
EGFR	Epidermal growth factor receptor
ER	Oestrogen receptor
FBS	Fetal bovine serum
G6P	Glucose-6-phosphate
GAPDH	Glyceraldehyde 3-phosphate Dehydrogenase
GPR55	G-protein coupled receptor 55

HCl	Hydrochloric acid
HER2	Human epidermal growth factor receptor 2
h	Hours
IDT	Integrated DNA Technologies
LC3	Light chain 3
LC3B	Light chain 3-phosphatidylethanolamine (PE)
IDT	Integrated DNA Technologies
M	Molar
MAPK	Mitogen-activated protein kinase
MC	Media control
MCF7	Michigan Cancer Foundation-7
min	Minutes
MIQE	Minimum Information for Publication of Quantitative Real-Time PCR Experiments
ml	Milliliter
mRNA	messenger RNA
MTT	3-(4,5-Dimethylthiazol-2-yl)-2,5 diphenyltetrazolium bromide
NCBI	National Center for Biotechnology Information
NADPH	Nicotinamide adenine dinucleic phosphate
nm	Nanometer
NR	Neutral red
OD	Optical density
OH	Oxyhydrogen
P/S	Penicillin/Streptomycin
PAC	Paclitaxel
PBS	Phosphate buffered saline
PCD	Programmed cell death
PE	Phosphatidylethanolamine
PFA	Paraformaldehyde
PI3K	Phosphoinositide 3-kinase
PR	Progesterone receptor
RDD	RNAse-free digestion buffer
RLT	RNA lysis buffer
RNA	Ribonucleic acid
ROS	Reactive oxygen species
RPLO	Ribosomal protein
RT	Room temperature
SAMRC	South African Medical Research Council
SERM	Selective oestrogen receptor modulators
SQTM1/P62	Sequestosome 1

Tam	Tamoxifen
THCV	Tetrahydrocannabivarin
TNC	Triple negative breast cancers
TRPV1	Transient receptor potential action channel subfamily V member 1
Δ^9 THC	Delta-9-Tetracannabidiol
ΔCq	Delta Quantification cycle
ΔΔCq	Delta Delta Quantification cycle
µg	Microgram
µl	Microliter
Mm	Microns
µM	Micromolar
%	Percent
°C	Degrees Celsius
Sec	Seconds

LIST OF FIGURES

Figure 1: A modified flow diagram showing a summary of the process of autophagy from induction and nucleation process requits atg complex proteins to form a phagophore. Phagophore recruits' molecules and expands to form an autophagosome. Autophagosome binds to lysosome to form an autolysosome. Autolysosome is the degraded 11

Figure 2: A flow diagram showing a summary model of the methodology used for the optimization of CBD concentrations using neutral red (cytotoxic assay) and a scratch assay (migration), and the determination of the optimal treatment duration. This was conducted on MCF7 cells. Following determination of the optimal CBD concentration and treatment duration on MCF7 cells, T47D cells were assessed for their response using the same neutral red assay and scratch assay. 16

Figure 3: A flow diagram showing a summary model of the methodology used for this study to assess inhibition of cell proliferation, CYP450 reductase enzyme activity; and protein and mRNA levels of *LC3B, P62* and *BECN1*. 17

Figure 4: A schematic diagram showing a confluent well before the creation of the scratch (A) and B shows a well with an exposed area which is the area of the scratch (white) after the scratch was created as well as the region that was measured in ImageJ (red). 23

Figure 5: A representative diagram of CellProfiler output images to show the pipeline. A: nuclei of 20-15 pixels within the cell identified using the " IdentifyPrimaryObjects module", B: BECN1 expression within the cell cytoplasm, identified using the " IdentifySecondaryObject module" and C: whole cell showing the cell nuclei and cytoplasm together as determined using the "IdentifyTertiaryObjects module. ..... **Error! Bookmark not defined.**

Figure 6: Dose response curves generated from GraphPad Prism showing the logIC50 concentration and cell viability in the single-dose treatment model (model 1) and the daily-replacement treatment model(model 2). The IC50 conentration as well as the r-squared value are also depicted on the graphs. 41

Figure 7:Line graphs showing the percent cell viability of MCF7 breast cancer cells treated with CBD, and combined CBD/Tamoxifen treatment, assessed by the neutral red assay. A: Model 1, single-dose treatment with CBD at 5 µM, 7,5 µM AND 10 µM. B: Model 2, daily-replacement treatment with CBD at 5 µM, 7,5 µM AND 10 µM C: Model 1, single-dose treatment with combined CBD and Tamoxifen treament . D: Model 2, daily-replacement treatment with combined CBD and Tamoxifen treament. In both Model 1 and Model 2, MCF7 cells were treated with diluent (sky blue), 2µM Tamoxifen (light blue), 5µM CBD or 2µM

Tamoxifen + 5µM CBD (light green), 7.5µM CBD or 2µM Tamoxifen +7.5µM CBD (yellow) and 10µM CBD or 2µM Tamoxifen +10µM CBD (red). Asterisks(*) matching the colour of the treatment group are used to show significant differences between treatment groups across time. Error bars as mean±SD. 43

Figure 8.A2: Photomicrographs with a scale bar of 100µm under the 10X objective showing changes in the scratch area (outlined in yellow and spanned by the yellow double arrow) of MCF7 cells treated with 5 µM CBD, 7.5 µM CBD and 10 µM CBD over 96 h. period in the single-dose treatment model (model 1) and the daily-replacement treatment model (model 2). 47

Figure 9: A: Line graphs showing percentage wound closure of MCF7 cells treated according to single-dose treatment model (model 1) and B: Shows MCF7 cells treated according to daily-replacement treatment model (model 2). In both Models MCF7 cells were treated with Media (dark blue), diluent (sky blue), 2 µM Tamoxifen (light blue), 5 µM CBD (orange), 7.5 µM CBD (violet) and 10 µM CBD (red). Asterisks(*) matching the colour of the treatment group are used to show significant differences between treatment groups across time with reference to 0 h. Error bars as mean±SD. 48

Figure 10:A: Photomicrographs at 100µm under the 10X objective showing changes in the scratch area (outlined in yellow and spanned by yellow double arrow) of MCF7 cells treated with media, diluent, 2 µM Tamoxifen, 2 µM Tamoxifen + 5 µM CBD, 2 µM Tamoxifen + 7.5 µM CBD and 2 µM Tamoxifen + 10 µM CBD over 96h period in single-dose treatment (model 1) and daily-replacement treatment (model 2). 51

Figure 11: A: Line graphs showing percentage wound closure of MCF7 cells treated according to single-dose treatment model (model 1) and B: Shows MCF7 cells treated according to daily-replacement treatment model (model 2). MCF7 cells were treated with Media (dark blue), diluent (sky blue), 2µM Tamoxifen (light blue), 2µM Tamoxifen +5µM CBD (orange), 2µM Tamoxifen +7.5µM CBD (violet) and 2µM Tamoxifen +10µM CBD (red). Asterisks(*) matching the colour of the treatment group are used to show significant differences between treatment groups across time with reference to 0 h.Error bars as mean±SD. 52

Figure 12: Line graphs showing the percentage cell viability of T47D breast cancer cells alongside MCF7 cells treated with CBD, Tamoxifen and combined CBD/Tamoxifen, assessed by the neutral red assay. A *and* C: Model 1, single-dose treatment with 5 µM CBD (green), 2 µM Tamoxifen (light blue) and 5 µM CBD combined with 2 µM Tamoxifen (orange) in T47D (A) and MCF7(C) cells. B *and* D: Model 2, daily-replacement treatment with 5 µM CBD (green), 2 µM Tamoxifen (light blue) and 5 µM CBD combined with 2 µM Tamoxifen (orange) in T47D

(B) and MCF7(D) cells. The diluent control in both A and B is shown in (dark blue). Error bars as mean±SD. 56

Figure 13.A1: Photomicrographs at 100µm under the 10X objective showing changes in the scratch area outlined in yellow and spanned by yellow double arrow) of T47D cells treated with media, diluent and 2 µM Tamoxifen over 96 h period in single-dose treatment model (model 1) and daily-replacement treatment model (model 2). 59

Figure 14. A and C: Line graphs showing percentage wound closure of T47D cells (B) and MCF7 cells (D) treated according to model 1 (single-dose treatment) and B and D: Shows T47D cells(B) and MCF7 cells (D) treated according to model 2 (daily-replacement treatment). In both A and B T47D cells were treated with Media (dark blue), diluent (green), 2µM Tamoxifen (light blue), 5µM CBD (orange) and 2µM Tamoxifen +5µM CBD (red) and compared with MCF7 cells (C and D) for the same treatment. Asterisks(*) matching the colour of the treatment group are used to show significant differences between treatment groups across time with reference to 0 h. Error bars as mean±SD. 61

Figure 15. A: Box and whisker plots showing inhibition of cell proliferation as absorbance ratio of MCF7 and T47D cells treated according to single-dose treatment (model 1) and B: Shows bar graphs of MCF7 and T47D cells treated according to daily-replacement treatment model (model 2). The X within the box indicates the mean and the line within the box indicates the median value. In both A and B MCF7 (blue) and T47D (red) cells were treated with Media, diluent, 0.1 % triton, 2 µM Tamoxifen 5µM CBD *and* 2µM Tamoxifen + 5µM CBD. No significant differences ($p>0.05$) were observed across all treatment groups in both Model 1 and Model 2 and across cell lines. 66

Figure 16: Showing CPR activity of MCF7 and T47D cells at 15 min and at 30 min. MCF7 and T47D cells were treated with Media, diluent, 2µM Tamoxifen, 5µM CBD, 2µM Tamoxifen + 5µM CBD, Paclitaxel and 1X EBSS according to model 1 (single-dose treatment). Eror bars as mean ± SD. 69

Figure 17: Showing CPR activity of MCF7 and T47D cells at 15 min and at 30 min. MCF7 and T47D cells were treated with Media, diluent, 2µM Tamoxifen, 5µM CBD, 2µM Tamoxifen + 5µM CBD, Paclitaxel and EBSS according to model 2 (daily-replacement treatment). Eror bars as mean ± SD. 70

Figure 18: Photomicrographs showing P62 expression (green fluorescence) in MCF7 and T47D breast cancer cells treated with media, diluent, tamoxifen, CBD, combined CBD and tamoxifen, Paclitaxel and 1X EBSS. White arrow (Dapi stained nuclei) and grey arrow (P62 in the cytoplasm). Scale bar= 100 µm (not 75

Figure 19: Box and Whisker plots showing P62 expression levels in breast cancer cells treated with media, diluent, tamoxifen, CBD, combined CBD and tamoxifen, Paclitaxel and 1X EBSS. The X within the box indicates the mean and the line within the box indicates the median value. A: MCF7 Model 1, B: MMCF7 Model 2, C: T47D Model 1 and D: T47D Model 2. 76

Figure 20: Photomicrographs showing BECN1 expression (red fluorescence) in MCF7 and T47D breast cancer cells treated with media, diluent, tamoxifen, CBD, combined CBD and tamoxifen, Paclitaxel and 1X EBSS. White arrow (Dapi stained nuclei) and grey arrow (BECN1 in the cytoplasm). Scale bar= 100 µm (not shown on the images to avoid obscuring fluorescence in some areas. 77

Figure 21: Box and Whisker plots showing *LC3B, P62 and BECN1* fold change in T47D breast cancer cells treated with media, diluent, tamoxifen, CBD, combined CBD and tamoxifen, Paclitaxel and 1X EBSS ($p>0.05$). The X within the box indicates the mean and the line within the box indicates the median value. A: T47D Model 1(M1) *LC3B* and Model 2(M2) *LC3B*, B: T47D Model 1(M1) *P62* and Model 2(M2) *P62* and C: T47D Model 1(M1) *BECN1* and Model 2 (M2) *BECN1.* 81

List of tables

Table 1: A table showing controls and experimental samples for Tamoxifen pre-treatment and CBD and Tamoxifen treatment, alongside the abbreviations used in labelling the samples. * Indicates pre-treatment with Tamoxifen for 24 h. 21

Table 2: Optimised treatment protocol for MCF7 and T47D cells 24

Table 3: Showing the constituents of sample wells and control wells for CPR activity assay 28

Table 4: The reference genes and genes of interest that were investigated in this study and their accession numbers 37

Table of Contents

Declaration: I

Abstract II

Acknowledgements IV

Dedication VII

List of abbreviations and symbols VIII

List of Figures XI

List of tables XV

1.Introduction 1

1.1. *Cannabis sativa* and its derivatives 1

1.2. Medicinal potential of cannabidiol and its metabolism 2

1.3. Breast cancer 4

1.4. The use and limitations of tamoxifen as a therapy for hormone-dependant breast tumours 6

1.5. The effects of CBD and Tamoxifen on the crosstalk between apoptosis and autophagy 8

1.6. Aim 13

1.7. Objectives 14

2.Materials and methods 15

2.1. Cell culture 18

2.2. Subculture of MCF7 and T47D cells 18

2.3. Plating cells for experimentation 19

2.4. Preparation of Tamoxifen and CBD solutions 19

2.5. CBD and Tamoxifen treatments 19

2.6. Establishment of treatment models 20

2.7. Determining optimal treatment concentration of CBD using the MCF7 cell line 22

2.7.1. Neutral Red assay 22

2.7.2. Scratch assay 23

2.7.3. Optimal CBD concentration and duration of treatment 24

2.8. Assessing the effects of optimal CBD concentration and duration of treatment on cell viability and cell migration in T47D breast cancer cells 25

2.8.1. T47D Neutral red and Scratch assay at optimal CDB concentration 25

2.9. Assessing the effects of optimal CBD concentration and Tamoxifen treatment in MCF7 and T47D breast cancer cells over 48h 25

2.10. Effects of CBD and Tamoxifen on *CYP450 reductase* (CPR) activity 26

2.10.1. CYP450 reductase (CPR) activity Assay 26
2.11. Effects of CBD and Tamoxifen treatment on protein and mRNA levels *of LC3B, P62* and *BECN1* in MCF7 and T47D breast cancer cells 29
2.11.1. Immunofluorescence 29
2.11.2. Determination of mRNA expression of genes involved in drug metabolism and autophagy 34
3.Results 39
3.1. Determining optimal CBD concentration and treatment duration using MCF7 cell line 39
3.1.1. Cell viability – the Neutral red assay in MCF7 cells 39
3.1.2. Wound closure - Scratch assay in MCF7 cells 44
3.1.3. Optimal CBD concentration and treatment duration 53
3.2. Cell viability and Cell migration in T47D cells in comparison to MCF7 cells 53
3.2.1. Cell viability – the Neutral red assay in T47D cells 53
3.2.2. Wound closure-Scratch assay in T47D cells 57
3.3. Cell proliferation in MCF7 and T47D, the single-dose treatment model (model 1) and the daily-replacement treatment model (model 2) 62
3.3.1. Proliferation inhibition induced by combined CBD and Tamoxifen in MCF7 and T47D cells (model 1, single-dose treatment) 62
3.3.2. Proliferation inhibition induced by combined CBD and Tamoxifen in MCF7 and T47D cells (model 2, daily-replacement treatment) 64
3.4. CYP450 enzyme activity in MCF7 and T47D cells 67
3.4.1. CPR activity with single-dose treatment (model 1) in MCF7 and T47D cells. 67
3.4.2. CPR activity with daily-replacement treatment (model 2) in MCF7 and T47D cells. 68
3.5. Immunolocalization of LC3B, P62 and BECN1 71
3.5.1. Antibody optimization 71
3.5.2. P62 and BECN1 protein expression with single-dose treatment model (model 1) -MCF7 and T47D cells. 71
3.5.3. P62 and BECN1 protein expression with daily-replacement treatment model (model 2) - MCF7 and T47D cells 73
3.6. Gene expression of *LC3B*, *P62* and *BECN1* 78
3.6.1. LC3B, P62 and BECN1 gene expression with single-dose treatment model (model 1) -T47D cells 78
3.6.2. LC3B, P62 and BECN1 expression with daily-replacement treatment model (model 2) -T47D cells 79
4.Discussion 82

4.1. The effects of combined CBD and Tamoxifen on MCF7 and T47D cell viability, migration, and proliferation. 83
4.2. The metabolic effects of Tamoxifen and CBD in MCF7 and T47D cells 86
4.3. The effects of Tamoxifen and CBD on LC3B, P62 and BECN1 mRNA and Protein expression in MCF7 and T47D cells 88
4.4 Limitations of the study and future perspectives 89
5.Conclusion 90
References 92
Appendix A-Drugs and reagents preparation and Tamoxifen pre-treatment. 107
Appendix B – Neutral red assay raw data and normality test results 110
Appendix C – Scratch assay optimization results 118
Appendix D- CYP450 assay reagents' preparation 119
Appendix E-ICC primary antibody optimization 120
Appendix F-qPCR nanodrop results 122
Appendix G-MTT statistical output 127
Appendix H- CYP450 assay statistical output 128
Appendix I- ICC results and statistical ouput 130
Appendix J-Gene amplification gaphs and qPCR statistical outputs 137
Appendix K- Proof of ethical clearance 142
Appendix L- Turnitin report 144

1.Introduction

1.1. *Cannabis sativa* and its derivatives

To date, actions to decriminalize and legalise *Cannabis sativa* in South Africa are gaining momentum (Venter, 2020; Rothberg, 2017). Cannabis originates from *Cannabis sativa*, with *Cannabis indica* and *Cannabis ruderalis* as its subspecies which contain cannabinoids, namely, Cannabidiol (CBD), Cannabinol (CBN) and Tetrahydrocannabivarin (THCV) and delta-9 - Tetracannabidiol (Δ^9 –THC) (Jooste *et al*., 2021) . The most studied cannabinoids are Δ^9 –THC which exhibits psychotropic effects, and CBD which is non-psychotropic and thus has been given preference over Δ^9 –THC for medicinal purposes (Mokoena *et al*., 2019; Rothberg, 2017) .

Increasing scientific evidence suggests medicinal and economic benefits of *Cannabis sativa* derivatives (Odieka *et al*., 2022; Venter, 2020; Mokoena *et al*., 2019; Rothberg, 2017). After many calls to legalize *Cannabis sativa*, in February 2014, the medical innovation bill was introduced in South Africa, it includes the legalization of the medical use of Cannabis (SAMRC policy brief, 2016). Furthermore, access laws were passed first by legalizing the private use of Cannabis, followed by amendments to the schedules of the medicines and related substances Act No.101 of 1965 which reduced the Cannabis plant from schedule 7 to the lower schedule where Δ^9 –THC was moved to schedule 6 and CBD was moved to schedule 4 (Government notices, no.43347, 2020; Donvito *et al*., 2017; Jooste *et al*., 2021) . Following these policy amendments, breast cancer patients have resorted to taking CBD alongside breast cancer treatment drugs to alleviate symptoms associated with chemotherapy.

Over the years, studies have shown that CBD can reduce the use of opioids due to its anti-nociceptive effects in inflammation models, causing a decrease in heroin-seeking behavioural traits (Jooste *et al*., 2021). CBD is reported to show anti-tumour effects which are yet to be proven; furthermore, it exhibits anti-inflammatory, analgesic, anti-emetic properties amongst other health benefits (Dobovišek *et al*., 2022; Odieka *et al*., 2022; Atalay *et al*., 2019) . The increase in diagnosed breast cancer cases per year and deaths resulting from breast cancer

globally have led to more breast cancer research involving the use of CBD to investigate the anti-tumour properties of CBD and possible interactions with standard cancer treatments (Ritchie and Roser, 2018) .

1.2. Medicinal potential of cannabidiol and its metabolism

Following the discovery of cannabinoid (CB) receptors, cannabis research increased remarkably (Wu, 2019; Kendall and Yudowski, 2017) .Currently, there are two known CB receptors, cannabinoid receptor 1 (CB_1) and cannabinoid receptor 2 (CB_2). CB_1 receptors are primarily confined to the central and peripheral nervous system and are engaged in motor behaviour, memory, learning, emotions, and perception (Almogi-Hazan, 2020; Wu, 2019; Kendall and Yudowski, 2017) and are involved in the stimulation of growth in haematopoietic lineages and glia cells (Vicente-Acosta *et al*., 2022; Devinsky *et al*., 2014) . CB receptors shed some light on the mechanism of action of cannabinoids (Wu, 2019; Kendall and Yudowski, 2017; Pertwee,2008). Currently cannabinoid receptors have been found to be widely distributed in human tissues including the central and peripheral nervous system and in the cells of the immune system (Including lymphocytes, natural killer cells, monocytes, and neutrophils) which are mainly localised in the spleen, lymph nodes and peripheral blood (Almogi-Hazan *et al*, 2020; Spiller *et al*., 2019; Freundt-Revilla *et al*., 2017; Klein *et al*., 2001)

Cannabinoid receptors are G-protein coupled receptors (GPCRs) and their agonists (synthetic CBD and synthetic-THC) have been shown to stimulate apoptotic cell death (Shahbazi *et al*., 2020; Cianchi *et al*., 2008; Pertwee, 2008) . CBD has a low affinity for CB_1 and CB_2 receptors whereas Δ^9 - THC has a high affinity for these receptors (Seltzer *et al*., 2020) hence the non-psychotropic effects of CBD. Δ^9 - THC activity mainly depends on CB_1 and CB_2 receptor stimulation. CBD not only acts via CB receptors but can also act via the transient receptor potential action channel subfamily V member 1 (TRPV1) and the G-protein coupled receptor 55 (GPR55). CBD binding to CB_1 inhibits the uptake and degradation of synthetic THC by the cells (Śledziński *et al*., 2018; Devinsky *et al*., 2014; Ryan *et al*., 2009; Pertwee, 2008) . At low concentrations, CBD activates TRPV1 receptor in breast cancer cells, resulting in increased calcium ion influx and elevated ROS thus leading to apoptosis (Muller *et al*., 2019; Ligresti *et al*., 2006) but inhibits G protein-coupled

receptor 55 (GPR55) which is involved in breast cancer cell metastasis (Devinsky *et al*., 2014; Pertwee, 2008; Ryan *et al*., 2009) .

CBD has been shown to attenuate the adverse drug reactions of chemotherapy drugs such as loss of appetite, nausea, and vomiting at low concentrations (0.5-2.5 mg/ml) in *Suncus murinus* treated with cisplatin (a chemotherapy drug) (Bathula and Maciver, 2023; Rock *et al*., 2012; Ligresti *et al*., 2006; Kwiatkowska *et al*., 2004).Moreover, advances in cannabis research have identified potential anti-cancer effects induced by CBD including pro-apoptotic effects, anti-proliferative effects, and inhibition of tumour metastasis *in vitro* in colorectal, lung and breast cancer cell lines by measuring amongst other parameters the reactive oxygen species (ROS) levels (Almeida *et al*., 2023; Massi *et al*., 2013; Shrivastava *et al*., 2011; Ramer *et al*., 2010; Jacobsson *et al*., 2000),however, further research needs to be done to understand how to exploit these reported anti-cancer properties of CBD taking into consideration possible drug interactions which may result from the use of similar metabolic enzymes for CBD and cancer drugs. CBD was shown to regulate the amount of ROS, endoplasmic reticulum stress, and immunomodulation thus suggesting that it may have anti-cancer activity (Almeida *et al*., 2023; Gill *et al*., 2016; Zhang *et al*., 2016; Jacobsson *et al*., 2000).A dose-dependent response to CBD has been observed with a half maximal inhibitory concentration (IC50) of 5 µM/ml in ER^+ (MCF7, T47D, ZR-75-1), and triple negative breast cancer (TNBC) cell lines (MDA-MB-231, MDA-MB-468, SK-BR3, SUM159, 4T1UP, MVT-1, and SCHP3) (Dobovišek *et al*., 2022; Shrivastava *et al*., 2011; Ligresti *et al*., 2006).

Studies have made advances in explaining the pharmacokinetics of CBD, which is mainly administered orally or through inhalation (Vinette *et al*., 2022; Devinsky *et al*., 2014). The primary metabolic pathway of CBD is through the oxidation of the carbon atom at the 7^{th} position which is then followed by hydroxylation in the pentyl side chain and terpene moiety primarily occurring in the liver with secondary metabolism occurring at other sites such as kidneys, placenta, intestines and blood plasma (Smith and Gruber, 2023; Jiang *et al*., 2011).The enzymatic processes involved in the formation of CBD metabolites involve CYP (Cytochrome P450) enzyme family primarily expressed in the endoplasmic reticulum of liver cells (Zhao *et al*., 2021; Ujváry and Hanuš, 2016). Interestingly, CBD is not only a substrate of CYP450 enzymes but it is also a

competitive inhibitor of these enzymes and therefore it can interfere with the metabolism of other drugs (Jiang *et al*., 2011; Pertwee, 2005).CBD is metabolized by CYP2D6 and CYP3A4 enzymes to form 7-OH and 4-OH CBD respectively (Jiang *et al*., 2011), in an extensive primary metabolism phase which accounts for the low bioavailability (referring to the amount of substance absorbed and available at the site of action) of CBD as most of it is excreted intact (Smith and Gruber, 2023; Millar *et al*., 2018; Ujváry and Hanuš, 2016) . CYP3A4 inducers reduce plasma levels of CBD while CYP3A4 inhibitors increase the plasma levels of CBD (Ujváry and Hanuš, 2016). CBD active metabolite, 7-OH is further oxidized to form CBD-7-oic acid which is the major CBD metabolite, and these are excreted in the faeces (Ujváry and Hanuš, 2016; Huestis, 2007).

1.3. Breast cancer

Breast cancer is the second leading cause of cancer-related death in women worldwide and it accounts for about 36% of all cancer patients worldwide (Smolarz *et al*., 2022). Over 2.3 million women were diagnosed with breast cancer and as of 2022, about 670 000 women died from breast cancer (WHO,2024). Breast cancer incidence rates have gained momentum in all regions of the world, with the highest incidence rates in developed countries (Azubuike *et al*., 2018; Moodley *et al*., 2016). While developing and underdeveloped countries have low incidence rates, they are presented with the highest mortality rates due to poor infrastructure and poor treatment modalities (Smolarz *et al*., 2022; Azubuike *et al*., 2018). In Africa, the mortality rates due to breast cancer are estimated to be disproportionately higher (50%) relative to the incidence rates (Smolarz *et al*., 2022; Azubuike *et al*., 2018). Southern Africa has been reported to account for 16526 of the new incidences of breast cancer in 2020 and 5090 of the mortalities globally (Arnold *et al*., 2022). Breast cancer remains one of the most prevalent cancers and therefore, more insight on the disease and the development of better diagnostic and treatment modalities is necessary.

Breast cancer tumours are heterogeneous, differing from patient to patient and within the tumour itself (Lawson *et al*., 2018; Ellsworth *et al*., 2017). Intratumoural heterogeneity is the diversity in the morphological, genomic, transcriptome and proteomic compositions of cell

populations within a single tumour, thereby posing challenges in the precision of diagnosis and chosen therapeutic modalities (Guo *et al*., 2023; Turashvili and Brogi, 2017; Tellez-Gabriel *et al*., 2016). Tumour heterogeneity adds to the many challenges in breast cancer treatment and therefore highlights a need to further optimize other treatment options in addition to standard hormone therapy.

Breast cancer is classified into distinct molecular subtypes based on hormone receptor status, human epidermal receptor-2 (HER2) status and Kiel-67 (Ki-67) protein levels. The first subtype is the normal-like phenotype, where breast tumour expression profiles are like that of non-cancerous breast tissue (Al-thoubaity, 2020; Prat and Perou, 2011; Sørlie, 2004). The second subtype is the Luminal subtype which refer to oestrogen receptor (ER) or progesterone receptor (PR) positive tumours that also express varying levels of epithelial markers such as E-cadherin (which maintains tissue structure through adhesion) and cytokeratins (CK), CK8, CK18 and CK19, which enable cells to resist mechanical stresses (Al-thoubaity, 2020; Nazarali and Narod, 2014; Prat and Perou, 2011; McAllister *et al*., 2007; Sørlie, 2004). Luminal subtype breast cancers are further divided into Luminal (sub)phenotypes; A ($ER^+/PR^+/HER2^-$/low Ki-67) and B ($ER^+/PR^+/HER2^{-/+}$/high Ki-67) (Al-thoubaity, 2020; Ahn *et al*., 2015) . The luminal A breast phenotype is the most prevalent, it accounts for about 75% of all breast cancer cases (Al-thoubaity, 2020; Kudela *et al*., 2020) . These tumours have low invasiveness and are associated with better survival rates (Al-thoubaity, 2020; Turashvili and Brogi, 2017; Caffarel *et al*., 2012) . However, the luminal B phenotype tumours have been associated with poor prognosis and an increased risk of relapse (Turashvili and Brogi, 2017; Cho, 2016; Li *et al*., 2016) .

The third subtype is HER2 tumours which includes ER^-HER2^+ or ER^-/PR^-HER2^+ tumours (Al-thoubaity, 2020; Nazarali and Narod, 2014; Prat and Perou, 2011; McAllister *et al*., 2007; Sørlie, 2004). The fourth subtype is the basal-like phenotype also known as the triple negative breast cancer ($ER^-/PR^-/HER2^-$) (Al-thoubaity, 2020; Yin *et al*., 2020) which is the most aggressive subtype where a robust cluster of genes coding for proteins such as epidermal growth factor receptor (EGFR), tumour protein 53 (p53) and basal cytokeratins (CK5/CK6/CK14/CK16 and CK17) (Nazarali and Narod, 2014; Prat and Perou, 2011; McAllister *et al*., 2007;Sørlie, 2004) are expressed.

Cell culture systems have been used extensively to evaluate molecular mechanism (such as those mediating metabolism, apoptosis, drug uptake and cell proliferation) with breast cancer cells being a useful model in these studies to explore *in vitro* drug effects (Mirabelli *et al*., 2019; Niu and Wang, 2015). The use of *in vitro* culture systems of breast cancer cell lines provides a platform to enable investigators to improve understanding of the mechanisms that drive cell behaviours (Kitaeva *et al*., 2020; Casbas-Hernandez *et al*., 2011). Behavioural mechanisms such as cell differentiation, migration and growth have been extensively studied using cell culture (Chen *et al*., 2021; Du *et al*., 2018). The Michigan cancer foundation-7 (MCF7) cell line is the most used cell line due to its genomic instability and its ability to adapt and evolve, it closely mimics human breast cancer cells which can undergo genetic and translational evolution thus altering cell responses to hormone therapy (Ben-David *et al*., 2018; Vantangoli *et al*., 2015; Aka and Lin, 2012). Following the MCF7 cell line, the T47D cell line is also commonly used in breast cancer research *in vitro* (Wright *et al*., 2022; Yu *et al*., 2017; Aka and Lin, 2012) . Both MCF7 and T47D breast cancer cells are hormone-dependent, and they express oestrogen receptors and often *in vitro* studies use synthetic chemotherapy drugs such as tamoxifen to investigate cellular responses.

1.4. The use and limitations of tamoxifen as a therapy for hormone-dependant breast tumours

Standard hormone therapy options for ER-expressing breast tumours, include selective oestrogen receptor modulators (SERM), of which tamoxifen remains the standard of care in hormone therapy, both in pre-menopausal and post-menopausal women (Howell and Howell, 2023; Johänning *et al*., 2017) ; and aromatase inhibitors, such as Anastrozole and Letrozole, which are predominantly administered in post-menopausal women, inhibit aromatase-an enzyme that converts androgens into oestrogens (Tong *et al*., 2018; Brueggemeier *et al*., 2005). Tamoxifen is administered orally at 20 mg per day and patients on Tamoxifen adjuvant therapy (i.e. therapy administered after primary therapy to prevent disease recurrence) remain on treatment for 5 years or longer as this has been proven to significantly increase survival rates (Farrar, 2023). Tamoxifen is an ER antagonist (inhibits oestrogen production at a cellular level) and agonist (inducing oestrogen responsive genes) (Mortimer *et al*., 2007). When acting as an antagonist, tamoxifen competes with oestrogen and oestradiol for binding to the ER and when bound to the

ER it hinders DNA synthesis and cellular responses to oestrogens, hence promoting cell death in breast cancer patients (Heery *et al*., 2018; Nazarali and Narod, 2014;; Singh *et al*., 2011; Lorizio *et al*., 2011; Mortimer *et al*., 2007).

Tamoxifen is ingested orally as a pro-drug (Johänning *et al*., 2017), following ingestion its metabolism is catalysed by the cytochrome P450 (CYP450) enzyme system. CYP450 enzyme subtypes catalyse the conversion of tamoxifen into its primary metabolites which bind to the oestrogen receptors (4-hydroxylation and N-demethylation) through the oxidation of nicotinamide adenine dinucleotide phosphate (NADPH) by cytochrome P450 reductase (CPR) in the endoplasmic reticulum of liver cells (Klein *et al*., 2013). CPR accepts one hydrogen and one electron from NADPH and transfers two electrons to CYP450. Although majority of the metabolism of drugs occurs in the liver, *CYP450* genes have been found to have basal expression in other non-hepatic cells, including cancer cells (Alzahrani and Rajendran, 2020; Kuhn *et al*., 2020).

Breast cancer cells are amongst the cancer cells that express CYP450 subtypes, which can either activate or deactivate chemotherapy drugs in these cells (Kuhn *et al*., 2020; Sneha *et al*., 2021 Murray *et al*., 2010). The formation of 4-hydroxyl Tamoxifen is catalysed by CYP2D6 (the rate limiting enzyme), and this active metabolite has been shown to be effective in inhibiting human breast cancer MCF7 cell proliferation in patients and *in vitro* (Ahmed and Wober, 2020; Maximov *et al*., 2014). N-dimethyl Tamoxifen formation is catalysed by CYP3A4 and CYP3A5, and is the primary ER binding metabolite of Tamoxifen, although it can be further metabolized into a secondary metabolite, Endoxifen(Cronin-Fenton, Damkier and Lash, 2014; Klein *et al*. 2013; Kumar, Chambers and Pertwee, 2001). The active metabolites of tamoxifen are mainly excreted in the faeces with some excreted in the bile and urine. Tamoxifen has been successfully used in the treatment of breast cancer, but its limitations and side-effects such as hot flashes, venous thrombosis and increased risk of endometrial cancer continue to be of great concern (Heery *et al*., 2018; Lorizio *et al*., 2011).

To relieve the pain associated with cancer, many cancer patients resort to self-medication using CBD alongside treatment with tamoxifen. Tamoxifen has a high bioavailability with around 65%

of the ingested drug being excreted over a period of two weeks, with an initial half-life (i.e. time taken for half of the substance to be eliminated from the body) of 7 hours (h) and a terminal half-life (i.e. time taken after blood concentrations of the substance reach equilibrium for the blood concentrations of the substance to gradually decline again) of 7 - 11 days (Klein *et al*., 2013) while oral ingestion of 20 mg CBD results in a half-life of only about 1 h and 97 sec (Millar *et al*., 2018). CBD has been shown to reduce p-glycoprotein transporters which are ATP-dependent efflux pumps localized on the plasma membrane that participate in multidrug resistance by removing drugs from the cells before they have a chance to exert their cytotoxic effects (Holland *et al*., 2008; Zhu *et al*., 2006). Tamoxifen has also been shown to reverse the drug-resistance effects of p-glycoprotein by directly binding to p-glycoprotein transporters and inhibiting drug transport out of the cell (Bosch *et al*. 2023; Callaghan, Higgins and Ary,1995). These pharmacokinetic parameters impact CBD interactions with other drugs and therefore it is essential to understand these interactions to better guide the use of CBD alongside Tamoxifen by breast cancer patients.

While the traditional treatment method for investing the effects of drugs and reagents in cell culture involve administering a single dose of treatment, it is of interest to mimic the administration of tamoxifen and CBD in patients on cell lines. The frequency of drug administration and how long the cells take to metabolize the drugs affects their response and therefore two treatment models (a single-dose treatment model and a daily-replacement treatment model) will extrapolate the observation of cell responses to treatment based on the treatment models.

1.5. The effects of CBD and Tamoxifen on the crosstalk between apoptosis and autophagy

Programmed cell death (PCD), which is a mechanism essential to tissue development and homeostasis under normal physiological conditions is desired in cancer treatment to eradicate malignant cancer cells, reduce tumour size and prevent drug resistance (Tompkins and Thorburn, 2019; Panawala and Between, 2017; Thorburn, 2008). Autophagy and apoptosis are both

pathways for PCD (Tompkins and Thorburn, 2019; Panawala and Between, 2017; Thorburn, 2008). Apoptosis is induced by a set of sequential molecular events using two main pathways: the activation of surface death receptors (extrinsic pathway) or through the mitochondrial release of cytochrome c (intrinsic pathway), depending on the origin of the stimuli inducing cell death (Jain *et al*., 2013; Gump and Thorburn, 2011; Elmore, 2007; Gupta, 2001). Apoptosis is characterized by morphological changes such as cell shrinkage, blebbing, nuclear condensation and loss of cell to cell adhesion or cell to extracellular matrix (ECM) adhesion (Ouyang *et al*. 2012; Elmore, 2007) .Extrinsic apoptosis is through the binding of ligands such as the Fas ligand to the Fas receptor which results in the binding of the Fas adaptor death domain to the cell death signalling complex which induces the autocatalysis of procaspase-8 to caspase 8 to initiate apoptosis(Ouyang *et al*. 2012; Elmore, 2007). Intrinsic apoptosis is through stimuli that is independent of surface receptors but induces mitochondria-mediated intracellular signals that act directly on the targets within the cell and cause direct cleavage of caspse-3 by caspase-9 to initiate apoptosis (Ouyang *et al*. 2012; Elmore, 2007).

Autophagy is characterized by the formation of vesicles called autophagosomes in the cytoplasm of the cell which engulf cellular micro-molecules which include carbohydrates, lipids, proteins, and nucleic acids, and organelles which are fragmented when the autophagosomes fuse with lysosomes (Panawala and Between, 2017; Gump and Thorburn, 2011; Djavaheri-Mergny *et al*., 2007) and is characterized by morphological changes such as increased vacuolisation and loss of intracellular organelles such as mitochondria, peroxisomes, lysosomes, endoplasmic reticulum, and the nucleus (Shrivastava *et al*., 2011;Djavaheri-Mergny *et al*., 2007; Deng *et al*., 2010). The autophagy process is regulated by autophagy related gene (ATG) proteins and multiple upstream signalling pathways such as the phosphoinositide 3-kinase (PI3K), mitogen-activated protein kinase (MAPK), and calcium signalling pathways amongst others. Autophagy related protein 8 (ATG8), also known as light chain 3 (LC3), and ATG12 are activated by ATG7 leading to their conjugation to lipid phosphatidylethanolamine (PE) and ATG5, respectively (Gavilán *et al*., 2015; Thorburn, 2008). The LC3-PE (LC3B) and ATG12-Atg5 conjugates are associated with the autophagosome (Gavilán *et al*., 2015; Thorburn, 2008). Autophagy involves multiple steps, namely, induction, nucleation, elongation, maturation, and degradation (Figure 1). Initiation

occurs at ER-associated structures (amegasomes) in mammals where cytoplasmic materials are sequestered by a double membrane structure called a phagophore. This phagophore undergoes nucleation, a process where ATG complexes are recruited to the phagophore (Parzych and Klionsky 2014; Sun *et al*. 2013; Wang and Klionsky, 2003) . In a process called elongation, the phagophore membrane expands to form a spherical autophagosome (Parzych and Klionsky 2014; Sun *et al*. 2013; Wang and Klionsky, 2003). In the maturation and closure steps, the autophagosome membrane fuses with the outer lysosome membrane to form a double-membrane autolysosome (Parzych and Klionsky 2014; Sun *et al*. 2013; Wang and Klionsky, 2003). When the autolysosome is degraded, LC3-B conjugate remains associated with the autophagosome so LC3B is often used as a measure of a decrease or an increase in autophagy (Thorburn, 2008; Djavaheri-Mergny *et al*.,2007).

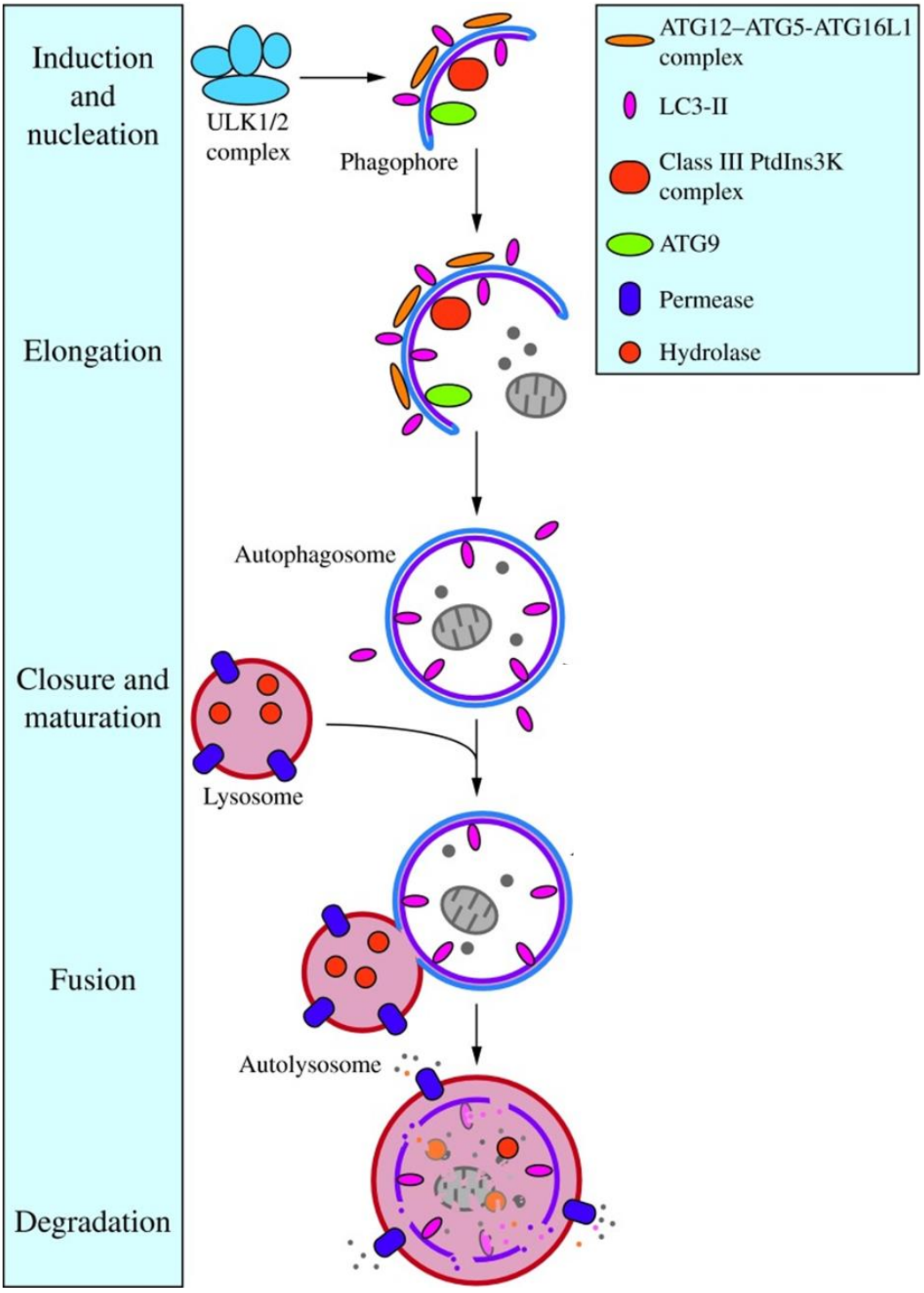


Figure 1: A modified flow diagram showing a summary of the process of autophagy from induction and nucleation process requits ATG complex proteins to form a phagophore. Phagophore recruits' molecules and expands to form an autophagosome. Autophagosome binds to lysosome to form an autolysosome. Autolysosome is the degraded (Parzych and klionsky 2014).

Interestingly, autophagy can be pro-survival or pro-death, depending on the molecular context (Gump and Thorburn, 2011; Maiuri *et al*., 2008; Thorburn, 2008). Autophagy under normal physiological conditions is usually pro-survival, protecting the cell against stresses such as nutrient deprivation by clearing damaged organelles, proteins, and pathogens, and additionally provides the cell with energy during starvation (Gump and Thorburn, 2011) . However, under pathophysiological conditions it has been shown to be associated with pro-death processes that are caspase independent and result from extensive degradation of the contents of the autolysosome (Wirawan *et al*.,2012; Dalby *et al*.,2010; Djavaheri-Mergny *et al*.,2007).

Tamoxifen induces apoptosis at higher concentrations (0,25-10 µM) in breast cancer cells (Bekele *et al*., 2016; Nazarewicz *et al*., 2007) and CBD can induce either apoptosis or autophagy. CBD induced autophagy involves multiple pathways, in triple negative breast cancer cells the increase in ROS levels mediated by cell G_0/G_1 cell cycle arrest and p53 induced autophagy associated with the activation of the heat shock protein 70 (Hsp70) system. Inhibition of Hsp70 results in a shift from CBD-induced autophagy to caspase-mediated apoptosis. Furthermore in hormone-sensitive breast cancers CBD-induced apoptosis is via mitochondria-mediated signalling pathways (Shrivastava *et al*., 2011) . Tamoxifen stimulates oxide synthase enzyme which causes an increase in mitochondrial nitride oxide and an increase in reactive oxygen species (ROS) within the mitochondria (Bekele *et al*., 2016; Nazarewicz *et al*., 2007) . Increased ROS results in tamoxifen-induced autophagy (Shrivastava *et al*., 2011).

Apoptosis can either co-operate with or oppose autophagy. When apoptosis cooperates with autophagy to bring about cell death, two main proteins are involved; Sequestosome 1 (SQTM1/P62), which plays a role in the selective autophagic degradation of proteins and the mitochondria, and beclin-1 (BECN1), a pro- apoptotic protein (Jain *et al*., 2013; Gump and Thorburn, 2011). Apoptosis can oppose autophagy via the caspase-3 cleavage of BEC N1 to produce a truncated protein incapable of promoting autophagy (Luo and Rubinsztein, 2009) . Autophagy, on the other hand, can oppose apoptosis by specifically degrading components of the apoptotic machinery such as the mitochondria and caspase-8 (Gump and Thorburn, 2011).

The cytotoxic effects of CBD on breast cancer cells are mainly through apoptosis, autophagy and cell cycle arrest (Shrivastava *et al*., 2011; Ligresti *et al*., 2006). In MCF7 cell lines, CBD was shown to either cause cell cycle arrest at the G_1 phase (for cell growth)/ S phase (for DNA synthesis) of the cell cycle to prevent cell proliferation or induce apoptosis but in TNBC, it was mainly apoptotic (Seltzer *et al*., 2020; Ligresti *et al*., 2006). While the anti-proliferative effects of CBD exerted through the G_1/S or G_2/M (G2- DNA synthesis checkpoint/M-mitotic division) phase arrest may exhibit desirable anti-cancer effects, the ability of breast cancer cells to escape from cell cycle arrest is concerning. Cells that escape cell cycle arrest at either G_1/S or G_2/M phase, regain their proliferative potential following treatment with chemotherapy drugs (Granada *et al*., 2020) . The escape from cell cycle arrest has been observed in breast cancer where cells escape senescence (a dynamic mechanism that results in permanent cell cycle arrest as a result of therapy -induced stress) and consequently cannot be cleared by the immune system (Sirinian *et al*., 2022; De Blander *et al*., 2021). Senescence escape enables breast cancer cell proliferation and facilitates breast cancer progression (Sirinian *et al*., 2022; De Blander *et al*., 2021). An understanding of the intersection between apoptosis and autophagy will help elucidate whether the use of Tamoxifen alongside CBD promotes the co-operation of these processes which would be a more beneficial effect compared to using tamoxifen alone, or whether it causes one process to inhibit or antagonise the other. Considering the biphasic role of autophagy, it is of vital importance to understand the impact of combined CBD and Tamoxifen treatment to better guide the use of CBD alongside Tamoxifen and to provide caution where pro-cancer cell survival effects may result.

Research question

Does CBD have an effect on the therapeutic role of tamoxifen in hormone dependent breast cancer cell lines?

1.6. Aim

To investigate the effects of combining CBD and Tamoxifen treatment and exposure to MCF7 and

T47D breast cancer cells on death and cell survival mechanisms using two treatment models.

1.7. Objectives

1. To establish an optimal treatment concentration of CBD and treatment duration through assessment of cell viability (NR assay) and cell migration (scratch assay) in MCF7 breast cancer cells across two treatment models as follows.
    - Single-dose treatment model (model 1)
    - Daily-replacement treatment model (model 2)
2. To assess the effects of optimal CBD concentration (as established from objective 1) on cell viability (using the neutral red assay) and cell migration (using the scratch assay) in T47D breast cancer cells across the two treatment models (model 1 and model 2)
3. To examine the activity of CPR enzyme in MCF7 and T47D breast cancer cells in response to Tamoxifen and CBD treatment (optimal concentration) using the cytochrome P450 reductase assay across the treatment models (model 1 and model 2).
4. To assess cell proliferation in response to Tamoxifen and CBD treatment (optimal concentration) in MCF7 and T47D breast cancer cells using the MTT assay across two treatment models (model 1 and model 2).
5. To examine changes in key markers involved in autophagy (LC3B, P62 and BECN1) following treatment with Tamoxifen and CBD (optimal treatment) in MCF7 and T47D breast cancer cells across two treatment models (model 1 and model 2) as follows.
    5.1 Assess gene expression using qPCR
    5.2 Assess protein expression using immunocytochemistry

2.Materials and methods

Ethical clearance was obtained from the University of the Witwatersrand, Human Research Ethics Committee, with the ethical clearance number M190522.

In summary (Figure 2), MCF7 cells (obtained from Prof Raquel Duarte, University of the Witwatersrand, Department of Internal Medicine at passage number 12) and T47D cells (donated by Prof Sharon Prince, University of Cape Town with at passage number 26) which represent luminal-A breast cancer cells were cultured in a monolayer under standard culture conditions (humidified environment at 5% CO2 and 37 degrees Celsius). To establish optimal concentrations of CBD in MCF7 and T47D cells, cytotoxicity of CBD was first established using cytotoxicity assays; neutral red assay and assessment of migration (scratch assay). CBD concentrations tested include 5 µM, 7.5 µM, 10 µM (Shrivastava et al,2011) and an optimal treatment duration including 24 h, 48 h and 72 h, was also tested. Two treatment models were used which included a single-dose model (Model 1), where cells received a once-off treatment during the culture period, and a daily-replacement model (Model 2), where cells received daily treatment over the culture duration. The different CBD concentrations tested were combined with 2 µM Tamoxifen which a=had been previously optimised in our lab (Pather, 2020.; Pather et al., 2019). Briefly, 2 µM Tamoxifen had been selected as the optimal concentration (IC50) following toxicity assays (neutral red assay and the lactate dehydrogenase assay) at a range of concentrations (0.5 µM, 1 µM, 1.5 µM, 2 µM, 2.5 µM) (Pather, 2020). Tamoxifen pre-treatment was included in this study to mimic patient treatment whereby CBD would only later be used to mitigate Tamoxifen-induced side effects, either as a once-off (model 1) or daily (model 2). Following the establishment of optimal treatment conditions for both treatment models, cultures were prepared to assess proliferation (using MTT assay), CPR activity (using cytochrome P450 assay), gene expression (using qPCR) and immunocytochemical localization of autophagy markers (P62, LC3B and BECN1) (Figure 2).

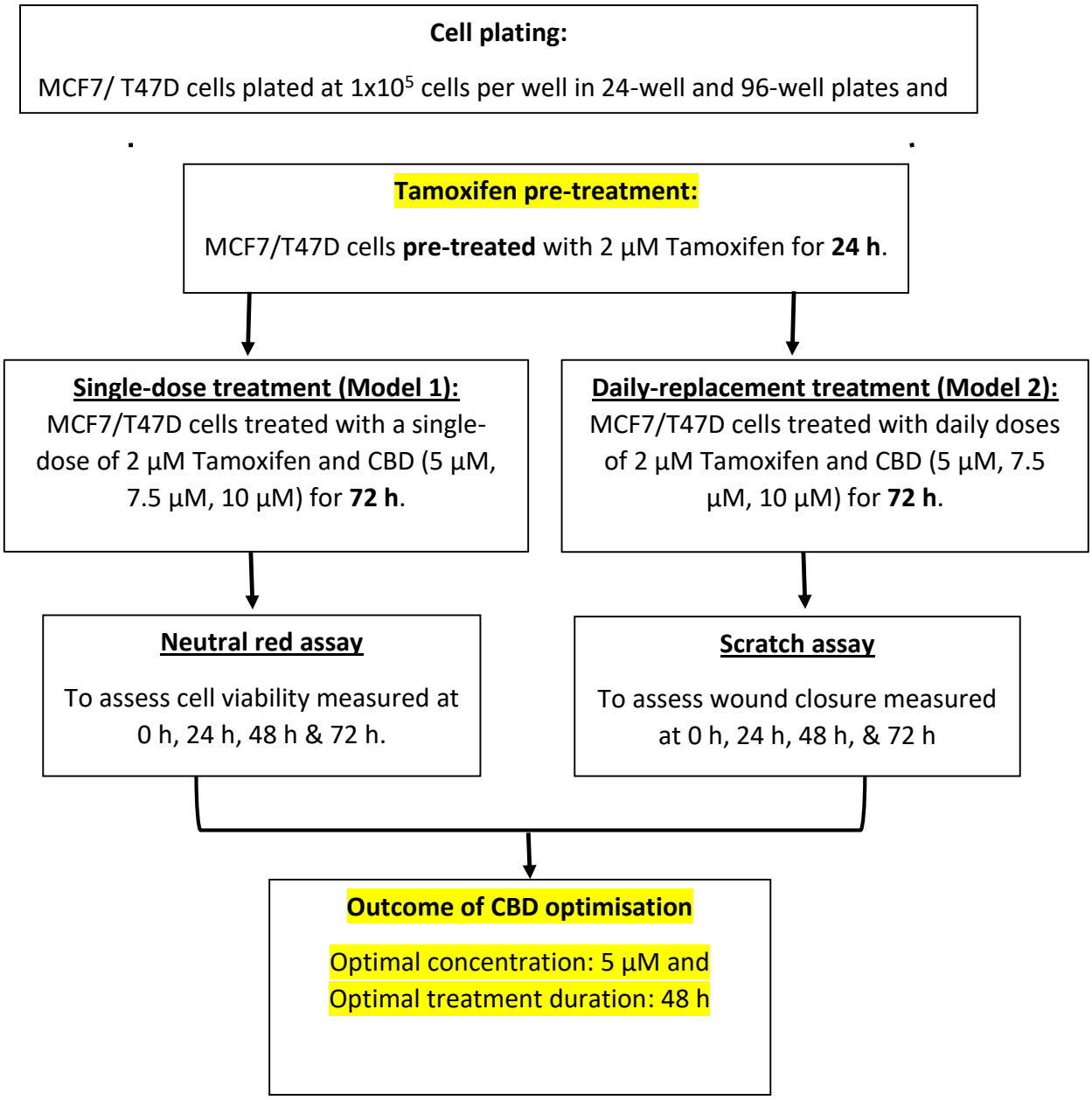


Figure 2: A flow diagram showing a summary model of the methodology used for the optimization of CBD concentrations using neutral red (cytotoxic assay) and a scratch assay (migration), and the determination of the optimal treatment duration. This was conducted on MCF7 cells. Following determination of the optimal CBD concentration and treatment duration on MCF7 cells, T47D cells were assessed for their response using the same neutral red assay and scratch assay.

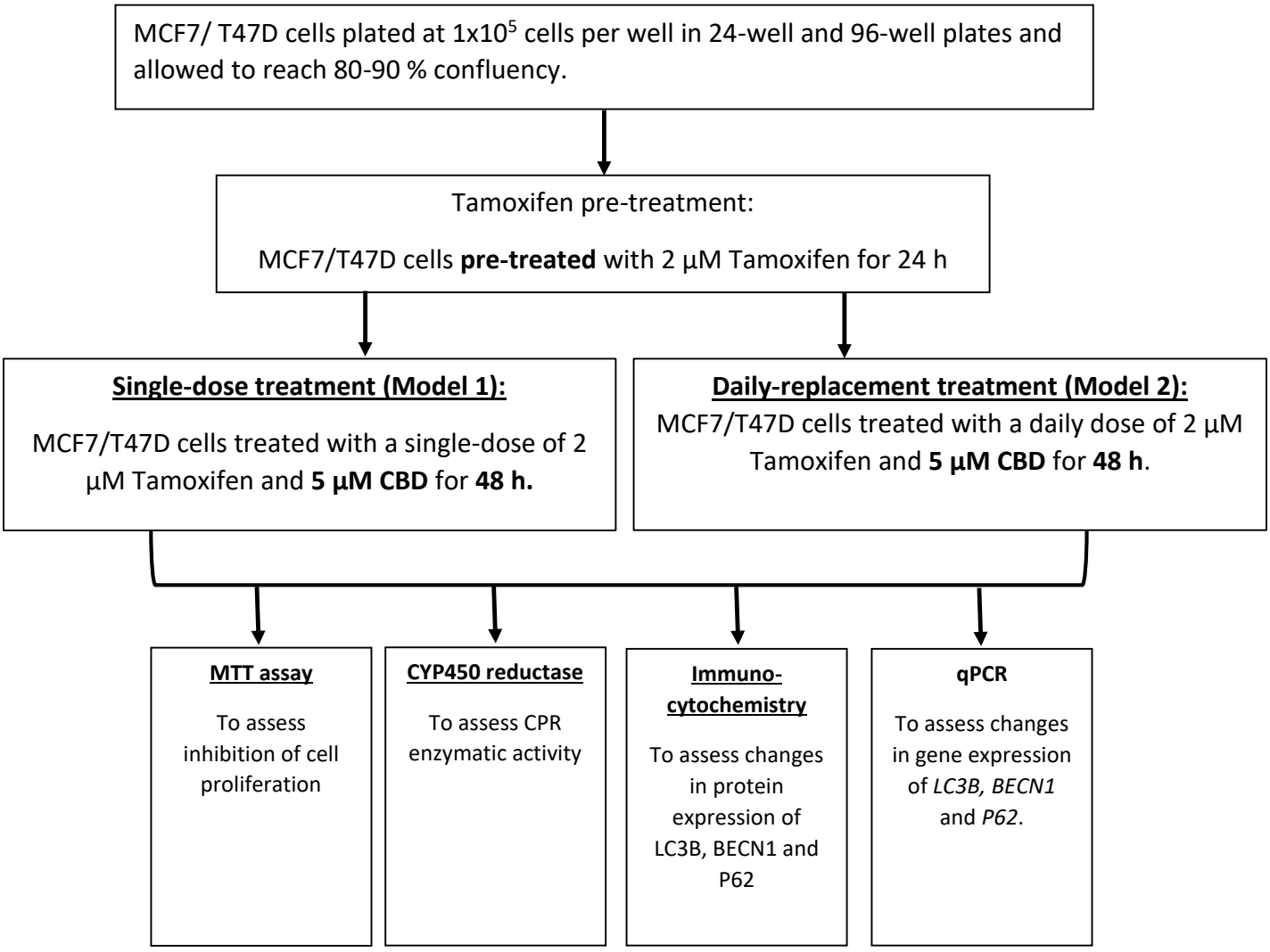


Figure 3: A flow diagram showing a summary model of the methodology used for this study to assess inhibition of cell proliferation, CYP450 reductase enzyme activity; and protein and mRNA levels of *LC3B, P62* and *BECN1*.

2.1. Cell culture

MCF7 breast cancer cells starting at passage number 12 (obtained from Prof Raquel Duarte, University of the Witwatersrand, Department of Internal Medicine) were cultured in Dulbecco's Modified Eagles Medium (DMEM) (Pan Biotech, P04-03590) supplemented with 10% Fetal Bovine Serum (FBS) (Thermo Fisher Scientific, Waltham, USA; 10499044) and 0.1% Penicillin/Streptomycin(P/S) (Lonza, Basel, Switzerland; OMB 206) in T75 (a surface area of 75 cm2) flasks (Greiner bio one, Frickenhausen, Germany, 658170) .T47D cells starting from passage number 26 (donated by Prof Sharon Prince, University of Cape Town) were cultured in Roswell Park Memorial Institute (RPMI) 1640 media (PAN Biotech, Honeydew, South Africa, P04-18500) supplemented with 1.6% human insulin (Sigma-Aldrich, Kempton Park, South Africa, I9278-5ML), 10% FBS and 0.1% P/S in T75 flasks cells were incubated at 37 °C and 5% CO2 in a humidified Heracell CO2 incubator which regulates the pH of the cell culture media (Thermofisher Scientific) until they reached 70 – 90% confluency following which they were used for subculture.

2.2. Subculture of MCF7 and T47D cells

Once the cells reached ~70-90% confluency, they were washed twice with 1X Phosphate buffered saline (PBS) (pH 7.4) (Appendix A). Then 4 ml of 0.25% Trypsin/Ethylenediaminetetraacetic acid (EDTA) (Thermofisher Scientific, 25200072) was added to each T75 culture flask and placed into the incubator at 37 °C and 5% CO_2 for 10 min to allow the cells to detach. The flask was retrieved and 4 ml of appropriate culture media for each cell line was added to neutralize the reaction. The cell suspension was gently transferred to a 15 ml centrifuge tube (Greiner bio one,188261) and centrifuged at 400xg for 5 min using the Rotofix 32 A centrifuge (Labotech). The supernatant was discarded, and the pellet resuspended in 1 ml of appropriate culture media. Ten (10 µl of the cell suspension was transferred into a 1.5 ml microcentrifuge tubes (Thermofisher Scientific,69715) and stained with 10 µl of trypan blue. Using the trypan blue exclusion assay and a TC20 automated cell counter (Bio-Rad), cell viability was determined. MCF7 and T47D cells were either cryopreserved in 10% of cell culture grade Dimethyl sulfoxide (DMSO) (Saarchem, Honeydew, South Africa, 186500), with 60% FBS and 30% of the appropriate cell culture media and stored in

a Glacier -86 °C ultralow temperature freezer (Nuaire); or plated for experimentation.

2.3. Plating cells for experimentation

For experimentation, a minimum of 80% live cells were used (as determined by the TC20 cell counter). 1x105 cells were seeded, in duplicate, into either 24-well plates (Greiner bio one, 662160) or 96 well plates (Greiner bio one,655160) and incubated at 37 °C and 5% CO2 for 5 min to allow the cells to attach. Cells plated for immunocytochemistry were plated onto glass coverslips in 24 well plates. The appropriate culture media was added to obtain a final volume of 200 µl incubated at 37 °C and 5% CO2. MCF7 cells were incubated for 48 h and T47D cells for 72 h to achieve 80-100% confluency.

2.4. Preparation of Tamoxifen and CBD solutions

Both Tamoxifen (Sigma-Aldrich, T5648) and CBD (Sigma-Aldrich,51853) were dissolved in ethanol (Appendix A). Tamoxifen was diluted in 100% ethanol due to its highly lipophilic nature to make up a stock solution of 2500 µM which was diluted to obtain 2 µM Tamoxifen in the appropriate culture media per well (Appendix A). CBD was resuspended in 100% ethanol at a concentration of 3200 µM (Appendix A), and further diluted in complete culture media to achieve the desired concentrations tested (Table 1). A diluent control consisting of 0.8% ethanol in the respective media was prepared. Paclitaxel (Biocom, Centurion, South Africa, AB120143_10), was used as a positive control for apoptosis, and was dissolved in 100% ethanol at a stock concentration of 243 µM and diluted in appropriate media to achieve 0.1 µM paclitaxel concentration which was used to treat cells.

2.5. CBD and Tamoxifen treatments

For optimisation of the appropriate concentration of CBD and duration of treatment (Figure 2), MCF7 cells were plated as stated previously (section 2.3) and pre-treated with 2 µM Tamoxifen, for 24 h at 37 °C, 5% CO_2. Tamoxifen pre-treatment meant that the cells were exposed to 2 µM Tamoxifen only for the first 24 h before treatment with any other drugs or treatment solutions and this was done for subsequent experiments after the establishment of optimal treatment

conditions. This concentration and duration of treatment had been previously established in our lab (Pather *et al.*, 2019). Following the 24 h of pre-treatment with 2 µM Tamoxifen, MCF7 cells were then treated with a range of CBD concentrations: 5 µM, 7.5 µM and 10 µM CBD (Shrivastava *et al.,*2011) using two culture models (Section 2.6). A viability test i.e. the neutral red assay and a migration test.i.e. the scratch assay, were conducted (Section 2.7). 5 µM CBD was found to be the optimal CBD concentration because its cytotoxic effects did not result in complete cell loss thus sufficient cells maintained viability for downstream experiments post 48 h of treatment with CBD (Section 3.1) and was used for further investigations on both MCF7 and T47D cells. Earle's balanced salt solution (EBSS), an isotonic solution comprised of inorganic salts (sodium chloride, potassium chloride, calcium chloride, magnesium sulphate, sodium dihydrogen phosphate, sodium bicarbonate) and a carbohydrate (glucose) was used as the autophagy positive control, inducing starvation (Zhu *et al*, 2017). Paclitaxel at 0.1 µM (a chemotherapy drug) was used as positive control (for apoptotic cell death) for the subsequent experiments (Armat *et al*., 2016; Ofir *et al*., 2002).

2.6. Establishment of treatment models

Two treatment models were explored following pre-treatment with Tamoxifen to investigate the effects of frequency of dual CBD and Tamoxifen administration. In the single-dose treatment model (Model 1) cells were treated with a single-dose of the treatment for the entire treatment duration with no replacement of media. In the daily-replacement treatment model (Model 2), the treatment solution was replaced at 24 h intervals by aspirating the old treatment media (with all its constituents including dead and or non-adherent cells) and replacing it with 200 µl of fresh treatment media for the treatment duration. The single-dose treatment model (Model 1) was used to evaluate the effects of the treatment when taken in a single-dose over a prolonged period (Maximov *et al.*, 2014; Benz *et al.*, 1992). The daily-replacement treatment model (Model 2) was used to evaluate the effects of treatment mimicking a clinical scenario where patients take treatment daily (McCowan *et al*., 2008; Etienne *et al*., 1989 . Cells were treated as shown in Table 1.

Table 1: A table showing controls and experimental samples for Tamoxifen pre-treatment and CBD and Tamoxifen treatment, alongside the abbreviations used in labelling the samples. * Indicates pre-treatment with Tamoxifen for 24 h.

Treatment group	**Description**
Media control (MC)	Cells (MCF7/T47D) in appropriate media
Earle's balanced salt solution (EBSS)	Cells (MCF7/T47D) in EBSS
Paclitaxel (Pac)	Cells (MCF7/T47D) in 0.1 µM Paclitaxel
Diluent control (DC)	Cells (MCF7/T47D) in 0.8% ethanol
2 µM Tamoxifen (Tam)*	Cells (MCF7/T47D) in 2 µM Tamoxifen
5 µM CBD	Cells (MCF7/T47D) in 5 µM CBD
7.5 µM CBD	Cells (MCF7) in 7.5 µM CBD
10 µM CBD	Cells (MCF7) in 10 µM CBD
2 µM TAM + 5 µM CBD*	Cells (MCF7/T47D) in 2 µM Tamoxifen and 5 µM CBD
2 µM TAM + 7.5 µM CBD*	Cells (MCF7/T47D) in 2 µM Tamoxifen and 7.5 µM CBD
2 µM TAM + 10 µM CBD*	Cells (MCF7/T47D) in 2 µM Tamoxifen and 10 µM CBD

2.7. Determining optimal treatment concentration of CBD using the MCF7 cell line

2.7.1. Neutral Red assay

The Neutral red assay measures the uptake of neutral red dye into the lysosomes of viable cells through their plasma membrane (Ates *et al*, 2017; Borenfreud and Puemer, 1985). To determine the cytotoxic effects of CBD following treatment (section 2.5) a neutral red assay was conducted at 24 h, 48 h, and 72 h in both Models on the MCF7 cells. Following treatment, the media was removed from the wells and cells were rinsed three times with 1M PBS (pH 7.4) to remove any residue and improve the purity of the sample for subsequent experiments. Cells were then incubated with 100 µg/ml of neutral red dye (Gurr BDH Chemicals, Poole, England, P34056) in appropriate culture media for 3 h at 37 °C and 5% CO_2. The neutral red medium was removed, and cells were washed with 1M PBS three times. Subsequently, 100 µl of Neutral red desorb solution (1% acetic acid in 50% ethanol) was added to each well and the 24-well plate was placed on a Micromixer Mx2 microplate shaker (FINEPCR) at 400xg for 10 min. The supernatant was then transferred into corresponding wells of a 96-well plate and absorbance levels were measured at 560 nm on a Glomax Promega microplate reader at room temperature (RT) (School of Anatomical Sciences, Wits University). Serum-free media was used as a technical control.

Data analysis

Data was managed in Microsoft Excel and descriptive statistics were calculated. Absorbance was corrected by subtracting the absorbance of the serum free medium from all values and used to draw IC50 graphs. The corrected average absorbance values for each group were used to calculate cell viability as follows (Ates et al., 2017):

$$Viability(\%) = \frac{corrected\ absorbance\ of\ sample}{corrected\ absorbance\ of\ media\ control} \times 100.$$

2.7.2. Scratch assay

To conduct this assay as a measure of migratory capacity, cells were seeded in 96-well plates, as previously described (section 2.3). 96-well plates were selected over 24-well plates following optimisation, because cells became confluent at a shorter period in 96 wells and the entire area of the 96 well could be imaged (Appendix C). When cells had reached 90-100% confluence in each well (48 h for MCF7 cells), media was removed, and cells were washed in PBS. Thereafter a 'scratch' was created using a p10 pipette tip (a pipette tip used for volumes from 0.1-10 µl) (Figure 4). Cells were rinsed once in 1X PBS to remove detached cells. To administer pre-treatment with Tamoxifen, 200 µl of 2 µM Tamoxifen was added to each well and images were taken immediately (day 0) using a 10X objective on the Olympus 1.5X inverted microscope (School of Anatomical Sciences, University of the Witwatersrand). Thereafter, cells were incubated at 37 °C and 5% CO2 for 24 h. Cell treatment was administered according to the treatment strategy for each model (section 2.5 and 2.6). Assessment of wound closure was conducted by imaging the scratch area at 0 h then subsequently at 24-hour intervals: 24 h, 48 h, 72 h, and 96 h.

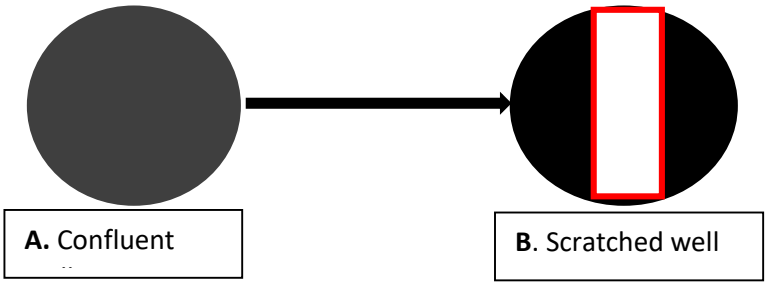


Figure 4: A schematic diagram showing a confluent well before the creation of the scratch (A) and B shows a well with an exposed area which is the area of the scratch (white) after the scratch was created as well as the region that was measured in ImageJ (red).

Data analysis

The Olympus iX51 microscope c-mount camera and CellSens software (Olympus) were used to capture images. Photomicrographs were imported into ImageJ software V1.8 (Preziosi, 2013) and the total surface area of the scratch was outlined manually on the ImageJ software. This was measured across the different time points.

The formula for calculating percentage wound closure $(\text{Yue } et\ al., 2010)$ was used to calculate the % closure of the scratched surface as follows:

$$\textit{Wound closure}(\%) = [(ave\ Area_{0hrs} - ave\ Area_{t})/ave\ Area_{0hrs}] \times 100$$

2.7.3. Optimal CBD concentration and duration of treatment

It was determined that 5 µM is the optimal CBD concentration (presented in Results Section 3.1.3). Further assays were conducted using only 5 µM CBD for a duration of 48 h in both culture models. Controls included the diluent control (0.8% ethanol medium), 0.1 µM Paclitaxel as a positive control for apoptosis and 1X EBSS (Appendix A) as a positive control for starvation induced autophagy**.**

Table 2. Optimised treatment protocol for MCF7 and T47D cellsTable 2: Optimised treatment protocol for MCF7 and T47D cells

	Duration	**Treatment**
Cell adherence	48h (MCF7) 72h (T47D)	Complete culture media for each (as stated in section 2.1)
Pre-treatment	24h	2 µM Tamoxifen
Combined Treatment	48h	5 µM CBD and 2 µM Tamoxifen (as follows); -Single dose (Model 1) -Daily-replacement (Model 2)

2.8. Assessing the effects of optimal CBD concentration and duration of treatment on cell viability and cell migration in T47D breast cancer cells

2.8.1. T47D Neutral red and Scratch assay at optimal CDB concentration

T47D cells were plated as per Section 2.3 and incubated for 72 h to reach confluency, due to their longer doubling time they required a longer period to reach the required confluency (90-100%) for further experimentation. Similarly, T47D cells were first pre-treated with 2 µM Tamoxifen for 24 h in both treatment models. This was followed by treatment with 5 µM CBD and 2 µM Tamoxifen for 48 h in both models (Table 2). The neutral red assay and scratch assay were conducted as previously described; section 2.7.1 and 2.7.2, respectively.

2.9. Assessing the effects of optimal CBD concentration and Tamoxifen treatment in MCF7 and T47D breast cancer cells over 48h

To investigate the inhibition of cell proliferation due to combined CBD and Tamoxifen treatment, the Roche 3-(4,5-Dimethylthiazol-2-yl)-2,5 diphenyltetrazolium bromide (MTT) proliferation assay kit was used (Roche, Midrand, 11465007001). MCF7 and T47D breast cancer cells treated according to Table 2 were retrieved from the incubator. 10 µl of MTT labelling agent was added to each well in the last four hours of the 48 h treatment period (at 44 h) and the 24-well plates were incubated at 37 °C and 5% CO_2. At the conclusion of the 48h treatment period, the MTT reagent was aspirated and 100 µl of MTT at 5mg/ml solubilizing agent (10% Sodium dodecyl sulphate in 0.01 M hydrochloric acid) was added to each well. The plates were incubated overnight at 37 °C and 5% CO_2. Following overnight incubation, the plates were retrieved from the incubator, and the solution was transferred to corresponding wells on a 96 well plate and absorbance was measured at optical density (OD)= 560 nm using the Promega Glomax explorer microplate reader. The following controls were included; high control (1% Triton-X-100) (Sigma Aldrich, X100) which permeabilizes cell membranes, serum free media control, complete media control and the diluent control (0.8% ethanol).

Data analysis

The duplicate readings for each sample were averaged and the culture medium background value (complete media only) was subtracted from the assay readings to find the corrected absorbance. Inhibition of proliferation was calculated using the equation (Ding *et al*., 2009).

$$inhibition\ of\ cell\ proliferation\ (absorbance\ ratio) = \frac{Corrected\ Mean\ OD560\ of\ treated\ cells\ (\ sample - control)}{corrected\ mean\ OD560\ of\ media\ control}.$$

2.10. Effects of CBD and Tamoxifen on *CYP450 reductase* (CPR) activity

2.10.1. CYP450 reductase (CPR) activity Assay

Following single-dose treatment (Model 1) and the daily-replacement treatment (Model 2) over 48 h in 200 µl of relevant treatment medium in 96-well plates, cytochrome P450 reductase activity (CPR) was assessed using the cytochrome P450 reductase activity assay kit (Abcam, ab204704, Biocom Africa, Pretoria) in both MCF7 and T47D cells by making use of manufacturer's methodology. Although the majority of drug metabolism occurs in the liver, CYP enzymes are present in breast cancers and there has been evidence of Intratumoural-mediated metabolism of a selection of drugs is showing to be of consequence (Luo et al., 2021; Sneha et al., 2021). Cytochrome P450 reductase activity assay measures the oxidation of NADPH by cytochrome P450 reductase (CPR) to the reduction of a colourless probe into a brightly coloured product with an absorbance at OD=460 nm. The absorbance measured by the rate of colour generation is directly proportional to CPR activity. The investigation of CYP reductase activity of importance to better understand the effects of Intratumoural-mediated metabolism of tamoxifen and CBD in breast cancer cells.

The following kit reagents: CPR buffer, G6P standard, NADPH substrate mix, G6P standard developer, and Human CPR positive control, were brought to room temperature (25 °C) 1 hour before the start of the assay procedure to thaw, whereas 10mM diphenyleneodium chloride was

thawed in the incubator at 37 °C and 5% CO2. Reagents were then resuspended or diluted in CPR buffer as shown in Appendix D, Table B1. This assay was used to assess whether CBD and Tamoxifen increase the activity of the CYP450 reductase which is essential for CYP450 enzyme activity.

Development of a standard curve

Following reagent preparation, the standard solutions were prepared as per manufacturer's instructions. All standards were assayed in duplicate, in a 96-well plate (Greiner Bio-one, 655160). To each of the standard wells containing 90 µl of standard solution, 5 µl of NADPH substrate mix and 5 µl of Glucose-6-phosphate (G6P) standard developer were added and mixed gently by pipetting up and down. The 96-well plate was covered in foil and the standard wells were incubated in the dark at RT for 30 min. Following the incubation period, the standard wells were measured at OD= 460nm at RT on the Promega Glomax explorer microplate reader. A standard curve was prepared on excel (Appendix D, Figure B1).

Sample preparation

Once the standard wells were measured, experimental samples were prepared. Following treatment over 48 h (section 2.7.3) in 200 µl of relevant treatment, samples from the single-dose treatment model (Model 1) and the daily-replacement treatment model (Model 2) were retrieved from the incubator. The media was aspirated, and the cells were washed three times in 1X PBS (pH 7.4) at RT followed by two washes in cold 1X PBS (pH 7.4). Cells were additionally lysed using 500 µl of 1% Triton-X-100 in CPR buffer and placed in the incubator at 37 °C and 5% CO2 for 10 min. Cell scrapers (Greiner Bio-one, PGRE541070) were used to mechanically lift cells that remained adherent after the incubation period. Cells were then homogenized using a 20 - gauge needle and syringe by gently drawing and releasing the sample, sample was passed 10 times to ensure that a homogeneous mixture was obtained. The samples were then transferred into 1.5 ml microcentrifuge tubes (Thermofisher Scientific,69715) which were pre-chilled in the fridge overnight at (~4-8 °C) and incubated on ice for 5 min. Samples were centrifuged at 1,500 rpm for 5 min in a microcentrifuge (Eppendorf minispin, School of Anatomical Sciences,

University of the Witwatersrand) placed in a cold room at 4 °C. The supernatants were transferred to a second set of pre-chilled 1.5 ml microcentrifuge tubes and centrifuged at 12, 000 rpm for 5 min at 4 °C in a microcentrifuge. The supernatant was collected and transferred to a third set of 1.5 ml microcentrifuge tubes and stored on ice.

CYP450 reductase activity

Sample wells were prepared in duplicate alongside negative control wells (samples containing inhibitor) Table 3. Positive control wells and background control wells were prepared as outlined in Table 3 (also shown in the plate layout in Appendix D, Figure B2). 30 µl of the reaction mix (Appendix D, Table B2) was added to each well of a 96-well plate containing 50 µl of sample and incubated for 5 min at RT to allow the inhibitor [1 mM Diphenyleneodium chloride was used to inhibit the intracellular NADPH oxidase [1mM Diphenyleneodium chloride (Piszczatowska *et al*., 2020)] to bind.

Table 3: Showing the constituents of sample wells and control wells for CPR activity assay

Sample group	**Contents of the well (µl)**
Sample wells	50 µl sample + 20 µl CPR buffer
Negative control wells	40 µl sample + 10 µl Inhibitor + 10 µl CPR buffer
Positive control wells	5 µl Human CPR positive control + 55 µl CPR buffer
Background control	40 µl sample + 2 µl Inhibitor + 28 µl CPR buffer

A 20 mM G6P solution was prepared (Appendix D, Table B1) and 10 µl of the 20 mM G6P solution was added to each of the experimental wells, inhibitor wells and positive control wells.

Absorbance was measured at OD 460 nm at 0 min, 15 min, and 30 min at 25 °C on the Promega Glomax explorer microplate reader.

Data analysis

The readings for duplicates of the standards and samples were averaged. To get the corrected absorbance: mean absorbance value of the blank was subtracted from all standard and sample readings. The corrected absorbance of samples with inhibitor were subtracted from that of the same treatment group without inhibitor to yield specific CPR activity which was plotted against time and a standard curve (Appendix D, Figure B1) was drawn from which unknown G6P concentrations of samples were determined. The CYP450 reductase activity was calculated using the equation (as indicated in the product sheet).

$$CYPR\ activity\left(\frac{nmol\ /min}{mg}\right) = \frac{[G6P\ (nmol)]}{(T_2 - T_1\ (min)) \times (amount\ of\ initial\ sample\ added\ (mg))}$$

$$Specific\ CYPR\ activity\left(\frac{nmol\ /min}{mg}\right) = CYPR\ activity(\ inhibitor)\left(\frac{nmol\ /min}{mg}\right) - CYPR\ activity(no\ inhibitor)\left(\frac{nmol\ /min}{mg}\right)$$

2.11. Effects of CBD and Tamoxifen treatment on protein and mRNA levels *of LC3B, P62* and *BECN1* in MCF7 and T47D breast cancer cells

The protein levels were investigated using immunocytochemical localization of LC3B, P62 and BECN1 while the mRNA expression levels were investigated using qPCR.

2.11.1. Immunofluorescence

For this section, cells were plated at $1X10^5$ cells on glass coverslips (Lasec, Midrand, South Africa) in 24 well plates. MCF7 and T47D cells in both the single-dose treatment model (Model 1) and the daily-replacement treatment model (Model 2) were treated as previously described (section

2.7.3, Table 2). Samples were washed with 1X PBS (pH 7.4) three times. Cells were fixed in 500 µl 4 % paraformaldehyde (PFA) for 10 min at RT, rinsed three times with 200 µl ice cold 0.1 % Tween-20/PBS for 5 min per wash. Cells were then incubated with 500 µl 0.2 % Triton-X-100 for 10 min at RT. Following this incubation, cells were washed three times with 200 µl ice cold 0.1% Tween-20/PBS for 5 min per wash. 500 µl of 1% Bovine serum albumin (BSA) in 0.1% Tween-20/PBS was added to each well and incubated for 30 min at RT. Primary antibodies in 0.1% Tween-20/PBS; mouse monoclonal anti-LC3B (1:1000)(Abcam, ab243506), rabbit monoclonal anti-SQSTM1/p62 (1:1000)(Abcam, ab240635) and rabbit polyclonal anti-BECN1(1:1000)(Abcam, ab217179), were optimized by titration where a range of antibody concentrations were diluted and used to stain treated cells as shown in Appendix E, section 1 and cells were incubated with 50 µl of optimal primary antibody concentration (as determined by titration), overnight at 4 °C.

Following overnight incubation with primary antibodies, the solution was aspirated, and cells were washed three times with 200 µl of ice cold 0.1% Tween-20/PBS for 5 min per wash. Thereafter the solution was aspirated, and cells were rinsed and incubated in the dark at RT for 2 h with secondary fluorochrome-conjugated secondary antibodies; goat anti-mouse IgG Alexa Fluor 594 (1:1000)(Abcam, ab150116) for anti-LC3B, goat anti-rabbit (Alexa Fluor 488) (1:1000) (Abcam, ab150077) for anti-P62 and goat anti-rabbit IgG (Alexa Fluor 647) (1:1000) (Abcam, Ab175471) for anti-BECN1 in the determined optimal volumes (Appendix E, section 2). Cells were rinsed three times with 200 µl of ice cold 0.1% Tween-20/PBS for 5 min per wash, and incubated in 50 µl of 4’,6-damidino-2-phenylindole (DAPI) for 5 min to stain nuclei. Cells were then rinsed two times with 200 µl of ice cold 0.1% Tween-20/PBS for 5 min per wash, the solution was aspirated after the last wash and cells were left in 1 ml of 1 M PBS (pH 7.4). Negative controls for both primary and secondary antibodies were prepared using untreated cells with no exogenous inducer of apoptosis or autophagy. The positive control included cells treated with 1X EBSS which induces autophagy markers (Zhu *et al*., 2017) and 0 .1 µM paclitaxel which induces apoptosis markers (Saunders *et al*., 1997).

Coverslips were mounted onto slides using Fluoromount (Sigma Aldrich) and viewed using the Zeiss Laser Scanning Confocal Microscope 780 Life Science Imaging Facility, University of the

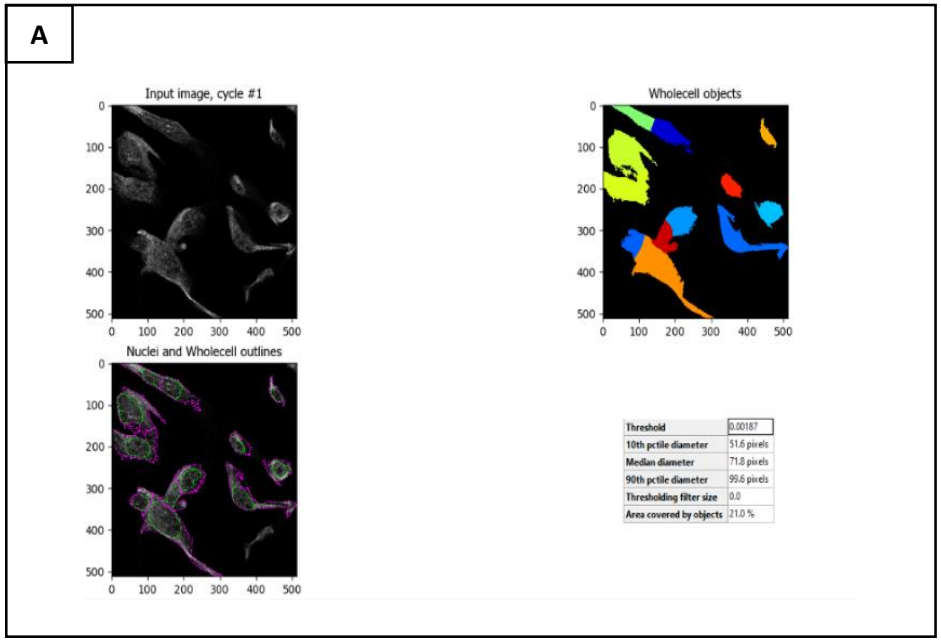
Witwatersrand). Images were taken using the Zeiss software and analysed with CellProfiler V.2.0 software (Kamentsky *et al*., 2011).

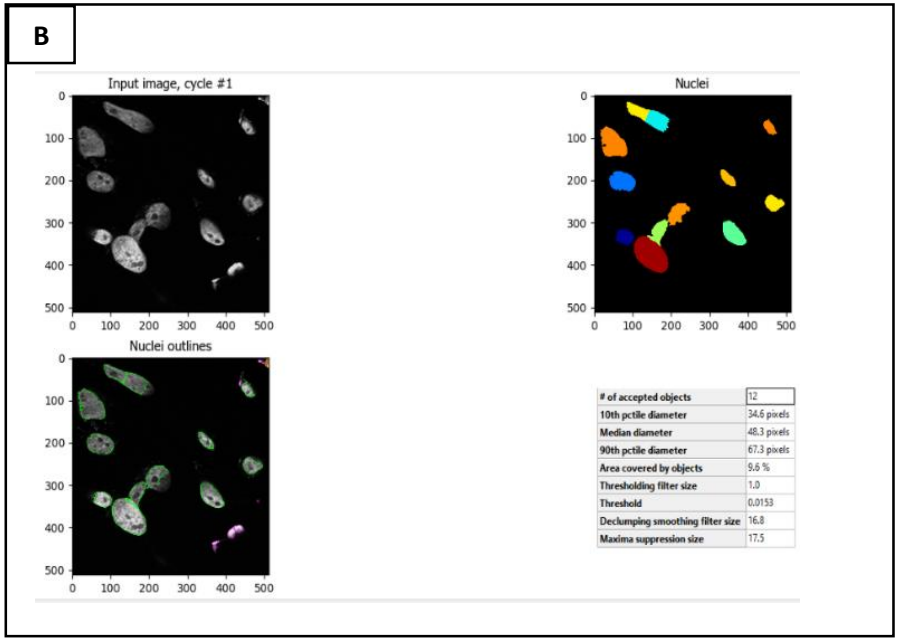
CellProfiler

A pipeline was created in CellProfiler for all the markers of interest; LC3B, P62 and BECN1. The metadata module was used to extract data about the images from image file headers and the "Names and types" module to input the names of the specific names of the objects to be identified. The "identify primary objects" module identified differences in pixels and the nuclei was identified as the high-intensity pixel objects. The size range of the nuclei identified was 25-100 pixels in diameter (Figure 5 A). Pixels outside the set range and those lying on boundaries were not considered. A global thresholding method was used and to distinguish clumped objects, the Otsu two classes strategy which measures the threshold separating two classes of pixels by reducing the variance within each class was used with a correction factor set at 1.

Clumped objects were distinguished by shape and the lines separating clumped objects were outlined by Propagate. The "identify secondary objects" module identified cells stained with fluorochrome bound antibodies (AF594 FOR LC3B, AF488 for P62 and AF647 for BECN1) where the proteins were expressed within the cytoplasm (Figure 5 B). The expression of the proteins was identified by "Propagation" using the "global" thresholding strategy and "minimum gross entropy" as the thresholding method with a correction factor indicated at 0.8. The lower bound was set at 0 and the upper bound at 1. Holes in the identified objects were filled and secondary objects touching the border were not discarded since the proteins of interest can be found even in the perinuclei border. Both the nuclei and the cytoplasm of the cells were identified using the "identify tertiary objects" module and smaller objects were shrunk prior to subtraction (Figure 5C). The intensity of LC3B, P62 and BECN1 was measured using the "measure object intensity" module and the "measure object size shape" module was used to measure the size and shape of the cells. The resulting integrated images from the "identify primary object" and the "identify secondary object" modules were saved using the "save images" module. All the data was

acquired from the “measure object intensity” and “measure object size shape” modules was exported into an excel spreadsheet using the “export to spreadsheet” module.





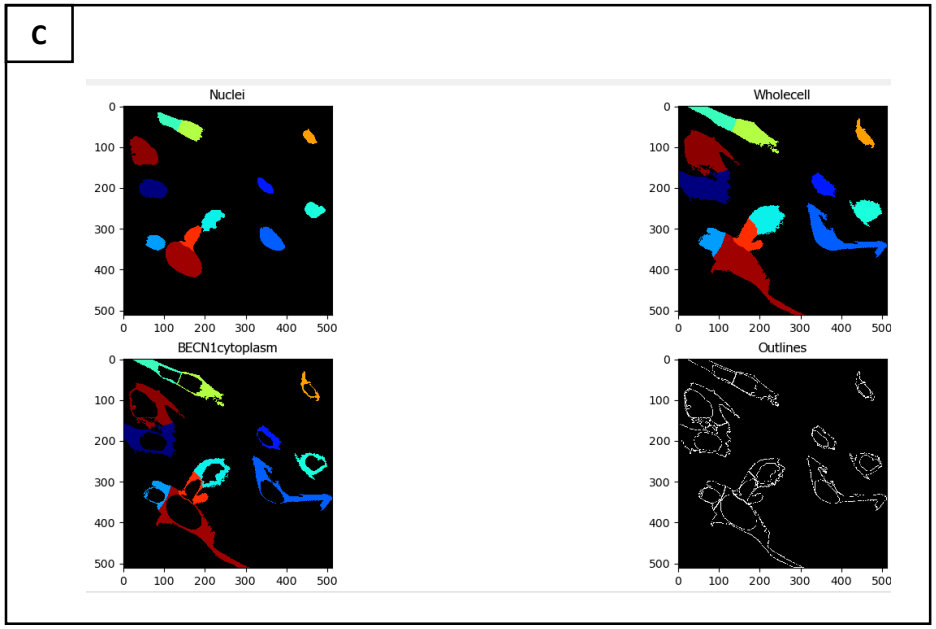


Figure 5: A representative diagram of cellprofiler output images to show the pipeline. A: nuclei of 20-15 pixels within the cell identified using the " identifyprimaryobjects module", b: becn1 expression within the cell cytoplasm, identified using the " identifysecondaryobject module" and c: whole cell showing the cell nuclei and cytoplasm together as determined using the "identifytertiaryobjects module.

Data analysis

Images were loaded into Cellprofiler, and the fluorescence of LC3B and BECN1 was quantified as mean fluorescence intensity. The values were exported into excel and used to plot graphs.

2.11.2. Determination of mRNA expression of genes involved in drug metabolism and autophagy

MCF7 and T47D cells, in the single-dose treatment model (Model 1) and the daily-replacement model (Model 2), were established and treated for 48 h (Section 2.7.3, Table 2)

RNA extraction

MCF7 cell samples underwent RNA extraction using the RNeasy kit (Qiagen, 74104), as per manufacturer's recommendation. Following treatment as outlined in section 2.7.3, Table 2, cells were washed three times in 1X PBS (pH 7.4). The PBS was aspirated, and cells were lysed with 350 µl of RNA lysis buffer (RLT) containing β-mercaptoethanol and homogenized using a 22-gauge needle with a 1 ml syringe. Following homogenisation, for MCF7 cells, two wells were pooled and for T47D four wells were pooled (due to low cell densities).

The 350 µl cell lysate was transferred to 1.5 ml microcentrifuge tubes to which 350 µl of 70% ethanol was added and gently mixed by pipetting and all samples were placed on ice to prevent denaturation of RNases in subsequent steps. The mixture was transferred to the corresponding RNeasy spin columns placed in 2 ml collection tubes and centrifuged (Eppendorf Minispin centrifuge) at 11,000 rpm for 30 sec. The flow through was discarded and on-column digestion was conducted as follows; 350 µl of RNA wash buffer (RW1) was added to each of the spin columns and they were centrifuged (Eppendorf Minispin centrifuge at 11,000 rpm) for 15 sec. The flow-through was discarded and DNase I incubation mixture was prepared to a final volume of 80 µl per sample by adding 10 µl of DNase I with 70 µl of Rnase-free DNase digestion buffer (RDD). The samples were incubated with the DNase I incubation mixture for 15 min at RT. Thereafter, 350 µl of RW1 was added to each of the Rneasy spin column and the samples were centrifuged (Eppendorf Minispin centrifuge) at 11,000 rpm for 15 sec, the flow through was discarded.

Foll owing on column digestion, 500 µl of the second RNA wash buffer RPE with ethanol was added to the samples and centrifuged (Eppendorf Minispin centrifuge) for 15 sec at 11, 000 rpm and the flow through was discarded. A second wash with 500 µl RPE buffer was performed, and samples were centrifuged (Eppendorf Minispin centrifuge) for 2 min at 11, 000 rpm. The flow through was discarded along with the collection tubes and the RNeasy spin columns were placed in new collection tubes and centrifuged (Eppendorf Minispin centrifuge) for 1 min at maximum speed (13, 400 rpm). The flow through was discarded and the spin columns were placed in new 1.5 ml collection tubes. 30 µl of RNAse free water was added to the spin columns and centrifuged (Eppendorf Minispin centrifuge) at 11, 000 rpm for 1 min to elute the RNA. To increase the RNA, yield the latter step was repeated and RNA was stored at -80 °C (Nuaire).

T47D cell samples underwent RNA extraction using the Agilent Absolutely RNA Miniprep kit (cat no. 400800), as per the manufacturer's recommendations. T47D cells treated as outlined in section 2.7.3, Table 2, were washed three times in 1X PBS (pH 7.4). The PBS was aspirated, and cells were lysed with 200 µl of RNA RLT buffer containing β-mercaptoethanol and mixed by repeated pipetting. The cell lysate was transferred to a 1.5 ml microcentrifuge tube and homogenized by vortexing the tube for 5 sec. 200 µl of 70% ethanol were added to the homogenized lysate and the tube was vortexed for another 5 sec. The 400 µl homogenized cell lysate was transferred into an RNA binding spin cup placed in a 2 ml receptable tube, the lid of the tube was closed tightly, and the sample was centrifuged at maximum speed (13, 400 rpm) for 30 sec. The flow through was discarded and the collection tube was placed under the spin column.

For on column DNase digestion, 600 µl of 1X Low-salt wash buffer was added to the spin column and the cap of the receptacle tube was snapped onto the spin cup. The mixture was centrifuged at maximum speed (13, 400 rpm) for 30 sec. The flow through was discarded and the spin cup and receptacle tube were retained, then they were spun at maximum speed (13, 400 rpm) for 2 min. 5 µl DNase I stock solution was added to 50 µl of DNAse digestion buffer and mixed by gentle inverting. The tube was centrifuged for 30 sec to collect residual liquid from the sides of the tube. 55 µl of DNase I incubation mix was added to the RNA spin cup and incubated at 37 ˚C for 15 min

in an incubator. Following this incubation, 600 µl of the 1X High-salt wash buffer was added to the spin cup and the mixture was centrifuge at maximum speed (13,400 rpm) for 30 sec. The flow through was discarded, the spin cup and the receptacle tube were retained. 600 µl of Low-salt wash buffer was added to the RNA spin cup to remove any contaminating agents; it was capped and centrifuged at maximum speed (13, 400 rpm) for 30 sec. The flow through was discarded, the spin cup in the receptacle tube was retained. The second wash was performed by adding 300 µl of Low-salt wash buffer to the RNA spin and centrifuging at maximum speed (13, 400 rpm) for 2 min.

To elute the RNA, the spin cup was transferred from the receptacle tube to a new 1.5 ml centrifuge tube. 30 µl of elution buffer was added to the spin columns, which were then incubated at RT for 2 min and then centrifuged at maximum speed (13, 400 rpm) for 1 min to elute the RNA. To increase the RNA yield, the latter step was repeated, and RNA was stored at -80 °C (Nuaire).

To quantify the RNA concentration and measure the purity for both MCF7 and T47D samples, the Nanodrop2000 (Thermoscientific, South Africa) was used and RNA with a 260/280 ratio of above 2 was considered pure (Appendix F, Table D1).

cDNA synthesis

The High-Capacity Reverse transcription kit (Thermofisher scientific,4368814) was used for cDNA synthesis. The cDNA master mix containing the following was prepared and added to each well; 1 µl of 10X RT buffer; 0.4 µl of 25X dNTP mix; 1 µl of 10X RT random primers, 2.1 µl of nuclease-free water and 0.5 µl of Multiscribe Reverse Transcriptase. Then, 5 µl of RNA (diluted to 20ng/µl) was added to appropriate tube containing 5 µl of master mix (Appendix F, Table 5) the tubes were centrifuged at 11, 000 rpm for 30 sec. Samples were then placed in the SimpliAmp thermal cycler (Thermofisher scientific), and cDNA was synthesized under the following conditions: 25 °C for 10 min; 37 °C for 120 min and 85 °C for 5 sec, then cDNA samples were stored at -20 °C (Defy).

Primer design

Sequence specific primers for *LC3B,BECN1* , and *P62* genes were designed in Eurofins Genomics software (www.eurofinsgenomics.eu), checked and validated using IDT (https://eu.idtdna.com/pages/tools/primerquet) and NCBI Primer-BLAST (https://www.ncib.nlm.nih.gov/tools/primer-blast/).

The following genes of interest and reference genes were used (Table 4).

Table 4: The reference genes and genes of interest that were investigated in this study and their accession numbers

Reference genes	**Primers**	**Accession Number**
ACTB3	F: GGCCGAGGACTTTGATTGCAC R: TTAGGATGGCAAGGGACTTCCTGT	NM_001101.3
RPLO	F: TGCAGCTGATCAAGACTGGAGACA R: TCCAGGAAGCGAGAATGCAGAGTT	BC001834.2
GAPDH	F: TGCACCACCAACTGCTTAGC R: GGCATGGACTGTGGTCATGAG	NM_002046.5
Genes of interest		
LC3B	F: GCAGCATCCAACCAAAATCC R: TGTGTCCGTTCACCAACAG	NM_022818.5
Beclin 1	F: GGCAAGATTGAAGACAGGAG R: TGAGGACACCCAAGCAAGAC	NM_003766.5
P62	F: TGAAGGGAGCATACAGAGAG R: TGGAATAAGGTGGGGAGAAG	NM_00655.3

qPCR reaction

Gene expression levels were determined using the SYBR green master mix (Applied Biosystems, 4309155) and samples were run at a final reaction volume of 10 µl consisting of; 0.2 µl forward primer, 0.2 µl reverse primer, 0.6 µl of RNAse-free water, 5 µl of SYBR Green Mastermix and 4 µl

of cDNA (2ng/reaction). qPCR was conducted with an Applied Biosystems QuantStudio1 PCR thermocycler (Thermofisher Scientific). Gene amplification was performed for 40 cycles under the following cycling condition: Holding stage at 95 °C for 10 min, cycling stage at 95 °C for 30 sec and 60 °C for 1 min to get data, melting curve at 95 °C for 30 sec and 60 °C for 1 min followed by 30 sec at 95 °C to get data. Data analysis was performed in accordance with the minimum information for publication of quantitative Real-Time PCR experiments (MIQE) guidelines.

Data analysis

The fold change in gene expression was calculated as outlined in (Hellemans *et al.,* 2007). First an average of the biological repeats was obtained, then the following formulae was applied to obtain fold change in gene expression:

$$Geometric\ mean\ of\ ref\ genes = \sqrt{(Ave\ Ref\ gene\ 1)(Ave\ Ref\ gene\ 2)(Ave\ Ref\ gene\ 3)}$$

$$\Delta Cq = Cq(Gene\ of\ interest) - AveCq(Geometric\ mean\ of\ ref\ genes)$$

$$\Delta Cq\ expression = (-\Delta Cq)^2$$

$$\Delta\Delta Cq = \Delta Cq(gene\ of\ interest) - \Delta Cq(Control)$$

$$Fold\ change = (-\Delta\Delta Cq)^2$$

Statistical analysis

All data from each study was exported into Microsoft excel for data management and exported into Statistica v14.0 for further analysis. A Shapiro-Wilk test for normality (Appendix B) indicated abnormal distribution of the data. Since the sample size is small non-parametric tests were used for further analysis. A Kruskal Wallis by Ranks Anova and post hoc test was used to determine how cells are altered in response to the different treatment groups. A Friedman test and Friedman's post hoc analysis were used to determine any significant differences in treatment across cell lines within each model; it was further used to determine any significant differences in treatment across the treatment models per cell line.

3.Results

3.1. Determining optimal CBD concentration and treatment duration using MCF7 cell line

3.1.1. Cell viability – the Neutral red assay in MCF7 cells

The media control is embedded in the calculation of the percentage cell viability and therefore it was not presented in the graphs, samples were compared with the diluent control and to each other. These findings indicated high neutral red uptake in the diluent control reflecting high percentage cell viability (greater than 80% viability) across both treatment models (Figure 7). This reflects the minimal effects of 0.8% ethanol diluent on cell viability. Notably, in the single-dose treatment model (model 1) (Figure 7 A) whereby cells were treated with a single-dose of 2 µM Tamoxifen, there was an increase in viability (not significant, $p>0.05$) from 84.2% at 24 h to 98.1% at 72 h, indicating cell recovery. This contrasted with the daily-replacement model (model 2), in which 2 µM Tamoxifen was replaced daily, resulting in a significant ($p<0.05$) decrease in cell viability at 72 h compared with 48 h and 24 h, showing that cells were unable to recover (Figure 7 B).

Cell viability: The effects of CBD

Assessing single treatments of CBD at 5 µM, 7.5 µM and 10 µM, a similar trend in cell viability across time (24 h-72 h) for these different concentrations was observed. In the single-dose treatment model (model 1) (Figure 7 A), there was lower cell viability from 24-48 h, but it was noted that from 48 h, cell viability increased. This may imply cell recovery due to decreased drug sensitivity in comparison to the daily-replacement treatment model (model 2) where cells die due to daily treatment which increases drug availability and consequently cytotoxicity. Cell viability decreased from 48 h through to 72 h (Figure 7 B, D). These results suggest that higher CBD concentrations (7.5 µM and 10 µM) when administered daily (model 2) for a period of 48 h and more, can reduce cell viability but when administered in a single-dose (model 1) over the same duration are less effective at reducing cell viability.

The results showed that a lower CBD concentration (5 µM CBD) is more effective at reducing cell viability in the single-dose treatment model (model 1) than in the daily-replacement treatment model (model 2) compared with the higher CBD concentrations (7.5 µM and 10 µM) in both treatment models, although no significant differences were identified ($p>0.05$). Similarly, CBD at all tested concentrations showed no significant effect on cell viability when compared with the diluent control, or the 2 µM Tamoxifen, in the single-dose treatment model (model 1) across all time points. A similar outcome was found within the daily-replacement model (model 2); however, percent cell viability with 2 µM Tamoxifen at 72 h was significantly higher ($p<0.05$) compared with percentage cell viability at 0 h.

The IC50 concentrations of CBD in single-dose and daily-replacement treatment models

The half maximum inhibitory concentration (IC50) was calculated using GraphPad prism (version 10.2.0) to measure the potency of CBD in inhibiting cell viability of MFC7 cells by fifty percent. Results from the neutral red assay were obtained at 24, 48 and 72 h after exposure to varying CBD concentrations (5 µM, 7.5 µM and 10 µM) and used to calculate cell viability which was then used to determine IC50 values of CBD at the different time points. The results obtained indicate low IC50 values in model 1 compared with model 2 at matched time points, thus indicating that that CBD has a high potency even at lower concentrations in model 1. In both models the IC50 values obtained across all time points were below 5 µM (the lowest tested CBD concentration) (Figure 6), thus indicating high potency of CBD even at the lowest concentration. Data obtained at 48h gave a good fit with an R-squared value of 1 compared with data obtained at 24 h and 72 h, thus indicating that at this time point the regression predictions fit the data.

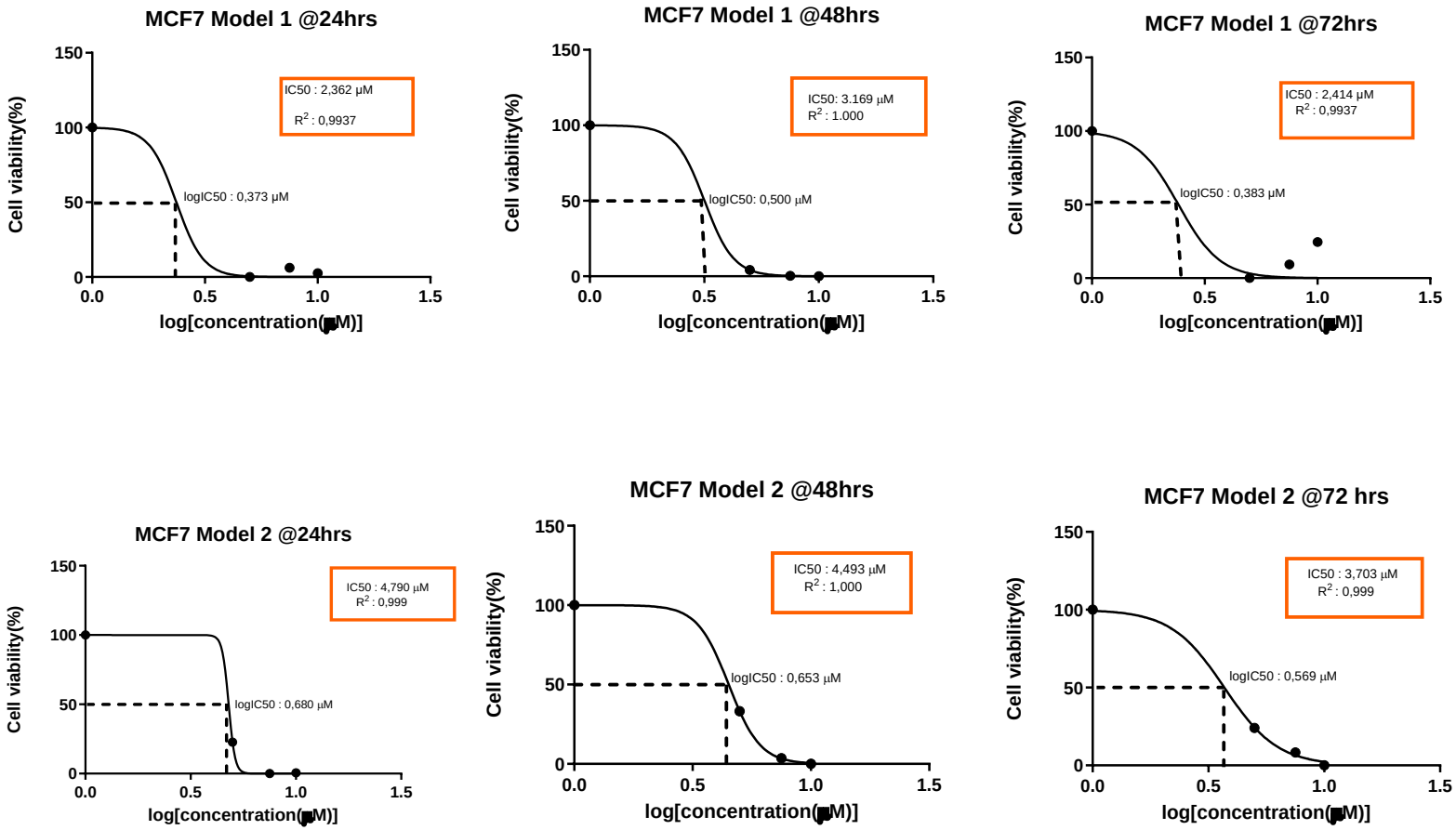


Figure 6: Dose response curves generated from GraphPad Prism showing the logIC50 concentration and cell viability in the single-dose treatment model (model 1) and the daily-replacement treatment model(model 2). The IC50 concentration as well as the r-squared value are also depicted on the graphs

Cell viability: The effects of CBD combined with Tamoxifen

The effect of the various CBD concentrations combined with 2 µM Tamoxifen on neutral red uptake were then investigated (Figure 7 C, D). The single-dose treatment model (model 1) showed that cell viability was not significantly altered with combined CBD (5 µM, 7.5 µM and 10 µM) and 2 µM Tamoxifen treatment compared with when CBD was administered alone. Percentage cell viability in the single-dose treatment (model 1) for all CBD concentrations (5 µM , 7.5 µM and 10 µM) increased from 28.16% to 60,19 % in CBD only treated cells (5 µM , 7.5µM and 10 µM) and from 28,35% to 59,63% in cells treated with combined CBD and Tamoxifen (5 µM CBD + 2 µM Tamoxifen , 7.5 µM CBD + 2 µM Tamoxifen and 10 µM CBD + 2 µM Tamoxifen), indicating that cells did not die due to this type of treatment at any of the time points (Figure 7 A, C).

Conversely, in the daily-replacement treatment model (model 2), 7.5 µM and 10 µM CBD alone and combined with 2 µM Tamoxifen induced ($p>0.05$) lower percentage cell viability compared with Tamoxifen only (Figure 7 B, D). No significant differences ($p>0.05$) were observed in the different treatment groups across all time points in both models. However, the results suggest that CBD is effective in reducing cell viability by itself and when combined with Tamoxifen, it increases the efficacy of Tamoxifen to reduce cell viability.

In summary these findings suggest that MCF7 cells were susceptible to CBD treatment across both models for the first 24 h of treatment but in the single dose treatment model (model 1) cell recovery was observed post 24 h of treatment. CBD concentrations caused a greater decrease in cell viability in the daily-replacement model (model 2) in a dose-dependent manner across all time points. Combined CBD and Tamoxifen treatment also shows increased efficacy at reducing cell viability, which is more significant in the daily-replacement treatment model (model 2).

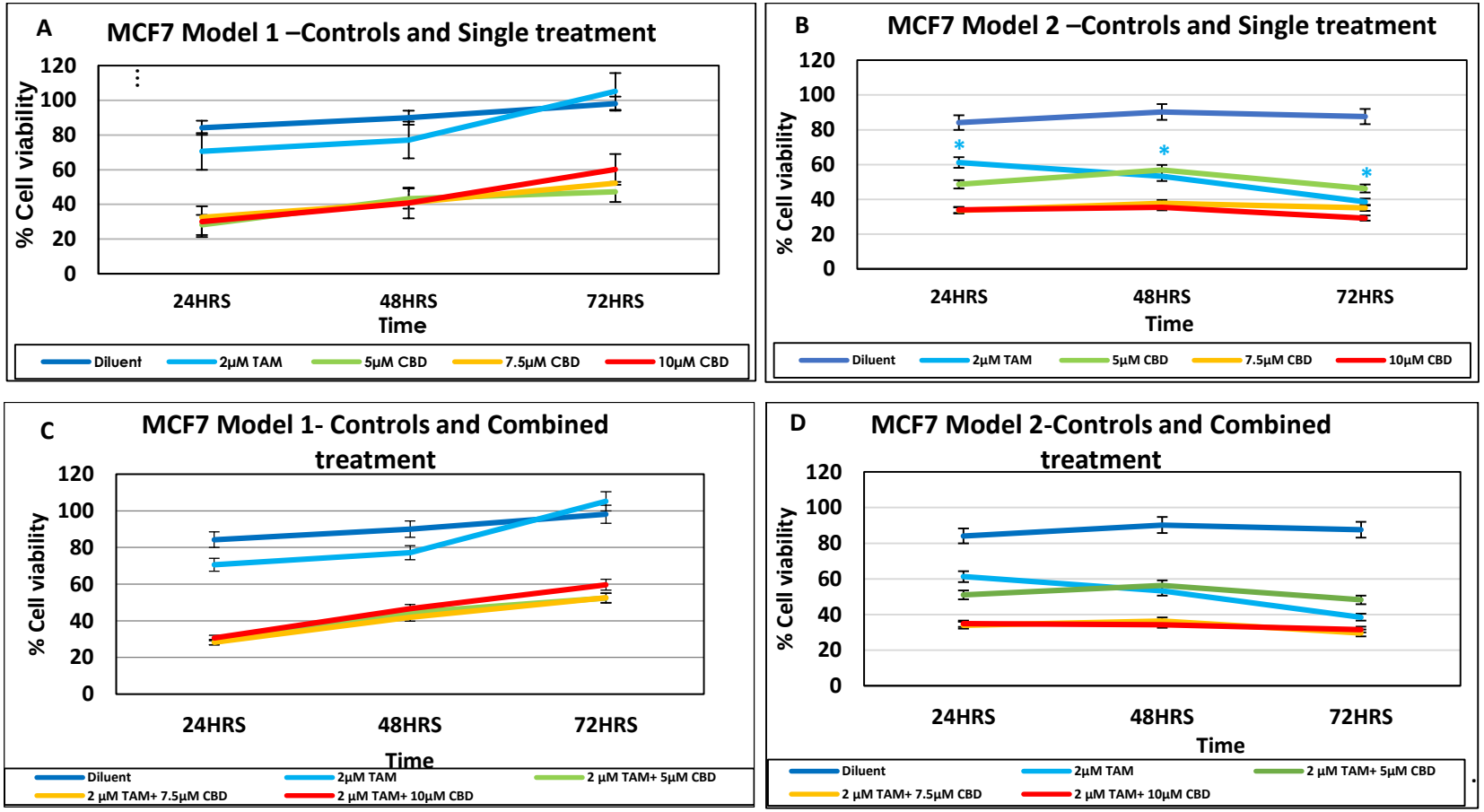


Figure 7:Line graphs showing the percent cell viability of MCF7 breast cancer cells treated with CBD, and combined CBD/Tamoxifen treatment, assessed by the neutral red assay. A: Model 1, single-dose treatment with CBD at 5 µM, 7,5 µM AND 10 µM. B: Model 2, daily-replacement treatment with CBD at 5 µM, 7,5 µM AND 10 µM C: Model 1, single-dose treatment with combined CBD and Tamoxifen treament . D: Model 2, daily-replacement treatment with combined CBD and Tamoxifen treament. In both Model 1 and Model 2, MCF7 cells were treated with diluent (sky blue), 2µM Tamoxifen (light blue), 5µM CBD or 2µM Tamoxifen + 5µM CBD (light green), 7.5µM CBD or 2µM Tamoxifen +7.5µM CBD (yellow) and 10µM CBD or 2µM Tamoxifen +10µM CBD (red). Asterisks(*) matching the colour of the treatment group are used to show significant differences between treatment groups across time. Error bars as mean±SD.

3.1.2. Wound closure - Scratch assay in MCF7 cells

The scratch assay, where a wound area is created at the center of a confluent monolayer is used as a measure of cell migration, where inhibition of cell migration associated with tumour development and metastasis is preferred (Liang, Park, and Guan, 2007; Bobadilla et al., 2019) . To quantitively analyze MCF7 cell migration, the wound closure percentage was calculated for the different time points and compared with the initial point of the creation of the scratch (0 h)(Grada et al., 2017) . Increasing positive wound percentage values indicate closure of the wound area and the decreasing negative values indicate widening of the wound area.

Wound closure- The effects of CBD treatments

In the media and diluent controls, the wound closed completely at 48 h and there was no significant increase ($p>0.05$) in the wound closure percentage in both the single-dose (model 1) and daily-replacement treatment model (model 2) with an increase in time (24 h – 72 h). Pre-treatment with Tamoxifen for 24 h heightened cell migration; however, replacement with CBD reduced migration of these pre-treated cells at 24 h in both Models (Figure 9 A). At 48 h of treatment with 2 µM Tamoxifen, the wound area in both treatment models (from 29.5% closure to -81.2% widening in the single-dose treatment model (model 1), and 42.9% wound closure to -42.4% widening in the daily-replacement model (model 2) (Figure 9 A, Figure 8), reflecting potential cell death with 2 µM Tamoxifen treatment for more than 24 h. Tamoxifen treatment did not significantly change wound closure across both models ($p>0.05$). However, the difference in cell response between the models with 2 µM Tamoxifen treatment was heighted at 72 h in the single-dose treatment model (model 1), cells recovered and promoted wound closure, showing an increase from -81.2% to 26.2% of wound closure at 96 h (Figure 9 A). In the daily-replacement treatment model (model 2), widening of the wound area was observed with Tamoxifen treatment for 48 h and the increase in wound size ceased at 96 h, showing that prolonged treatment with Tamoxifen caused complete loss of cell adhesion and the floating dead cells were discarded with the aspirated media during replacement of treatment (Figure 9 B).

In the single-dose treatment model (model 1), all CBD concentrations (5 µM, 7.5 µM and 10 µM) increased wound closure at 24 h post-CBD treatment. After 24 h, higher CBD concentrations (7.5 µM and 10 µM) induced a slight decrease ($p>0.05$) in wound closure percentage and from 48 h there was no further change in the size of the wound area. In comparison, 5 µM CBD after 48 h showed a greater reduction in percentage wound closure until 72 h which then started to increase, peaking at 52.75% at 96 h (Figure 9 A). In daily-replacement treatment (model 2), in which daily doses of CBD were administered, percentage wound closure decreased substantively with an increase in CBD concentration at 48 h from values between 20-55% in the single-dose treatment (model 1) to values between 60-82% in the daily-replacement model (model 2) (Figure 9 B). Significant differences ($p<0.05$) were observed in the diluent control at 72 h and 96 h where wound closure percentage increased: 5 µM CBD at 48 h and 96 h, 7.5 µM CBD at 24 h and 48 h and 10 µM CBD at 24 h and 48 h showed a significant decrease ($p<0.05$) in wound closure percentage in comparison to 0 h. 7.5 µM CBD and 10 µM CBD at 72 h and 96 h in the single-dose treatment model (model 1) induced greater wound closure compared with the daily-replacement model (model 2). As illustrated in Figure 8 A, there was a complete loss of cells in the wells from 48 h to 72 h in Tamoxifen treated and CBD treated wells in the daily-replacement model (model 2). This loss of cells may be due to the loss of adhesion molecules causing cells to detach from the surface and from each other in response to treatment, thus leading to the cells being washed off when treatment was replaced every 24 h.

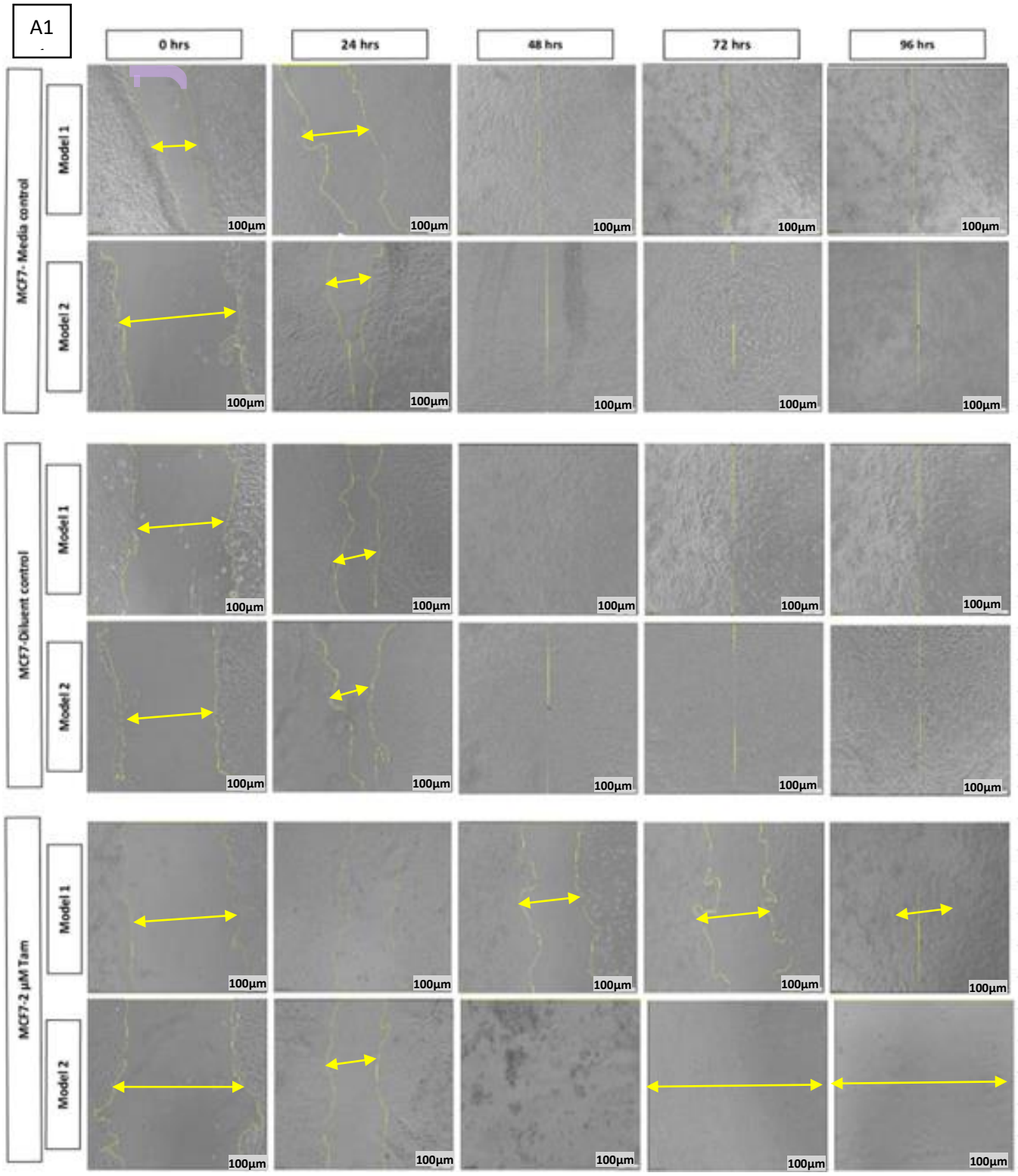


Figure 8.A1: Photomicrographs with a scale bar of 100 µm under the 10X objective showing changes in the scratch area (outlined in yellow and spanned by the yellow double arrow) of MCF7 cells treated with media, diluent and 2 µm Tamoxifen over 96 h. Period in the single-dose treatment model (model 1) and the daily-replacement treatment model (model 2).

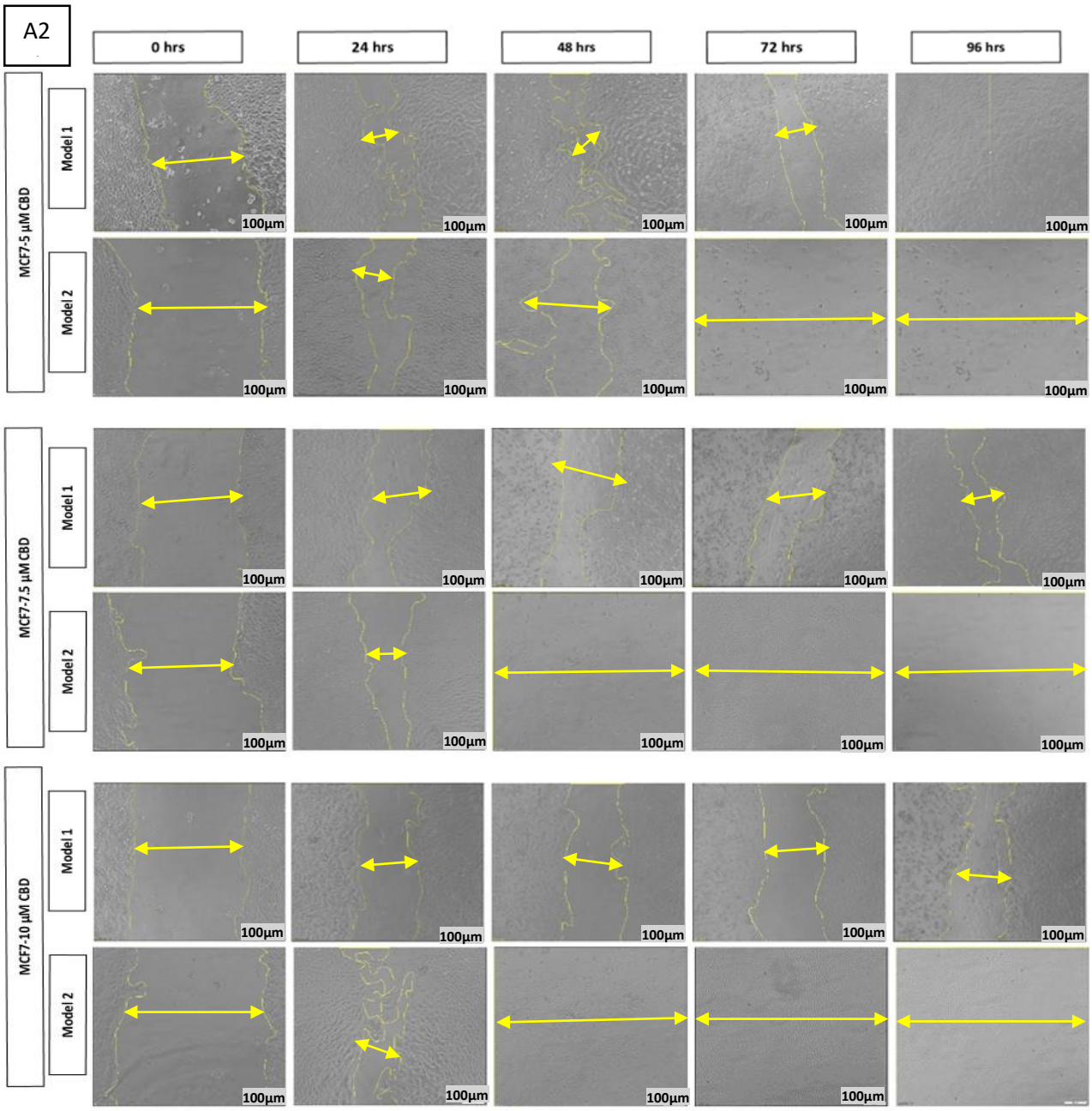


Figure 8.A2: Photomicrographs with a scale bar of 100 µm under the 10X objective showing changes in the scratch area (outlined in yellow and spanned by the yellow double arrow) of MCF7 cells treated with 5 µM CBD, 7.5 µM CBD and 10 µM CBD over 96 h. period in the single-dose treatment model (model 1) and the daily-replacement treatment model (model 2).

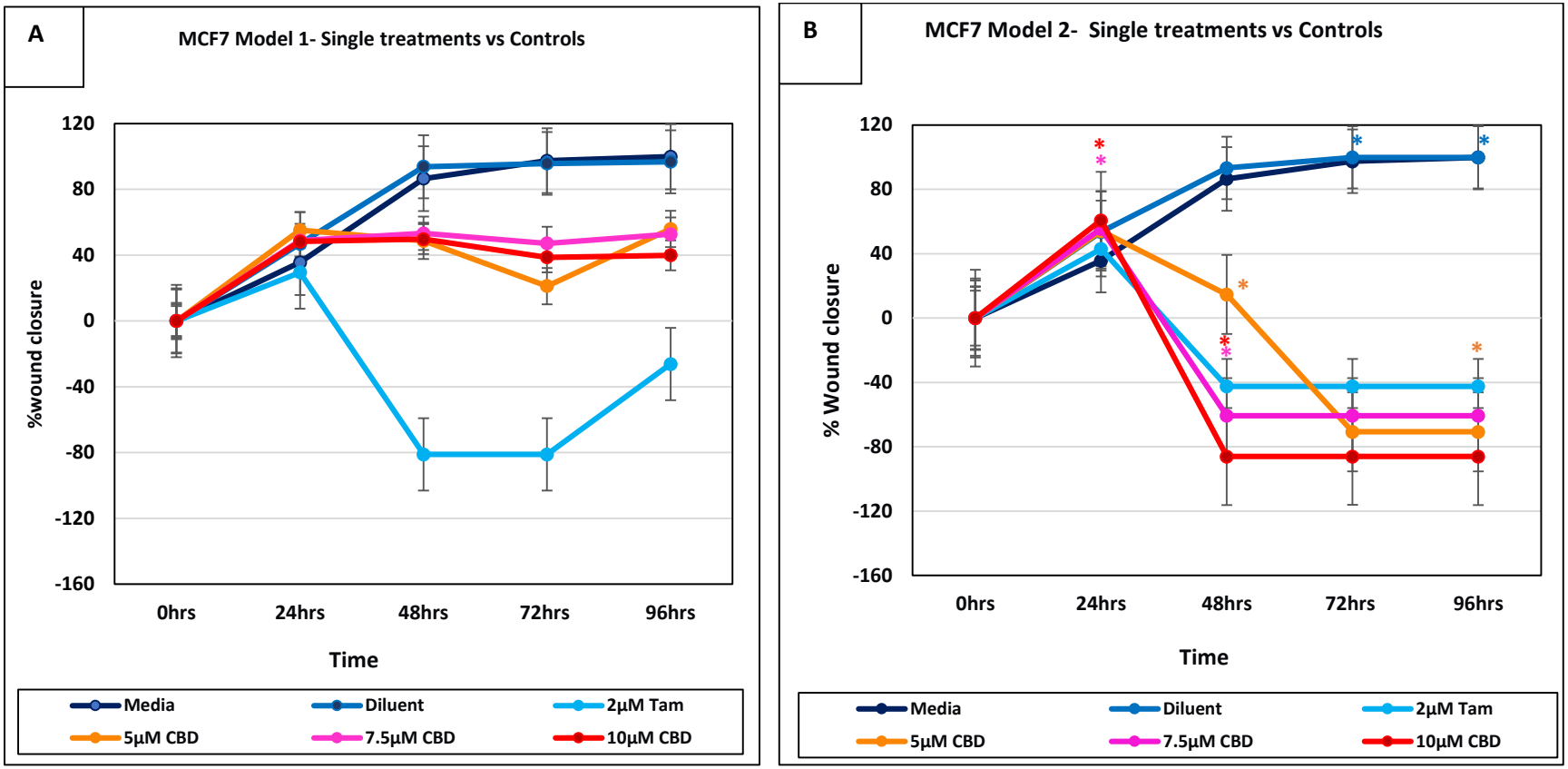


Figure 9: A: Line graphs showing percentage wound closure of MCF7 cells treated according to single-dose treatment model (model 1) and B: Shows MCF7 cells treated according to daily-replacement treatment model (model 2). In both Models MCF7 cells were treated with Media (dark blue), diluent (sky blue), 2 µM Tamoxifen (light blue), 5 µM CBD (orange), 7.5 µM CBD (violet) and 10 µM CBD (red). Asterisks(*) matching the colour of the treatment group are used to show significant differences between treatment groups across time with reference to 0 h. Error bars as mean±SD.

Wound closure-CBD and Tamoxifen combined treatment

When 2 µM Tamoxifen was combined with 5 µM, 7.5 µM and 10 µM CBD, there was a great decrease wound closure percentage .i.e. the wound area became wider compared with when the drugs were administered individually. In the single-dose treatment model (model 1), there was no loss of cells observed with an increase in CBD concentrations combined with Tamoxifen (Figure 10 and Figure 11 A). The wound area slightly increased over time, but these changes were not significant ($p>0.05$) and could not be clearly observed from 48 h to 96 h (Figure 10 and Figure 11 A).

In the daily-replacement model (model 2), increasing CBD concentrations combined with 2 µM Tamoxifen at 24 h increased wound closure percentage from 28,59% at the lowest concentration (5 µM CBD) to 64% at the highest concentration (10 µM CBD) which signifies reduction in the wound area relative to the original wound area; however, from 48 h to 96 h, the wound area widened substantially (from 28,59% to -56,26% at 5 µM CBD; 52,94% to -46,93% at 7,5 µM and 64,23% to -53,75% at 10 µM CBD) (Figure 11 B). The widening of the wound area may be due to cell death or the loss attachment of the cells from the surface, with qualitative assessment showing cells had washed off with the change in daily treatment hence the empty wells (Figure 10). This was more evident in the daily-replacement model (model 2). Significant differences in comparison to 0 h ($p<0.5$) were observed in the diluent control at 48 h, 72 h and 96 h (with an increase in % wound closure); 2 µM Tamoxifen+5 µM CBD at 96 h (with a decrease in % wound closure); 2 µM Tamoxifen +7.5 µM CBD at 24 h *and* 48 h (with a decrease in % wound closure) and 2 µM Tamoxifen+10 µM CBD at 24 h and 48 h (with a decrease in % wound closure). The same differences were noted across both models.

In summary it was shown that CBD inhibits wound closure at higher concentrations but at lower concentrations, cells can recover and promote wound closure after 72 h of treatment in single-dose treatment (model 1) whereas in the daily-replacement treatment (model 2) cells die due to treatment even with the lowest CBD concentration. Combined CBD and Tamoxifen treatment in the daily-replacement model (model 2) was more effective at inhibiting wound closure than in

the single-dose treatment model (model 1), resulting in wider scratch areas with an increase in treatment duration where after 48 h, there was complete cell loss in the daily-replacement model (model 2) treated samples.

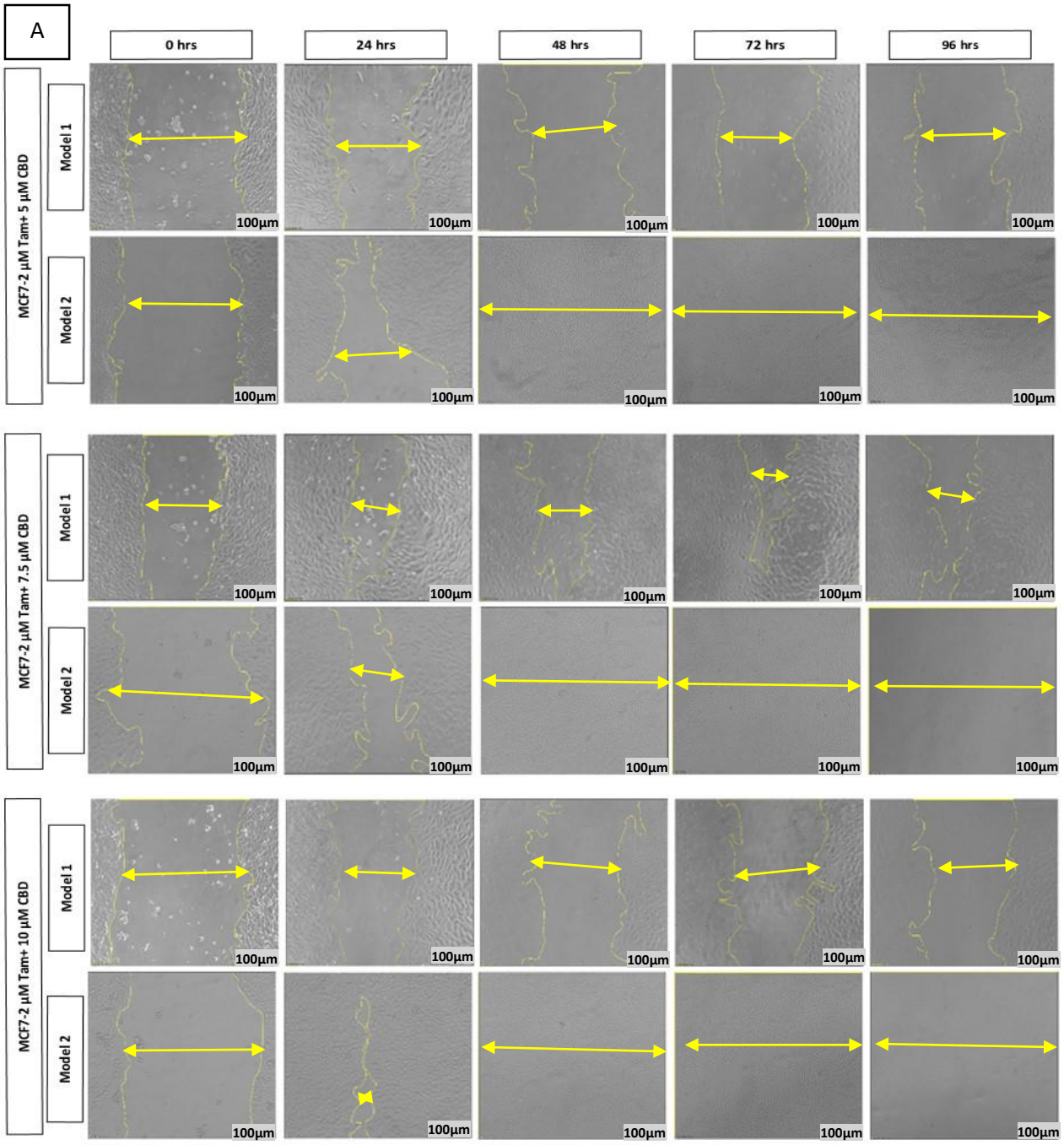


Figure 10:A: Photomicrographs at 100µm under the 10X objective showing changes in the scratch area (outlined in yellow and spanned by yellow double arrow) of MCF7 cells treated with media, diluent, 2 µM Tamoxifen, 2 µM Tamoxifen + 5 µM CBD, 2 µM Tamoxifen + 7.5 µM CBD and 2 µM Tamoxifen + 10 µM CBD over 96h period in single-dose treatment (model 1) and daily-replacement treatment (model 2).

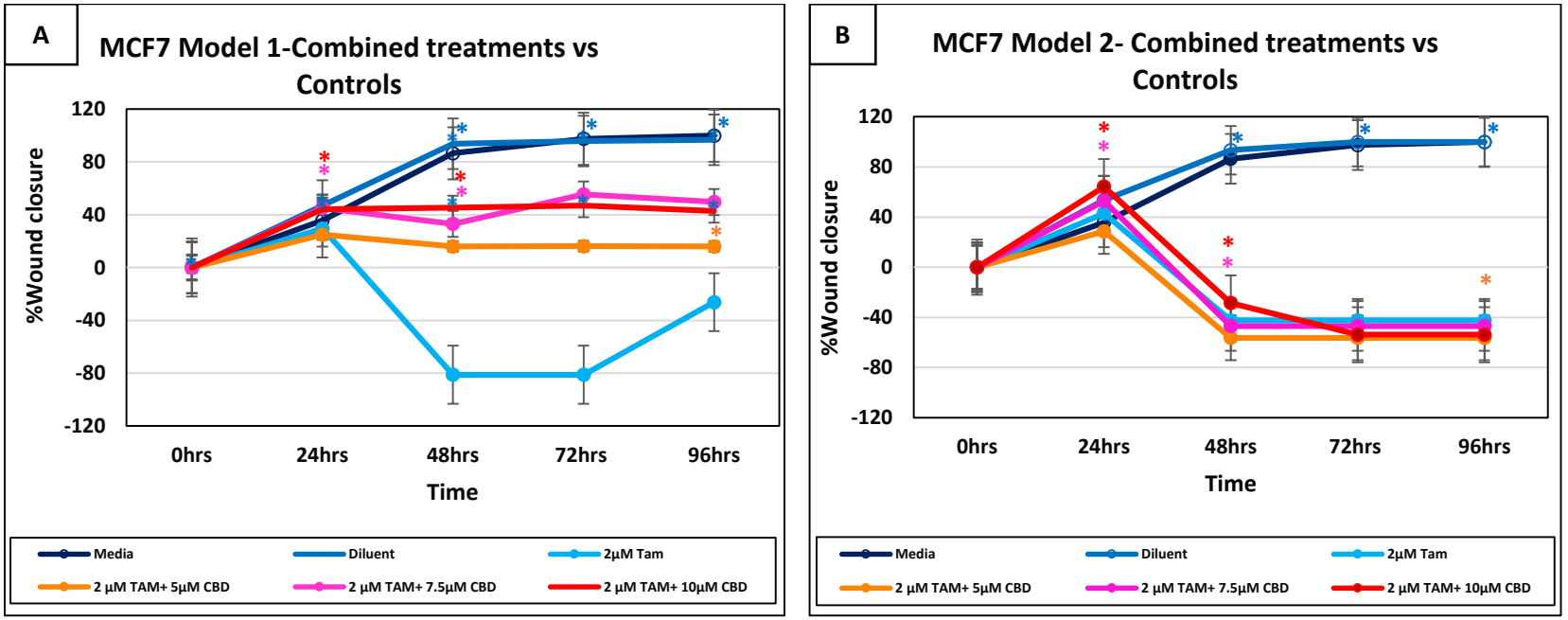


Figure 11: A: Line graphs showing percentage wound closure of MCF7 cells treated according to single-dose treatment model (model 1) and B: Shows MCF7 cells treated according to daily-replacement treatment model (model 2). MCF7 cells were treated with Media (dark blue), diluent (sky blue), 2µM Tamoxifen (light blue), 2µM Tamoxifen +5µM CBD (orange), 2µM Tamoxifen +7.5µM CBD (violet) and 2µM Tamoxifen +10µM CBD (red). Asterisks(*) matching the colour of the treatment group are used to show significant differences between treatment groups across time with reference to 0 h.Error bars as mean±SD.

3.1.3. Optimal CBD concentration and treatment duration

The cell viability and wound closure results showed that 5 µM CBD is the optimal CBD concentration because with the higher CBD concentrations (7.5 µM and 10 µM) there was a complete loss of cells as shown in Figure 8 and 10, and that cell viability was very low at these concentrations (Figure 12), especially in the daily-replacement model (model 2). At 24 h, there was an increase in cell viability and an increase in wound closure thus suggesting that after 24 h both cell viability and wound closure started decreasing thus indicating that the cells were sucumbing to treatment. Moreover, in both models the IC50 values obtained across all time points were below 5 µM (the lowest tested CBD concentration) (Figure 6), thus indicating high potency of CBD even at the lowest concentration. Data obtained at 48h gave a good fit with an R-squared value of 1 compared with data obtained at 24 h and 72 h, thus indicating that at this time point the regression predictions fit the data. Following observations from 0 h to 72 h, 48 h was the optimal treatment duration because beyond 48 h there were no notable changes in the behaviour of the cells in response to treatment.

3.2. Cell viability and Cell migration in T47D cells in comparison to MCF7 cells

3.2.1. Cell viability – the Neutral red assay in T47D cells

Following the determination of 5 µM CBD as the optimal CBD concentration and 48 h as the optimal treatment duration in the MCF7 cells, T47D cells an additional hormone-dependent breast cancer cell line was used to assess the effects of combined CBD and Tamoxifen on cell viability and cell migration. The data was managed as outlined in section 3.1.1 and compared with the initial data obtained for MCF7 cells in section 3.1.

Cell viability in response to 5 µM CBD and 2 µM Tamoxifen in T47D cells compared with MCF7 cells

No significant differences ($p>0.05$) were found in cell viability using the neutral red assay for all treatment groups from 24 h to 72 h of treatment in both the single-dose treatment model (model

1) and the daily-replacement model (model 2) treated MCF7 and T47D cells. T47D cells showed an exponential increase ($p>0.05$) in cell viability from 24 h to 48 h in the diluent control(64,23% to 90,68%) and a decrease from 48 h to 72 h (90,68% to 82,04%) with single-dose treatment (model 1) (Figure 12 A). Contrastingly, with the daily-replacement treatment model (model 2), a decrease ($p>0.05$) in cell viability was observed from 24 h to 48 h (96,56% to 81,71%) in the diluent control, which was followed by an increase in cell viability from 81,71% to 102,45% from 48 h to 72 h (Figure 12B). The decrease in T47D cell viability in the diluent control group with single-dose treatment model (model 1) contrasted with MCF7 cell viability at matched treatment. In MCF7 cells treated with the diluent, cell viability increased in response to treatment with an increase in incubation time (84,20% at 24 h to 98,09% at 72 h); daily-replacement treatment model (model 2) increased from 24 h to 48 h (84,09%-90,21%) and then decreased from 48 h to 72 h (90,21% to 87,61%) further contrasting the trend observed in T47D cells treated with the diluent solution.

Treatment with 2 µM Tamoxifen caused a decrease in T47D cell viability from 24 h to 48 h (58,05% to 35,87%) within the single-dose treatment model (model 1) and an increase in cell viability from 48 h to 72 h (35,87% to 48,03%). With the daily-replacement model (model 2), 2 µM Tamoxifen resulted in a decrease in T47D cell viability as the incubation time increases (74,60% at 24 h to 49,48% at 72 h). T47D cell response to Tamoxifen treatment contrasted that of MCF7 cells in the single-dose treatment model (model 1) for the first 48 h of treatment .i.e. cell viability decreased in T47D cells and only started increasing post 48 h of treatment whereas MCF7 cell viability increased from 24 h to 72 h (70,55% to 105,14%) within this treatment model. In the daily-replacement treatment model (model 2), T47D cell viability in response to Tamoxifen treatment was similar to that of MCF7 cells, with cell viability decreasing from 24 h to 72 h (74,60% to 49,58% in T47D cells and 61,26% to 38,51% in MCF7 cells).

An increase in T47D cell viability was observed in cells treated with 5 µM CBD from 24 h to 48 h in both Model 1 (60,55% to 97,28%) and Model 2 (90,26% to 99,61%). After 48 h T47D cell viability decreased in cells treated with a single-dose of CBD (97,28% to 77,21%) and with the daily-replacement treatment model (99,61% to 80,37%) (Figure 12 A and B). While MCF7 cell increased

from 24 h to 48 h and started decreasing post 48 h of incubation with CBD solution in the daily-replacement treatment model (model 2) as seen in T47D cells, in the single-dose treatment model (model 1), MCF7 cell viability exponentially increased from 0 h to 72 h(28,35% to 47,22%) at matched treatment .

In T47D cells, a decrease in cell viability was observed following treatment with 2 µM Tamoxifen and 5 µM CBD from 24 h to 48 h in the single-dose treatment model (model 1) (40,10% to 35,88%) and the daily-replacement treatment model (model 2) (81,28% to 37,95%), with the daily-replacement treatment model (model 2) exhibiting the greatest effects in decreasing cell viability. In the single-dose treatment model (model 1), MCF7 cell viability increased from 24 h to 72 h whereas T47D cell viability only started increasing post 48 h of treatment(Figure 12 A and C). Contrastingly, MCF7 cell viability in response to combined treatment increased in the daily-replacement treatment model (model 2) from 24 h to 48 h whereas it decreased in T47D cells at matched time points and treatment, post 48 h MCF7 cell viability started to decrease as T47D cell viability decreased further post 48 h of treatment (Figure 12 B and D). Overall, MCF7 cells showed the highest cell viability and less sensitivity to treatment compared with T47D across both Models.

In summary combined 5 µM CBD and 2 µM Tamoxifen have cytotoxic effects on both MCF7 and T47D cells, with T47D cells showing increased susceptibility to treatment than MCF7 cells across both models. While MCF7 cells in the daily-replacement treatment model (model 2) were able to recover from combined CBD and Tamoxifen treatment and promote cell viability, a greater number of T47D cells died following treatment with combined CBD and Tamoxifen treatment.

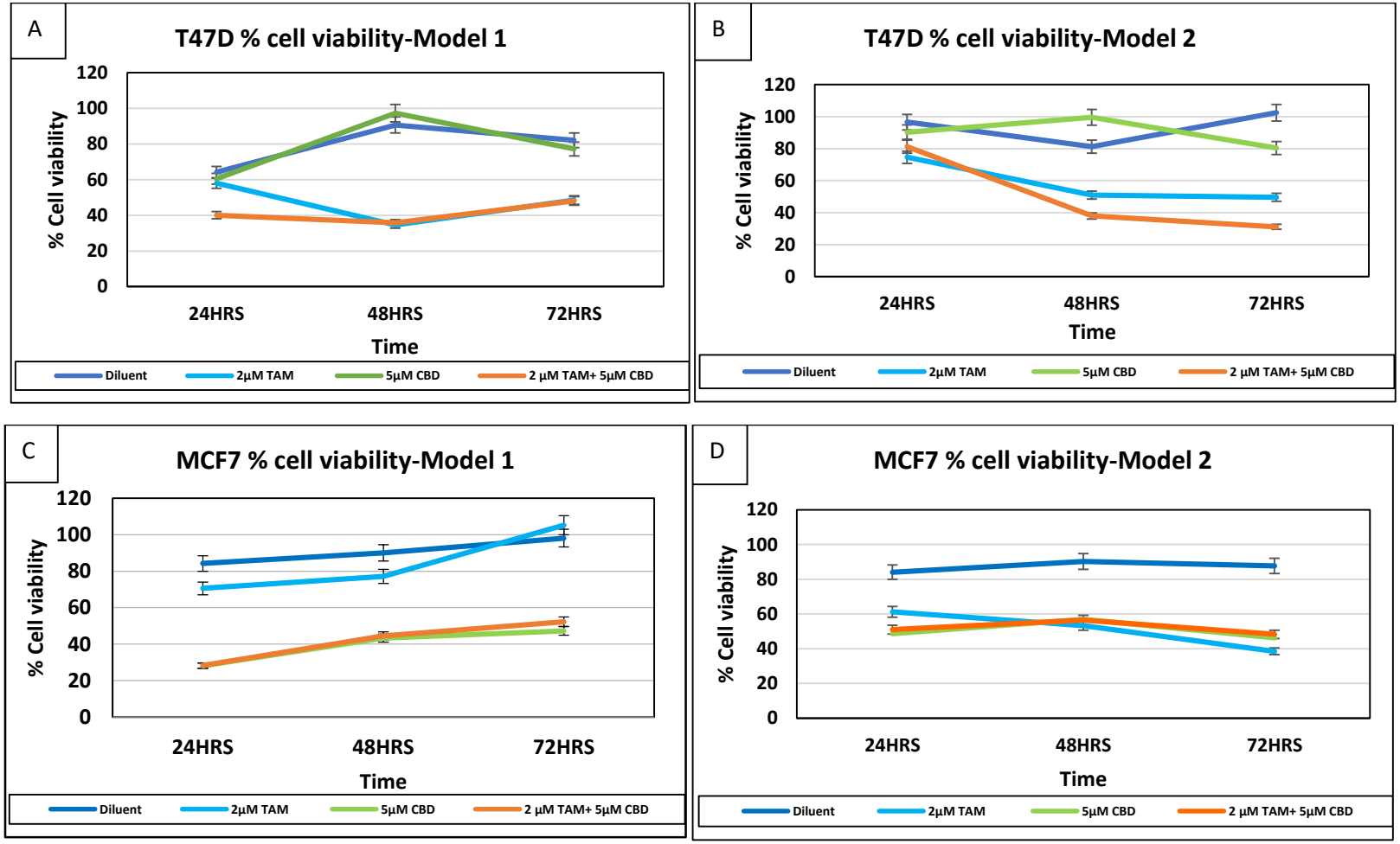


Figure 12: Line graphs showing the percentage cell viability of T47D breast cancer cells alongside MCF7 cells treated with CBD, Tamoxifen and combined CBD/Tamoxifen, assessed by the neutral red assay. A *and* C: Model 1, single-dose treatment with 5 µM CBD (green), 2 µM Tamoxifen (light blue) and 5 µM CBD combined with 2 µM Tamoxifen (orange) in T47D (A) and MCF7(C) cells. B *and* D: Model 2, daily-replacement treatment with 5 µM CBD (green), 2 µM Tamoxifen (light blue) and 5 µM CBD combined with 2 µM Tamoxifen (orange) in T47D (B) and MCF7(D) cells. The diluent control in both A and B is shown in (dark blue). Error bars as mean±SD.

3.2.2. Wound closure-Scratch assay in T47D cells

Cell migration in response to 5 µM CBD and 2 µM Tamoxifen in T47D cells compared with MCF7 cells

Complete wound closure was achieved at 24 h and there was no significant increase ($p>0.05$) in the wound closure percentage in both the single-dose and daily-replacement treatment models with an increase in time (24 h – 72 h) for media control and diluent control T47D cells, like that observed in MCF7 cells. Following Tamoxifen pre-treatment, in the single-dose treatment model (model 1), there was a significant ($p<0.05$) increase in wound closure with further 2 µM Tamoxifen treatment in T47D cells at 72 h compared with 0 h (Figure 13 and Figure 14 A) whereas in MCF7 cells, there was an increase in wound size which was not significant ($p>0.05$) (Figure 14 C). In the daily-replacement treatment model (model 2), 2 µM Tamoxifen daily-replacement treatment induced over confluence of the wells from 24 h to 48 h (99% to 112%) resulting in cell death as shown by the significant ($p<0.05$) decrease in wound closure percentage at 72 h and 96 h where there was complete cell loss in the wells (Figure 13A1 and Figure 14B). Contrastingly, in MCF7 cells, a significant ($p<0.05$) decrease in wound closure percentage was observed as early as 24 h post treatment with Tamoxifen and 96 h there was almost complete cell loss with the scratch area widening due to cell death (Figure 10 and Figure 14 B and D).

In T47D cells, treatment with 5 µM CBD resulted in increasing wound closure percentage from 0 h to 24 h and 24 h post treatment the wound area was 100% confluent and the confluence was maintained until at 96 h in both the single-dose treatment(model 1) and daily-replacement treatment model (model 2) (Figure 13) which signifies increased cell migration, significant ($p<0.05$) at 48 h, 72 h and 96 h compared with 0 h (Figure 14). Single-dose treatment with combined 2 µM Tamoxifen and 5 µM CBD resulted in complete wound closure 24 h post treatment in T47D cells, similar to what was observed in MCF7 cells. The wound closure then decreased from 48 h to 72 h due to cell death, at 96 h some of the viable cells moved into and obscured the scratch area with combine CBD and Tamoxifen treatment in the single-dose

treatment model. In T47D cells, a significant decrease in the wound size was observed only at 72 h post treatment whereas in MCF7 it was observed as early as 48h in the daily-replacement treatment model(Figure 14 A and C). Similarly, complete wound closure was observed in the daily-replacement treatment model (model 2) in T47D cells at 24 h, followed by a decrease in wound closure percentage from 99% to 48%, from 48 h to 96 h (Figure 14 B *and* D), significant ($p < 0.05$) at 72 h and 96 h. A similar trend was observed in MCF7 cells treated with combined CBD and Tamoxifen as early as 24 h post treatment, with a significant decrease in wound closure at 96 h due to cell death.

In summary, T47D cells in both treatment models promoted complete wound closure with 5 µM CBD whereas in MCF7 cells it induced widening of the wound area and these similar observations were noted even with combined CBD and Tamoxifen treatment. Combined CBD and Tamoxifen treatment in the daily-replacement treatment model (model 2) for T47D and MCF7 cells induced an increase in the wound area, with complete cell loss observed from 48 h of treatment.

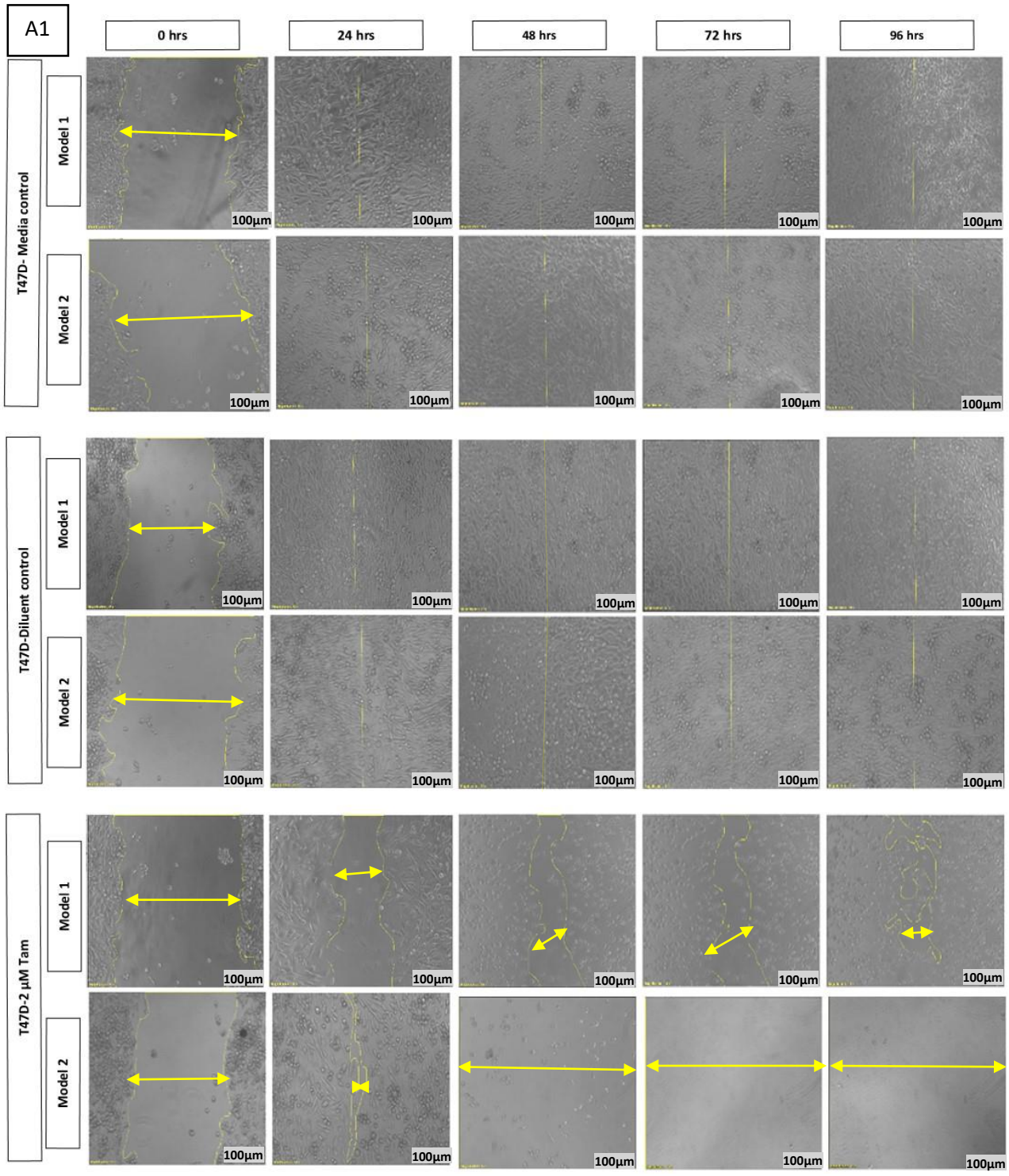


Figure 13.A1: Photomicrographs at 100µm under the 10X objective showing changes in the scratch area outlined in yellow and spanned by yellow double arrow) of T47D cells treated with media, diluent and 2 µM Tamoxifen over 96 h period in single-dose treatment model (model 1) and daily-replacement treatment model (model 2).

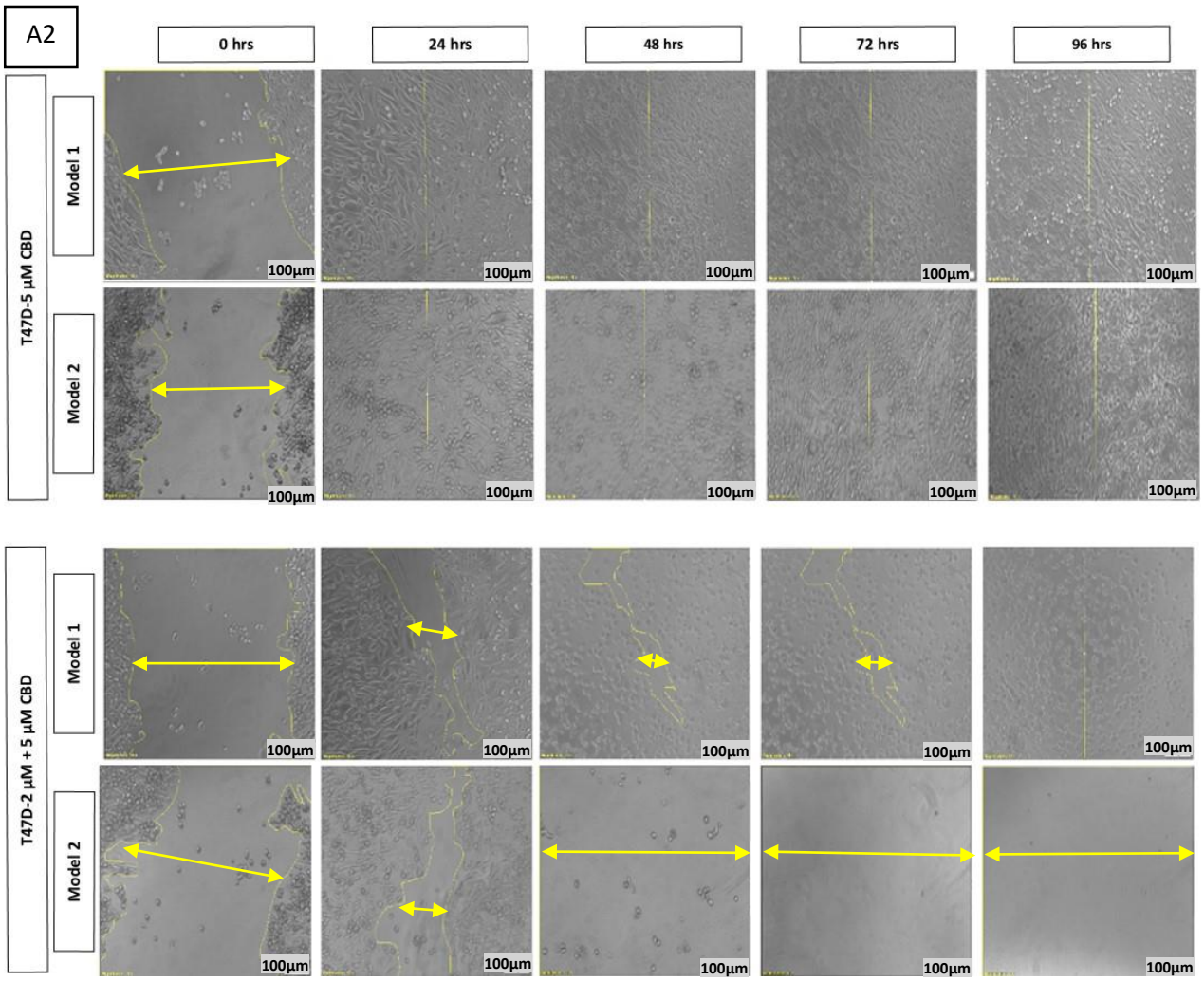


Figure 13.A2: Photomicrographs under the 10X objective showing changes in the scratch area outlined in yellow and spanned by yellow double arrow) of T47D cells treated with 5 µM CBD and 2 µM Tamoxifen + 5 µM CBD, over 96 h period in single-dose treatment model and daily-replacement treatment model (model 2). Scale bar at 100µm

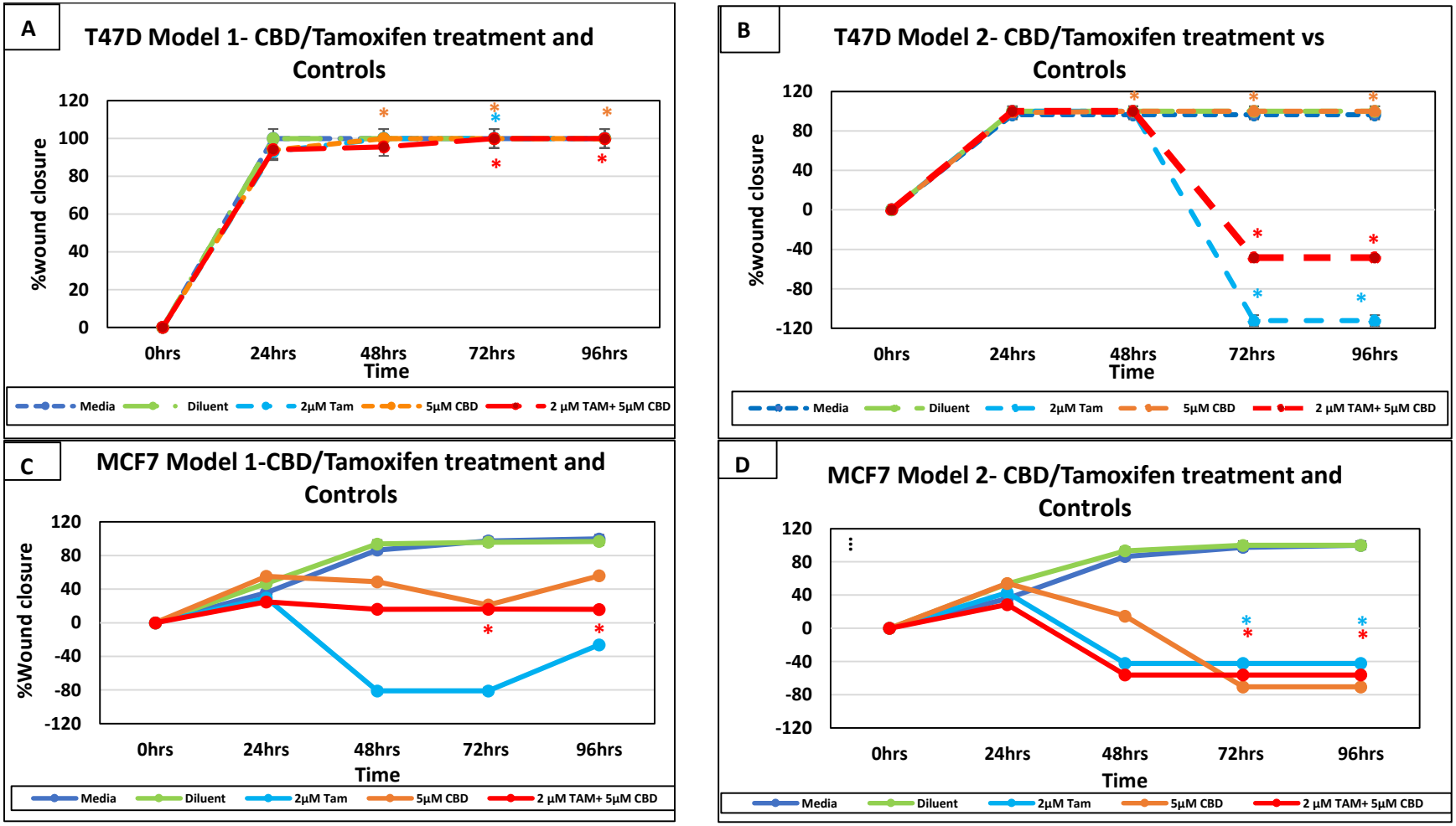


Figure 14. A and C: Line graphs showing percentage wound closure of T47D cells (B) and MCF7 cells (D) treated according to model 1 (single-dose treatment) and B and D: Shows T47D cells(B) and MCF7 cells (D) treated according to model 2 (daily-replacement treatment). In both A and B T47D cells were treated with Media (dark blue), diluent (green), 2µM Tamoxifen (light blue), 5µM CBD (orange) and 2µM Tamoxifen +5µM CBD (red) and compared with MCF7 cells (C and D) for the same treatment. Asterisks(*) matching the colour of the treatment group are used to show significant differences between treatment groups across time with reference to 0 h. Error bars as mean±SD.

3.3. Cell proliferation in MCF7 and T47D, the single-dose treatment model (model 1) and the daily-replacement treatment model (model 2)

The MTT assay was performed on MCF7 and T47D cells in both Models following treatment (Table 2) for 48 h. The results are represented as absorbance ratios with 1 as the baseline (ratios above 1 are considered high and indicate increased rate of cell proliferation whereas those below 1 are considered low and a reduced rate of cell proliferation) (Salati, Ahmad, and Khwaja, 2013;Klinsang et.al.,2023) .

3.3.1. Proliferation inhibition induced by combined CBD and Tamoxifen in MCF7 and T47D cells (model 1, single-dose treatment)

Following statistical analysis using the Kruskal Wallis by ranks Anova and post hoc tests, no significant differences ($p>0.05$) were noted across the treatment groups within the single-dose treatment model (model 1) (Appendix G, Figure E11).

As expected, treatment with 0.1% Triton-X-100 (High control) induced a decrease in cell proliferation in both MCF7 and T47D cells compared with the media only treated cells, with T47D cells showing the greatest decrease in cell proliferation. In the single-dose treatment model (model 1), MCF7 cells treated with diluent had the highest absorbance ratio (absorbance=1,46) than all other treatment groups in the single-dose treatment model (model 1) which may indicate that 0.8% ethanol increases rate of cell proliferation in MCF7 cells whereas in T47D cells it reduces the rate of cell proliferation (absorbance ratio=0.64), although these findings were not statistically significant. MCF7 cells with single-dose treatment (model 1) showed a higher rate of cell proliferation compared with the T47D cells across all treatment groups except with 5 µM CBD control which differed in T47D cells as it resulted in slightly more inhibition of cell proliferation (Figure 15 A). A slight increase in the inhibition of cell proliferation of MCF7 cells (absorbance ratio =0.87) was noted when cells were treated with 2 µM Tamoxifen and a greater reduction was noted in T47D (absorbance ratio=0.15) at matched treatment when compared with the media control. Treatment with 5 µM CBD showed increased inhibition of cell proliferation in MCF7 cells than in T47D cells, compared with the baseline media control cells. Combined CBD

and Tamoxifen treatment (2 µM Tamoxifen+ 5 µM CBD) showed the greatest increase in inhibition of cell proliferation of MCF7 cells (absorbance ratio=0.46) compared with all other treatments and a much greater decrease in T47D cells (Figure 15 A).

3.3.2. Proliferation inhibition induced by combined CBD and Tamoxifen in MCF7 and T47D cells (model 2, daily-replacement treatment)

Following statistical analysis using the Kruskal Wallis by ranks Anova and post hoc tests, no significant differences ($p>0.05$) were noted across the treatment groups within the daily-replacement treatment model (model 2) (Appendix G, Figure E1).

The rate of cell proliferation decreased across all treatment groups in both MCF7 and T47D cells with daily treatment replacement every 24 h for a duration of 48 h (Figure 15 B). A slight decrease in MCF7 and T47D cell proliferation compared with the media control was observed (MCF7 absorbance ratio= 0.75 and T47D absorbance ratio=0.72). Treatment with 0.1% Triton-X-100 (High control) showed a greater increase in the rate of inhibition of cell proliferation in both MCF7 (absorbance ratio= 0,32) and T47D cells (absorbance ratio=0.09), with T47D cells showing the greatest proliferation inhibition (Figure 15 B) in comparison with the media control. The rate of proliferation of MCF7 cells slightly decreased (absorbance ratio=0,79) when cells were treated with 2 µM Tamoxifen and an even greater decrease in the rate of cell proliferation was noted in T47D cells (absorbance ratio=0.17) in comparison with the media control (absorbance ratio=1). Treatment with 5 µM CBD showed a higher inhibition of cell proliferation in MCF7 cells (absorbance ratio=0.35) and only a slight inhibition of cell proliferation in T47D cells (absorbance ratio =0.95) compared with the baseline media control cells. Treatment with both 2 µM Tamoxifen and 5 µM CBD showed the greatest decrease in cell proliferation of MCF7 cells (absorbance ratio=0.23) compared with all other treatments and a decrease in T47D cell proliferation (absorbance ratio=0.15) at matched treatment. The daily treatment replacement model showed to be the most effective though non-significant ($p>0.05$) at reducing cell proliferation in both cell lines (MCF7 and T47D) among all treatment groups compared with the single-dose treatment model (model 1), except with 5 µM CBD.

In summary, T47D cells showed greater cell proliferation with 5 µM CBD compared with MCF7 cells across both models. In the single-dose treatment model (model 1), combined CBD and Tamoxifen treatment caused higher cell proliferation in MCF7 cells compared with T47D cells,

and this similar observation was noted even with the daily-replacement treatment model (model 2) treated cells.

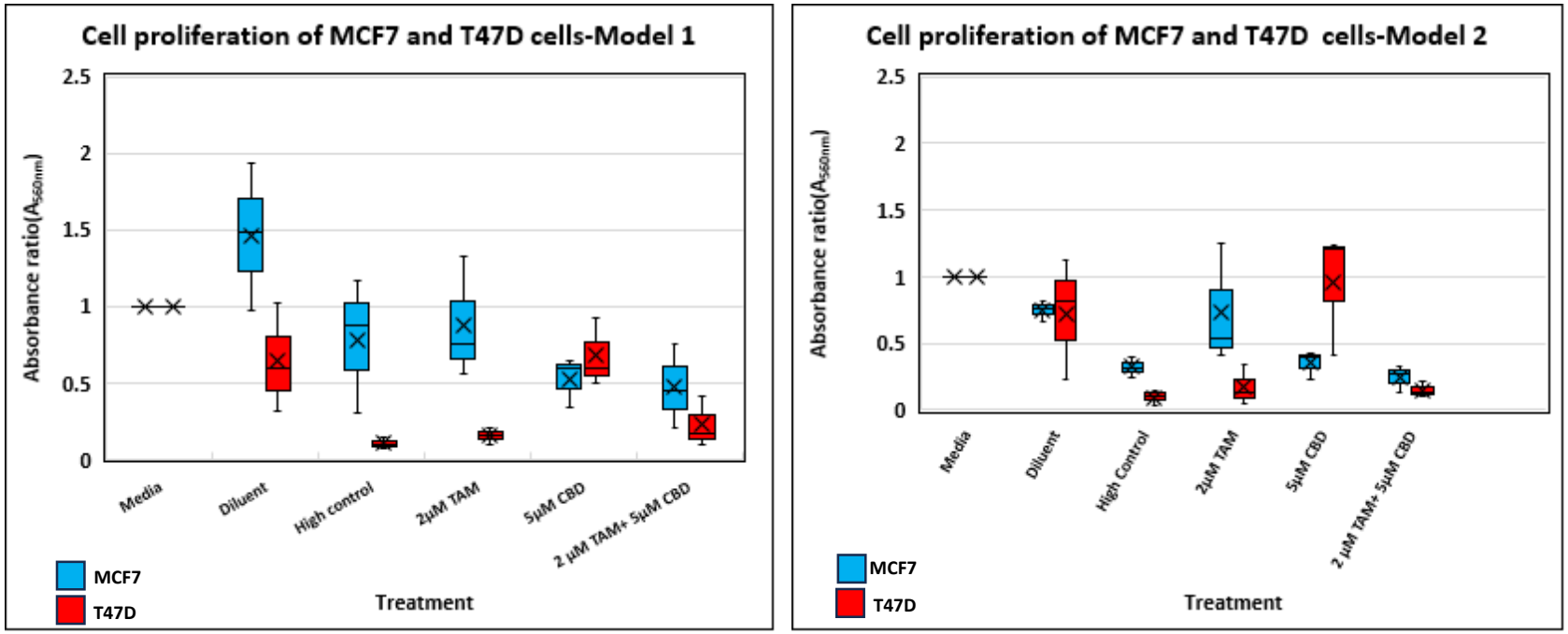


Figure 15. A: Box and whisker plots showing inhibition of cell proliferation as absorbance ratio of MCF7 and T47D cells treated according to single-dose treatment (model 1) and B: Shows bar graphs of MCF7 and T47D cells treated according to daily-replacement treatment model (model 2). The X within the box indicates the mean and the line within the box indicates the median value. In both A and B MCF7 (blue) and T47D (red) cells were treated with Media, diluent, 0.1 % triton, 2 µM Tamoxifen 5µM CBD *and* 2µM Tamoxifen + 5µM CBD. No significant differences ($p>0.05$) were observed across all treatment groups in both Model 1 and Model 2 and across cell lines.

3.4. CPR activity in MCF7 and T47D cells

CPR, an electron transfer protein is responsible for transferring electrons to many natural occurring electron acceptors, including CYP450 enzymes; therefore, CPR activity can indicate CYP450 enzyme activity (Gan et al., 2008). CYP450 enzyme activity in MCF7 and T47D cells was investigated through CPR electron transfer activity to establish the effects of treatment (section 2.10) on MCF7 and T47D cells across the single-dose treatment model (model 1) and the daily-replacement treatment model (model 2) after 48 h. Both CBD and Tamoxifen are substrates of CYP450 enzymes and can compete for binding to the active site. CPR activity measured in this assay will indicate the ability of CPR to transfer electrons from NADPH to CYP450 enzymes to activate them. Furthermore, it will give an indication of the rate of the CYP450 catalyzed reaction.

3.4.1. CPR activity with single-dose treatment (model 1) in MCF7 and T47D cells.

CPR activity detected was greater in T47D cells than in MCF7 cells, in all treatment groups. CPR activity in MCF7 cells treated with a single dose of treatment solutions decreased with an increase in time, with the lowest CPR activity being observed at 30 minutes in both the media control (0,059 mU/ml at 15 mins to no CPR activity at 30 mins) and diluent control (0,06 mU/ml at 15 mins to 0,02 mU/ml at 30 mins) and 5 µM CBD (0,15 mU/ml at 15 mins to 0,02 mU/ml at 30 mins). Similarly, CPR activity in T47D cells also decreased with an increase in time (CPR activity ranging between 2,56-4,11 mU/ml at 15 mins to 0,07-0,59 mU/ml at 30 mins) across all treatment groups. This reduction in CPR activity signifies reduction in the rate of electron transfer from NADPH to CYP450 enzyme therefore reducing the activity of this enzyme. The reduction in CYP450 activation results in reduction of the CYP450 catalysed reactions such as the conversion of drug compounds to their pro-drugs. While the control groups and 5 µM result in evident decrease in CPR activity with an increase in time, it is important to note the observed slight increase in CPR activity with 2 µM tamoxifen, combined CBD and tamoxifen, paclitaxel and 1X EBSS as time increases from 15 mins to 30 mins (Figure 16) in MCF7 cells. Overall CPR activity was high in T47D cells compared with MCF7 cells, thus showing an increased rate of CYP450 catalysis in T47D cells compared with MCF7 cells.

3.4.2. CPR activity with daily-replacement treatment (model 2) in MCF7 and T47D cells.

CPR activity at 15 min in MCF7 cells could not be detected and this was similar for all treatment groups even at 30 min but in T47D cells, CPR activity was high detected at 15 mins but not at 30 min for all treatment groups (Figure 17). This lack of CPR activity may be due to the loss of substrate (the cells) which are lost with the aspirated media in the daily-replacement treatment model therefore resulting in no substrate for the electron from NADPH to bind on and increase CPR activity. CBD and tamoxifen single treatment resulted in higher CPR activity at 15 minutes compared with combined CBD and Tamoxifen (Figure 17) thus indicating the increase in cytotoxic effects of combined treatment which results in accelerated cell loss. At 30 min, the was no enzyme activity for any of the treatment groups. Overall, T47D cells showed measurable CPR activity at 15 min thus indicating CYP450 activity at this time point but the activity of CYP450 was lost at 30 min thus suggesting that CPR substrate concentration decreased in T47D cells with an increase in time. The loss of CPR activity at 30 mistranslates to reduced efficacy of the CYP450 enzyme in catalysing the reaction that forms metabolites of the treatment compounds.

MCF7 and T47D cells, exposed to the single-dose treatment (model 1) exhibited higher CPR activity at 15 min and 30 min compared with the daily treatment replacement treatment model which showed low CPR activity at 15 and no CPR activity at 30 min. These finding suggests that cells given treatment daily were more likely to be susceptible to the effects of the treatment possibly due to higher drug availability which may inhibit enzyme activity by reducing the amount of substrate available for binding.

In summary the trend observed in the CPR activity of 5 µM CBD alone and 2 µM Tamoxifen + 5 µM CBD in both MCF7 and T47D at 30 min is similar for both single-dose treatment (model 1) and daily-replacement treatment and indicates that CPR activity decreases with an increase in time as less substrates are available for the activation of the CYP450 enzyme through CPR mediated electron transfer.

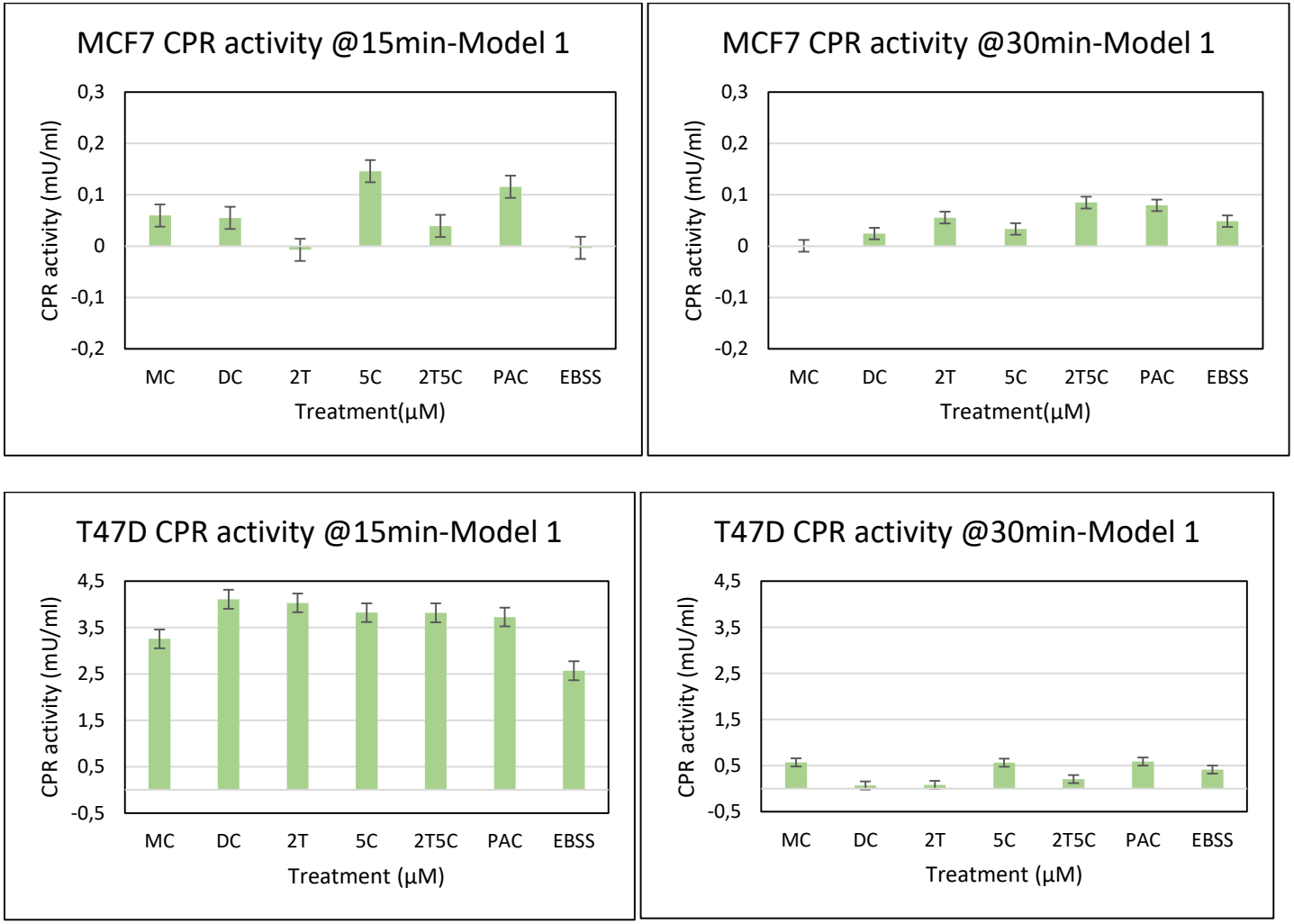


Figure 16: Showing CPR activity of MCF7 and T47D cells at 15 min and at 30 min. MCF7 and T47D cells were treated with Media, diluent, 2µM Tamoxifen, 5µM CBD, 2µM Tamoxifen + 5µM CBD, Paclitaxel and 1X EBSS according to model 1 (single-dose treatment). Error bars as mean ± SD.

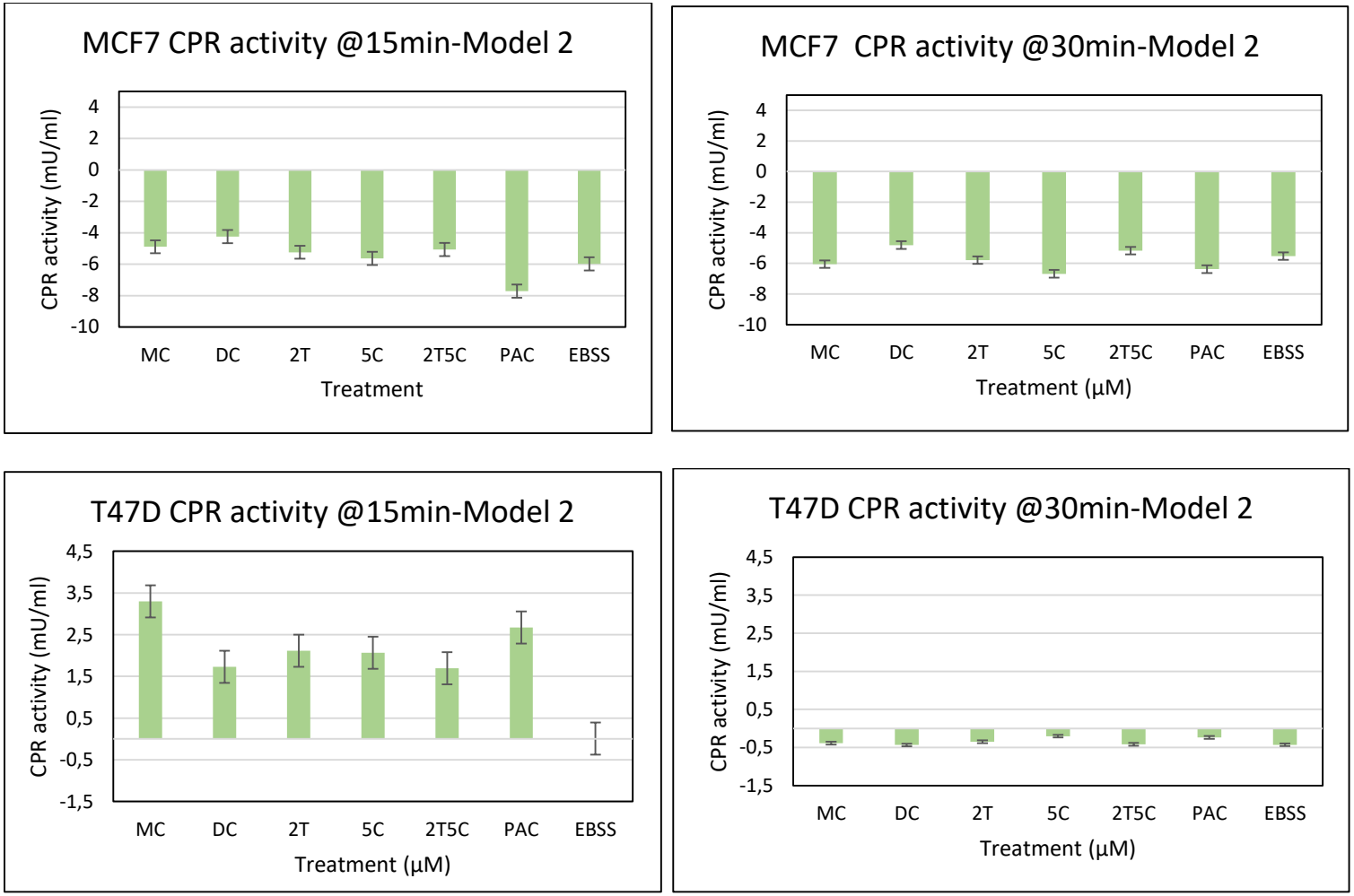


Figure 17: Showing CPR activity of MCF7 and T47D cells at 15 min and at 30 min. Negative values indicate no CPR activity detected. MCF7 and T47D cells were treated with Media, diluent, 2µM Tamoxifen, 5µM CBD, 2µM Tamoxifen + 5µM CBD, Paclitaxel and EBSS according to model 2 (daily-replacement treatment). Error bars as mean ± SD.

3.5. Immunolocalization of LC3B, P62 and BECN1

3.5.1. Antibody optimization

Primary and secondary antibodies for LC3B, P62 and BECN1 (each of these proteins plays a role in the autophagy cascade) were optimized for staining intensity, and the most appropriate concentrations which resulted in more punctate staining (provides information about the localization and activity of the protein of interest) and less background staining were chosen. For mouse monoclonal anti-LC3B, 1:500 was chosen, for rabbit monoclonal anti-SQSTM1/p62, 2.5 µg/ml was chosen and for rabbit polyclonal anti-BECN1, 1:50 was chosen as the optimal primary antibody concentration (Appendix I). All secondary antibodies (AF594, AF488 and AF647) were diluted at 1:1000 following optimization.

Note on the antibodies: LC3B, BECN1 and P62 primary antibodies expired in October 2021. Optimization of the antibodies was conducted in October 2021 and positive results were observed but the was a lag time of four months between the optimization and the experiments hence the varying outcomes in the antibody staining.

The decrease in the quality of staining or the loss of antibody staining completely was observed in all three proteins of interest (especially LC3B), across the various treatment groups in both the single-dose treatment model (model 1) and the daily-replacement treatment model (model 2). P62 exhibited levels of staining that could be quantified whereas LC3B staining could not be quantified as it was non-specific throughout and BECN1 could not be quantified because specific staining was observed in less than 50% of the treatment groups, therefore no further quantitative analysis could be performed on LC3B and BECN1 images (Appendix I). BECN1 images could only be analyzed by observation in the few treatment groups that showed specific staining.

3.5.2. P62 and BECN1 protein expression with single-dose treatment model (model 1) -MCF7 and T47D cells.

The expression of P62 was measured in MCF7 and T47D cells across both treatment models. In treated MCF7 cells, P62 expression was low in most treatment groups including combined CBD and Tamoxifen treatment, single reagent treatment groups and positive controls but significantly higher in the diluent control (Figure 18 and Figure 19; Appendix I). MCF7 cells treated with combined CBD and Tamoxifen showed low but detectable P62 expression levels as well as in the single reagent treatments (2 μM Tamoxifen alone and 5 μM CBD alone). The combination of Tamoxifen with CBD resulted in significantly higher P62 expression compared with Tamoxifen and CBD when administered individually (Figure 14 and Appendix I). Paclitaxel, a positive control for cell death and 1X EBSS, an inducer of autophagy, were significantly lower in P62 expression compared with all the other treatment groups in cells treated according to the single-dose treatment model (model 1) (Figure 18 and Figure 19; Appendix I).

In the single-dose treatment model (model 1) T47D cells, P62 expression was significantly lower in cells treated with combined CBD and tamoxifen and single treatments in comparison to the media and diluent controls. Furthermore, P62 expression in the combined CBD and tamoxifen treatment group was significantly higher compared with paclitaxel expressing the lowest levels of P62 across all the treatment groups.

In MCF7 cells treated according to the single-dose treatment model (model 1), BECN1 expression was not observed in the combined CBD and tamoxifen treatment group, single treatment groups, positive controls, and diluent control but punctate BECN1 expression was observed in the media control group. For the T47D cells, in the single-dose treatment model (model 1), combined CBD and tamoxifen treatment, single reagent treatment, positive controls and media control cells had little BECN1 expression within their cytoplasm, which is indicated by the grey arrows (Figure 18), but the diluent control cells expressed high BECN1. T47D cells were expressing more BECN1 in the combined CBD and tamoxifen treatment group and across the other treatment groups compared with MCF7 cells.

3.5.3. P62 and BECN1 protein expression with daily-replacement treatment model (model 2) - MCF7 and T47D cells

In MCF7 cells treated according to the daily-replacement treatment model (model 2), P62 expression in cells treated with combined CBD and tamoxifen was significantly higher (as seen by the high mean value which signifies a significant difference in protein expression) than the diluent control which showed the lowest levels of expression. All the other treatment groups showed higher P62 in comparison to paclitaxel and EBSS controls. T47D cells showed significant differences in P62 expression in the combined CBD and tamoxifen treated cells compared with all other treatment groups (Figure 18 and Appendix I). In T47D cells treated with combined CBD and tamoxifen and tamoxifen only, P62 expression was significantly lower than in cells treated with CBD only thus suggesting a more active role of CBD in P62 localization within the cytoplasm (Figure 18 and Appendix I).

In the daily treatment replacement model, MCF7 cells treated with combined CBD and tamoxifen expressed exceptionally low BECN1 and most of the treatment groups did not express BECN1, only cells treated with tamoxifen showed punctate BECN1 staining (Figure 20). In T47D cells, the combined CBD and tamoxifen, single reagent treatment and positive control groups showed significantly lower BECN1 levels compared with the diluent control cells which showed significantly higher BECN1 expression. T47D cells treated with tamoxifen only showed BECN1 staining but none was observed in the CBD only treated cells. The observed punctate BECN1 expression in combined CBD and tamoxifen treated cells may be due to the action of tamoxifen and not necessarily CBD.

In summary, P62 and BECN1 were expressed in both MCF7 and T47D cells across both treatment models. Combined CBD and tamoxifen treatment is effective at inducing P62 and BECN1 autophagy markers thus suggesting that it effectively promotes the initiation and nucleation steps of autophagy. P62 and BECN1 are highly expressed in T47D cells compared with MCF7 cells thus indicating less autophagic activity in T47D cells compared with MCF7 cells. The daily - replacement treatment model (model 2) is more effective at promoting P62 protein expression compared with the single -dose treatment model (model 1) with CBD and tamoxifen treatment.

T47D cells have higher P62 protein expression compared with MCF7 cells which signifies translational efficiency in T47D cells.

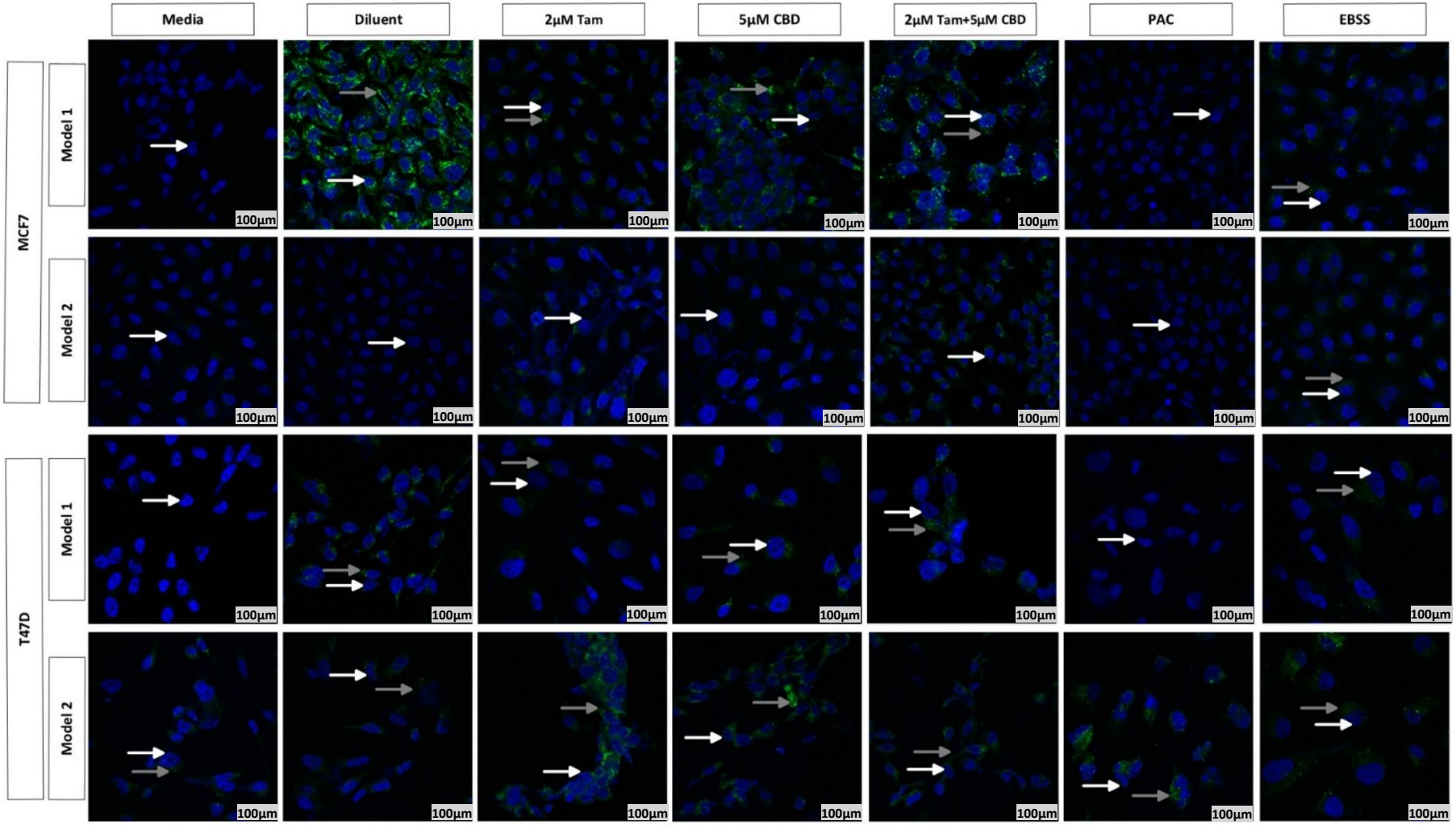


Figure 18: Photomicrographs showing P62 expression (green fluorescence) in MCF7 and T47D breast cancer cells treated with media, diluent, tamoxifen, CBD, combined CBD and tamoxifen, Paclitaxel and 1X EBSS. White arrow (Dapi stained nuclei) and grey arrow (P62 in the cytoplasm). Scale bar= 100 µm.

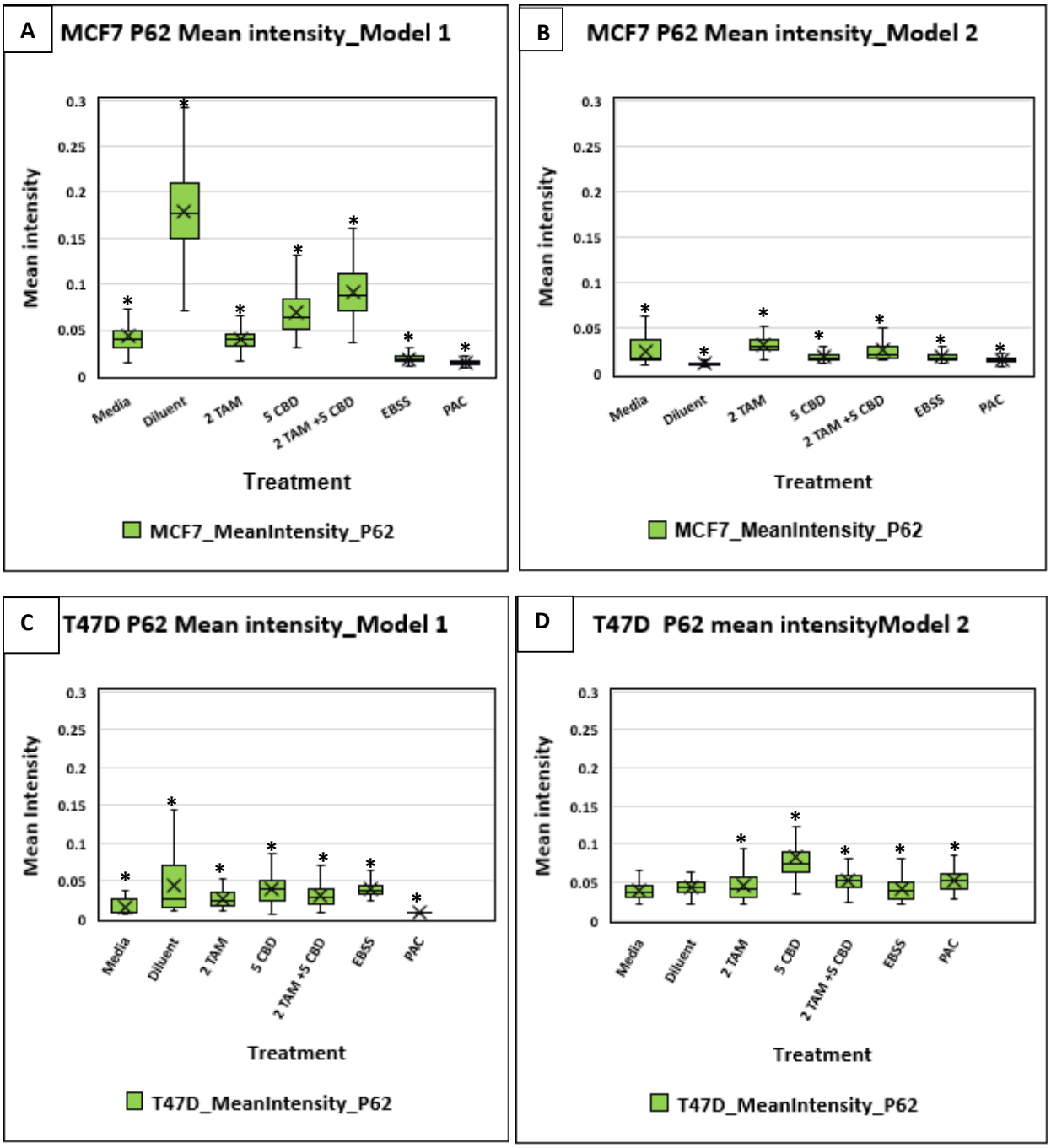


Figure 19: Box and Whisker plots showing P62 expression levels in breast cancer cells treated with media, diluent, tamoxifen, CBD, combined CBD and tamoxifen, Paclitaxel and 1X EBSS. The X within the box indicates the mean and the line within the box indicates the median value. A: MCF7 Model 1, B: MMCF7 Model 2, C: T47D Model 1 and D: T47D Model 2.

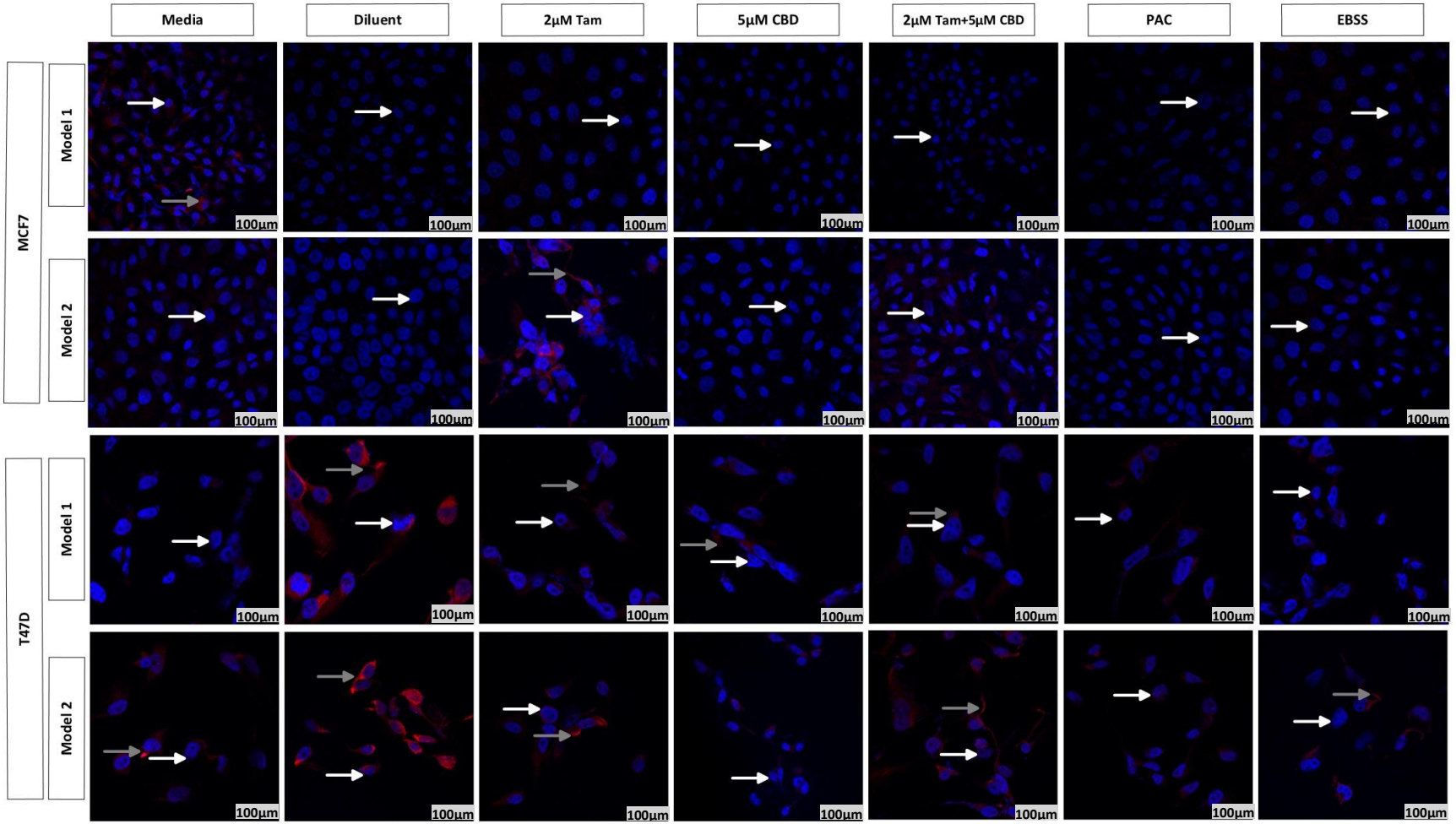


Figure 20: Photomicrographs showing BECN1 expression (red fluorescence) in MCF7 and T47D breast cancer cells treated with media, diluent, tamoxifen, CBD, combined CBD and tamoxifen, Paclitaxel and 1X EBSS. White arrow (Dapi stained nuclei) and grey arrow (BECN1 in the cytoplasm). Scale bar= 100 µm.

3.6. Gene expression of *LC3B*, *P62* and *BECN1*

P62, *BECN1* and *LC3B* genes that encode proteins involved in cell death and cell survival pathways were investigated to determine the effects of combined CBD and tamoxifen treatment in MCF7 and T47D cells. Baseline levels of expression were established in cells treated with media only (fold change=1) and were used as a reference for calculating fold change in gene expression. Fold change in gene expression was determined across all treatment groups in the single-dose treatment model (model 1) and the daily-replacement treatment model (model 2) in T47D cells (Appendix J). In MCF7 cells, gene expression was undetermined for all genes of interest across both treatment models. Undetermined Cq values in this cell line (MCF7) may have resulted from low amounts of target RNA or compromised sample integrity, these samples were not analysed further.

No significant differences in gene expression were found in the treatment groups within the quantified T47D cells and across the treatment models, but trends are presented here.

3.6.1. LC3B, P62 and BECN1 gene expression with single-dose treatment model (model 1) - T47D cells

LC3B expression was upregulated ($p>0.05$) in the diluent control cells compared with all other treatment groups treated according to the single-dose treatment model (model 1) (Figure 19A). Cells treated with combined CBD and tamoxifen showed slight *LC3B* upregulation ($p>0.05$) and similar *LC3B* upregulation was observed in CBD only and 1X EBSS treated cells. In tamoxifen-treated cells *LC3B* expression was highly upregulated compared with other treatment groups, thus suggesting increased potential for autophagic activity in cells treated with 2 µM tamoxifen only. In paclitaxel treated cells, *LC3B* expression was downregulated ($p>0.05$) in relation to the media control cells and the other treatment groups (Figure 21A). This suggests that T47D cells were less susceptible to Paclitaxel and *LC3B* transcription was suppressed (Figure 21A). Combined CBD and tamoxifen treatment resulted in *P62* downregulation($p>0.05$) (Figure 21C); however, *P62* expression was slightly upregulated in the rest of the treatment groups including CBD only

and tamoxifen only treated cells, with tamoxifen showing the greatest levels of upregulation ($p>0.05$). These findings suggest that CBD and tamoxifen are more effective at enabling *P62* upregulation when administered individually but this effect was reduced when administered together. *BECN1* expression was slightly upregulated ($p>0.05$) across all treatment groups, with 2 µM tamoxifen exhibiting the highest level of expression ($p>0.05$) which may suggest potential for autophagic activity (Figure 21).

3.6.2. LC3B, P62 and BECN1 expression with daily-replacement treatment model (model 2) - T47D cells

In T47D cells treated according to the daily-replacement treatment model (model 2), *LC3B* was upregulated ($p>0.05$) only in the 1X EBSS and Paclitaxel treated cells (Figure 21) and downregulated ($p>0.05$) in the rest of the treatment groups (Figure 21A) which may suggest down regulation of autophagy in these cells thus preventing intact autophagic activity. *P62* gene expression with the diluent control cells and drug treated cells (2 µM tamoxifen, 5 µM CBD and combined CBD and tamoxifen treatment) resulted in baseline levels of *P62* expression (Figure 21B). Like *LC3B* expression, the positive controls (Paclitaxel and 1X EBSS) resulted in slight *P62* upregulation ($p>0.05$) compared with the baseline levels of expression. *BECN1* expression was downregulated across the treatment groups except in the 1X EBSS treated cells where it was slightly upregulated ($p>0.05$) (Figure 21C). These findings suggest that, in the daily-replacement treatment model (model 2), combined CBD and tamoxifen treatment may have impaired autophagy and the same can be suggested for the single reagent treated cells.

In summary, combined CBD and tamoxifen treatment may have induced autophagy in the single-dose treatment model (model 1) as shown by slight upregulation of *LC3B* and *BECN1* expression ($p>0.05$). In contrast, in the daily-replacement treatment model (model 2), *LC3B* and *BECN1* expression was downregulated ($p>0.05$) in the combined CBD and tamoxifen treatment group and the single reagent treatment groups. These findings suggest that combined CBD and tamoxifen treatment promotes the expression of genes that encode for proteins involved in autophagy with the single-dose treatment model compared with the CBD only and positive controls, but less effective in promoting the expression of autophagy genes compared with

tamoxifen only treatment. In the daily-replacement treatment model combined CBD and tamoxifen may result in impaired autophagy as *LC3B* and *BECN1* expression levels are down regulated and remain below baseline levels. *P62* expression with combined CBD and single reagent treatments was upregulated with the single-dose treatment model (model 1) but remained at baseline levels in the daily-replacement model (model 2), thus suggesting that the single-dose treatment model (model 1) may promote an increase in autophagic activity compared with the daily-replacement model (model 2).

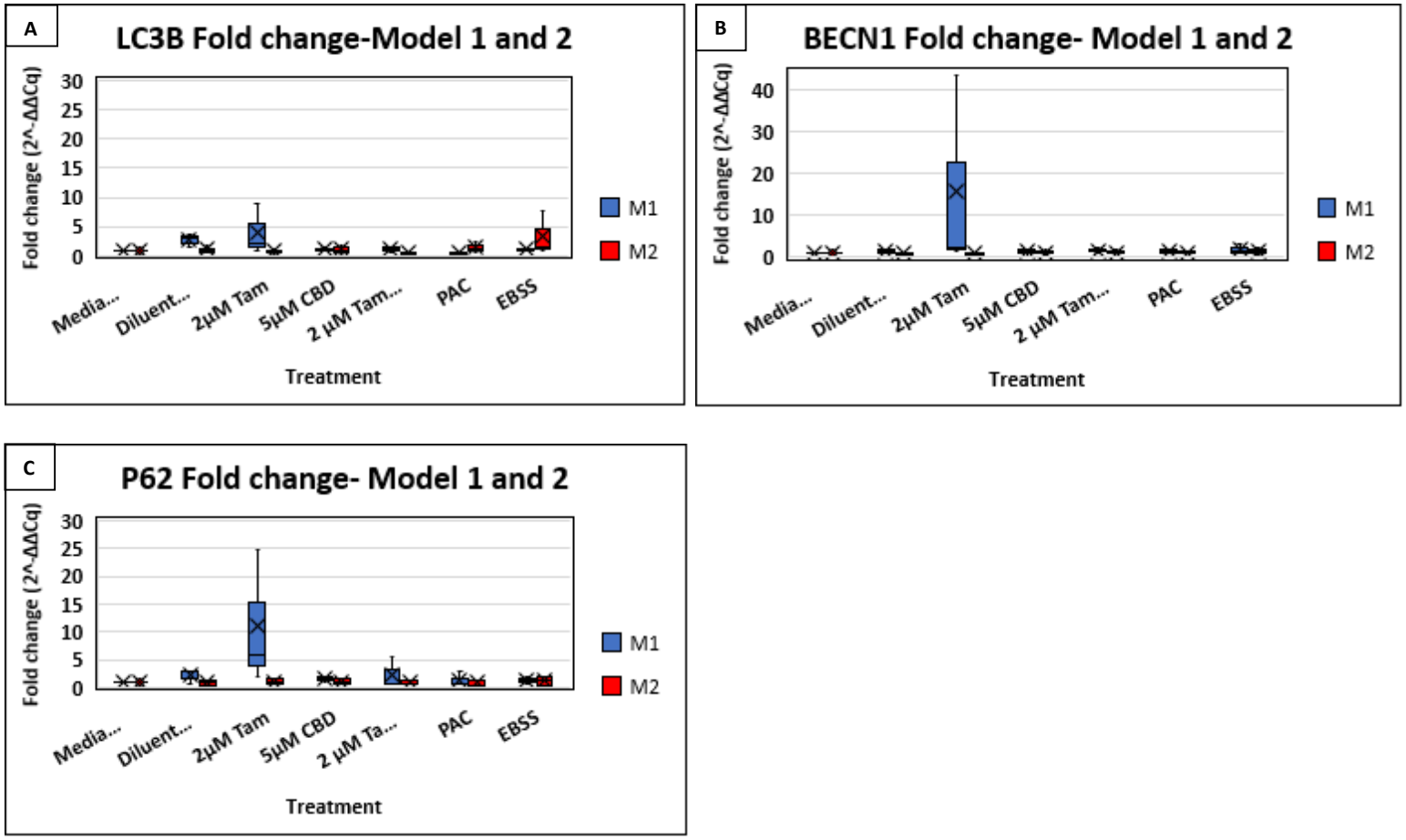


Figure 21: Box and Whisker plots showing *LC3B, P62 and BECN1* fold change in T47D breast cancer cells treated with media, diluent, tamoxifen, CBD, combined CBD and tamoxifen, Paclitaxel and 1X EBSS ($p>0.05$). The X within the box indicates the mean and the line within the box indicates the median value. A: T47D Model 1(M1) *LC3B* and Model 2(M2) *LC3B*, B: T47D Model 1(M1) *P62* and Model 2(M2) *P62* and C: T47D Model 1(M1) *BECN1* and Model 2 (M2) *BECN1.*

4.Discussion

This study aimed to investigate the effects of combined CBD and tamoxifen treatment on the cell death and cell survival mechanisms in hormone-dependent breast cancer cell lines, exemplified by the MCF7 and T47D cell lines. This is essential to know because there is increasing usage of CBD in combination with breast cancer treatment drugs and the interactions of CBD with these drugs may affect overall treatment outcomes. CBD has been shown to induce either pro-death or pro-survival autophagy in cancer where Beclin 1 and P62 have been shown to be key players in the balancing act between pro-death mechanisms and pro-survival mechanism (Gump and Thorburn, 2011; Schoeman *et al*., 2020; Sultan *et al*., 2018; Surapaneni *et al*., 2022). More studies targeting specific drugs in breast cancer cell lines are needed to help understand this balancing act. The interplay between metabolic enzyme activity, pro-survival autophagy and pro-death autophagy with combined CBD and tamoxifen treatment is of great interest as it may provide insight in the development of future treatment strategies.

To determine the cytotoxic effects of combined CBD and tamoxifen, multiple CBD concentrations (5 µM, 7.5 µM and 10 µM) which were previously tested in literature (Shrivastava *et al*., 2011), were investigated using two treatment models: single-dose treatment (model 1) and daily-replacement treatment (model 2) at different time points (24 h, 48 h, and 72 h). To assess the cytotoxic effects of the different concentrations on breast cancer cell lines, cell viability (using the neutral red assay) and cell migration (using the scratch assay) following which an optimal concentration was chosen for downstream experiments. Of all the three investigated concentrations, 5 µM CBD closely correlated with the IC50 value in the range 2-5 µM and was chosen as the optimal concentration and 48 h as the optimal treatment duration. The latter treatment conditions were used in subsequent techniques to determine cell proliferative potential, CPR activity, and the changes in the expression of autophagy markers (LC3, BECN1 and P62).

4.1. The effects of combined CBD and Tamoxifen on MCF7 and T47D cell viability, migration, and proliferation.

The neutral red assay and the scratch assay provide an indication of cell survival and are useful to optimize cell culture conditions. In this study, the neutral red assay cell viability and growth scratch assay were conducted on cells in media only to observe their normal cell viability and wound healing behavior against that of cells treated with CBD and tamoxifen over a period of 72 h. MCF7 cells which represent a model of early-stage breast cancer express less proteins compared to the T47D cells, although oestrogen receptor alpha is more abundant in MCF7 cells (Aka and Lin, 2012). Notably, T47D cells have a higher expression of oestrogen receptor beta than MCF7 cells and are considered a more highly aggressive luminal phenotype cell line (Pather and Augustine, 2020). Notably CBD can function not merely through CB1 and CB2 receptors but is also able to act via a range of GPCRs (Dobovisek *et al*., 2022;Seltzer *et al*.,2020). The variations in molecular profiles between the cell lines may explain the different responses to CBD and tamoxifen.

The findings of this study showed a decrease in cell viability in MCF7 and T47D cells across both treatment models with 5 µM, 2 µM tamoxifen and a combination of CBD and tamoxifen at these concentrations, when compared with cells exposed to the diluent. While the decrease in cell viability was observed in both cell lines, it is important to note that this decrease was accelerated in T47D cells, and this may be explained by the high protein profile of this cell line which suggests that there are more receptors, and varied receptors (Radde *et al*.,2014;Aka and Lin, 2012), available for CBD and tamoxifen to bind and exert their effects. The additive negative effects of combined CBD and tamoxifen on cell viability observed in this study in T47D cells align with those observed in a study by Dobovišek *et al*. (2022) where 5 µM CBD (which is the same concentration used in the present study) was added to cells treated with 2.5 µM tamoxifen (which is 0.5 µM higher than the concentration used in the present study) resulted in an accelerated decrease in cell viability. While similar effects of CBD and tamoxifen on cell viability were observed in MCF7 cells in our study, the results reported by Dobovišek *et al*., (2022) on MCF7 cells contradicted

these findings because combined CBD and tamoxifen treatment did not have an additive effect in decreasing MCF7 cell viability in their study.

In addition to inducing cell death to limit tumour growth, understanding the impact of CBD and Tamoxifen on the capacity of cells to migrate *in vitro* would shed light on the *in vivo* process of metastasis (Almeida *et al*., 2023; Massi *et al*., 2013; Shrivastava *et al*., 2011). In this study, the scratch assay evaluated the ability of cells to migrate back into the wound area following treatment with 5 µM CBD and 2 µM tamoxifen. Interestingly in T47D cells in the daily-replacement model (model 2), 5 µM CBD combined with tamoxifen enhanced tamoxifen-induced cell death (Zheng *et al*., 2007). The cell viability and cell migration results together suggest that the cell death effects of combined treatment are attenuated when only a single-dose of treatment is used but are enhanced when drugs are administered more than once (Shrivastava *et al*., 2011; Dobovišek *et al*., 2022). Moreover, the present study showed that CBD inhibits wound closure at higher concentrations but at lower concentrations, cells can recover and promote wound closure after 72 h of treatment in single-dose treatment (model 1) whereas in the daily-replacement treatment (model 2) cells die due to treatment even with the lowest CBD concentration. These findings further indicate how cell responses vary in a concentration, time, and cell type dependent manner (Pather *et al.*, 2019; Xulu, Duarte and Augustine, 2020) and the discovery of optimum combined treatment concentrations are of significant value in guiding the usage of CBD in conjunction with breast cancer hormone therapy. When a single-dose of tamoxifen was used, wound closure was promoted for the first 24 h, whereas from 48 h to 72 h widening of the scratch area was observed and cells were losing their migration capability as a result of the loss of cellular adhesions. In contrast, when tamoxifen was used daily (model 2), there was accelerated widening in the size of the scratch area, with complete loss of cells after 48 h of treatment in both cell lines. This may be due to the loss of substrate attachment (Pucci, Kasten and Giordano,2000), thus indicating increased potency of tamoxifen in inhibiting wound closure (Lu *et al*., 2020) . The morphological changes observed in MCF7 and T47D cells such as the loss of cell-cell attachment and single rounded cells are all characteristic of cellular stress. These findings were consistent with those of other studies (Pucci, Kasten and Giordano, 2002; Liang, Park, and Guan, 2007; Lu *et al*., 2021), showing that tamoxifen inhibits oestrogen receptor

positive breast cancer cell growth and development. Contrastingly, in other instances small viable cell clusters were observed, which may indicate aggressive cell profiles and pro-survival mechanisms in a subset of cells (Gao *et al*., 2020; Tu *et al*., 2010; Xulu *et al*., 2020).

Increasing CBD concentrations promoted wound closure for the first 24 h in the single-dose treatment group for both cell lines, following which no noteworthy changes in the wound area were observed. This suggests that a single-dose of 5 µm CBD for 48 h is insufficient to induce cell death. Contrastingly, when CBD was replaced daily, cell growth in the wound area was inhibited further with increasing concentrations. These findings are in line with other studies where cells were treated with 2.5 µM tamoxifen and a range of CBD concentrations from 5 to 30 µM (Shrivastava *et al*., 2011) . In the current study, the combination of CBD with tamoxifen had an increasing, additive negative effect on wound closure when treatment was replaced daily (model 2) as opposed to a single-dose (model 1) whereby few changes were observed in the wound area post the 24 h of treatment, except with 5 µM CBD. This suggests that a single-dose of 5 µM CBD is effective at promoting wound closure or permitting cell recovery, whereas multiple doses inhibit wound closure.

Shrivastava *et al.*, 2011, further showed that CBD combined with tamoxifen in T47D cells enhanced the efficacy of tamoxifen, and these were consistent with the findings in this study where 5 µM CBD combined with tamoxifen reduced cell viability and was further supported by the inhibition of wound closure compared with tamoxifen only. The inhibition of wound closure may translate to the ability of combined treatment to reduce tumour metastasis (Dobovisek *et al*., 2022;Seltzer *et al*.,2020), but this requires further evidence based on animal studies and clinical trials. Furthermore, at higher CBD concentrations combined with tamoxifen, T47D cells maintained their migration capability. This suggests that T47D cells may comprise of more growth stimulating proteins and an intact G2/M phase thus allowing enhanced cell division compared to MCF7 cells (Aka and Lin, 2012; Widowati *et al*., 2021).

Tamoxifen inhibits cell proliferation by oestrogen receptor dependent modulation of gene expression (Klein *et al*., 2013; Kumar *et al*., 2001), while CBD has been shown in selected *in vitro* studies to limit tumour cell proliferation (Lukhele and Motadi, 2016; Shrivastava et al., 2011). In the present study, treatment with combined 5 µM CBD and tamoxifen resulted in inhibition of cell proliferation in both MCF7 and T47D cells across both treatment models, with T47D cells showing substantial inhibition of cell proliferation. Interestingly, when CBD was administered alone in the daily-replacement model it did not inhibit T47D cell proliferation. These results further indicate the additive effects of combined CBD and tamoxifen treatment on cell proliferation, especially in MCF7 cells in a dose dependent manner. These findings suggest potential anti-proliferative effects of CBD as found in other studies (Lukhele and Motadi, 2016; Shrivastava et al., 2011), which are increased when CBD is combined with tamoxifen. These findings collectively suggest that CBD has an additive function on the cytotoxic effects of tamoxifen thus resulting in loss of cell viability, loss of cell migration and inhibition of proliferation and consequently cell death.

4.2. The metabolic effects of Tamoxifen and CBD in MCF7 and T47D cells

Tamoxifen is metabolized to its active metabolite by CYP450 family enzymes which play an essential role in drug metabolism by either activation or inactivating the pro-drugs (Singh, Francis, and Michael, 2011). CYP450 family enzymes metabolize tamoxifen into its active metabolites, which have a higher affinity for the ER, through a series of reactions mediated by the cytochrome P450 reductase (CPR) (Kumar *et al*., 2001) . Breast cancer cells express CYP450 subtypes, which can either activate or deactivate drugs in these cells (Kuhn *et al*., 2020; Murray *et al*., 2010; Sneha *et al*., 2021). Tamoxifen has been shown to be a substrate of CYP450 enzyme subtypes and thus to induce CPR activity (Cronin-Fenton,Damkier and Lash, 2014).

In the present study, in model 1 T47D cells had markedly higher CPR activity at 15 min compared to MCF7 cells. Under tamoxifen treatment in MCF7 cells, CPR activity was not detected at 15 min, but had risen by 30 min. Contrastingly, 5µM CBD alone induced greater CPR activity at 15 min which reduced at the 30 min mark. However, when combined with Tamoxifen, CBD enhanced

CPR activity at both timepoints, indicating the successful initiation of electron transfer from NADPH to the CYP450 enzymes which is catalyzed by CPR (Guengerich *et al*., 2009; Yim *et al*., 2005).T47D cells which had greater CPR activity at 15 min in all treatment groups, showed reduced CPR activity at 30 min. In T47D cells, CBD did not appear to affect CPR activity when combined with Tamoxifen. In all groups, the reduction in CPR activity from a higher level of activity reflects CYP450 catalysed reactions such as the conversion of drug compounds to their pro-drugs (Klein et al.,2013;Ortiz de Montellano,2013; Singh, Francis, and Michael, 2011). These results, when compared to controls, suggest that a single dose of CBD does not prevent the capacity of CPR to catalyse the formation of Tamoxifen metabolites via the CYP450 enzymes (Ahmed and Wober, 2020; Maximov *et al*., 2014), in T47D cell, and may enhance the process in MCF7 cells. These findings contrast with those of Nasrin *et al*., (2021), who found that CBD at varying concentrations (1 µM and 10 µM) was able to reversibly and directly inhibit CYP enzyme activity in microsomes derived from human embryonic kidney cells 293 (HEK293), echoing another study on human liver microsomes (Jiang *et al*., 2011). Notably, Nasrin *et al*, (2021) also found that CBD shows time-dependent inhibition of specifically CYP2D6, which is instrumental in metabolising both Tamoxifen and CBD (Ahmed and Wober, 2020; Maximov *et al*., 2014; Jiang*et al*.,2011).

In the present study, in contrast to the results obtained from the single-dose model, with the daily-replacement treatment model there was no CPR activity detected in MCF7 cells across both time points in all treatment groups. The lack of detection of CPR activity at 15 min in MCF7 cells, may be indicative of an increase in pro-drug bioavailability at an earlier time, or conversely, decreased efficacy of CPR in reducing CYP450 (Wiseman and Lewis, 1996; Jiang *et al*., 2011) . Further studies are required to unpack this finding. Contrastingly, in T47D cells there was CPR activity at 15 minutes which was lost 15 minutes later in all treatment groups. While CPR activity in extrahepatic tissues has been noted to be lower than in hepatocytes (the primary mediators of drug metabolism), CPR activity is also enhanced in aggressive, malignant tissues (Barata *et al.,* 2022). T47D cells are notably more aggressive than MCF7 cells (Pather and Augustine, 2020), and thus may have a greater potential for metabolic activity (Aka and Lin, 2012). These findings suggest that repeated use of CBD (model 2) has inhibitory effects on CPR in MCF7 cells specifically

and that such assays require kinetic evaluation that permit monitoring in real-time to gain an accurate understanding of enzymatic activity.

4.3. The effects of Tamoxifen and CBD on LC3B, P62 and BECN1 mRNA and Protein expression in MCF7 and T47D cells

Autophagy has a biphasic role, it can promote cell survival or induce cell death when two main proteins are involved: P62 which plays a selective role for autophagic degradation of proteins and BECN1, a pro-autophagic protein which is also involved in nucleation during the autophagy process (Gump and Thorburn, 2011; Luo and Rubinsztein, 2010). P62 plays a role in selective autophagy, whereby specific aggregates are directed to the lysosomes under nutrient rich environments (Lippai and Low, 2014) . In this study we aimed to investigate whether LC3B, P62 and BECN1 gene and protein expression levels are altered with combined CBD and tamoxifen treatment in MCF7 and T47D cells across two treatment models: the single-dose treatment model (model 1) and the daily-replacement treatment model (model 2). The mRNA expression was undetermined for all three genes of interest [*LC3B*, *P62 (SQTM1),* and *BECN1*] in MCF7 cells across both the single-dose treatment model (model 1) and the daily-replacement treatment model (model 2) but was quantified in T47D cells. Furthermore, in this study, LC3B and BECN1 protein expression levels could not be accurately quantified for both MCF7 and T47D cells due to the reduced fluorescence and therefore no further analysis was conducted for those proteins (LC3B and BECN1), only P62 was analysed further.

In T47D cells *P62* expression was substantially upregulated with tamoxifen only treatment and with combined CBD and tamoxifen treatment in the single-dose model. The upregulation of *P62* resulted in efficient translation in the cytoplasm and measurable P62 levels. P62 protein levels inversely correlate with autophagy. P62 protein promotes mammalian target of rapamycin complex 1 (MTORC1) activation by participating in its translocation to the lysosomes where it then promotes cell growth and inhibits autophagy (Nihira *et al*., 2014; Ning and Wang, 2018; Sánchez-Martın and Komatsu, 2018). The P62 protein expression levels with the daily-replacement treatment model (model 2) in T47D cells provides further evidence of the decreased

susceptibility of T47D cells to combined CBD and tamoxifen treatment as outlined in this study and other studies(Casbas-Hernandez, Fleming and Troester, 2011; Aka and Lin, 2012) .

Contrastingly, low P62 protein expression was observed in MCF7 cells, although combined CBD and tamoxifen treatment induced a significant increase under single-dose treatment. This was not observed in the same model in T47D cells, but rather combined CBD and tamoxifen treatment in the daily-replacement treatment model only marginally increased p62 mean intensity. The high cytoplasmic P62 levels may indicate autophagy impairment in MCF7 cells and the low *P62* and *LC3B* gene expression levels in T47D may indicate low levels of autophagy in the single-dose model (Lippai and Low, 2014) . However, for T47D cells in the daily replacement treatment model, low *LC3B* expression levels combined with the high P62 protein expression levels signify decreased autophagy (Adams *et al*., 2018).Collectively, the results of this study indicate that CBD when combined with tamoxifen may enhance cell death mechanisms in MCF7 breast cancer cells but in T47D cells, it may drive cell survival mechanisms.

4.4 Limitations of the study and future perspectives

4.4.1. Study limitations

- The lack of gene detection in MCF7 cells prevented us from deducing whether the autophagy markers of interest are upregulated or downregulated in these cells with combined CBD and tamoxifen treatment.
- Optimization of the antibodies for immunofluorescence was conducted in late 2021 just prior to the expiry date of the antibodies. Thus, while optimal fluorescence was established, by the time the antibodies were used for experiments in early 2022, there was less, or no specific staining observed for the autophagic markers of interest. The candidate quantified fluorescence for P62 and thus learned the software application, in addition to the immunofluorescence technique. However, conclusive information cannot be drawn from these results.

4.4.1. Future perspectives

- The immunofluorescence and qPCR of this study would need to be repeated to accurately ascertain whether combined CBD and Tamoxifen treatment induce autophagy. There is a need to investigate markers that are specifically involved in apoptosis such as Bcl-2 and caspase 3 activity alongside the autophagy markers to clearly deduce the interplay between cell death mechanisms due to combined CBD and cancer treatment drugs.
- The CYP450 subtypes that are specific for CBD and tamoxifen enzyme activity need to be investigated using a kinetic mode that would help unpack more accurately, the metabolic process.
- The effects of CBD using other chemotherapeutic drugs in other cell lines needs to be elucidated, with additional cytotoxicity assays employed.
- Experiments to determine whether tamoxifen or CBD, or a combination of both, induces the expression of P-glycoprotein and increases its activity.
- Use the Chou and Talalay method to perform combination experiments to determine drug interactions.

5.Conclusion

In summary these findings suggest that MCF7 cells are susceptible to combined CBD and tamoxifen treatment with evidence of the anti-tumour potential of this treatment through reduced cell viability, decreased metabolic activity and low cell proliferation. These desirable anti-cancer effects are enhanced with the daily-replacement treatment model (model 2) in both MCF7 and T47D cells. Moreover, in the single dose model MCF7 cells showed CPR activity, an indicator of CYP450 and thus Tamoxifen metabolism even in the presence of CBD, in the daily replacement model, this CPR activity was lost. T47D cells showed maintenance of CPR activity in both models, regardless of the treatment used. Combined CBD and tamoxifen treatment may induce autophagy as can be seen by the presence of measurable P62 (which is involved in the proteasomal degradation of ubiquitinated proteins in pro-survival autophagy). The accumulation of P62 with daily-replacement treatment, particularly in the T47D cells, signifies decreased efficacy of combined CBD and tamoxifen treatment at inducing pro-death autophagy

and this treatment may consequently promote breast cancer cell survival. The findings of this study need to be repeated, particularly with respect to understanding the role of autophagy in cell death and cell survival. Nevertheless, the results highlight the importance of carefully considering the administration of CBD alongside tamoxifen as differing molecular profiles can lead to either pro-death or pro-survival mechanisms being initiated.

References

Adams, O. & Janser, F.A. & Dislich, B. & *et al*. (2018) A specific expression profile of LC3B and P62 is associated with nonresponse to neoadjuvant chemotherapy in esophageal adenocarcinomas. *PLOS ONE*, 13 (6). doi: 10.1371/journal.pone.0197610

Ahmed, N.S. & Wober, J. (2020) Synthesis of novel flexible tamoxifen analogues to overcome CYP2D6 polymorphism and their biological evaluation on MCF-7 Cell Line. *Drug Development Research*, 81 (4): 444–455. doi:10.1002/ddr.21637

Ahn, H.J. & Jung, S.J. & Kim, T.H. & *et al*. (2015) Differences in clinical outcomes between Luminal A and B type breast cancers according to the St. Gallen Consensus 2013. *Journal of Breast Cancer*, 18 (2): 149. doi:10.4048/jbc.2015.18.2.149

Aka, J.A. & Lin, S.-X. (2012) Correction: Comparison of functional proteomic analyses of human breast cancer cell lines T47D and MCF7. *PLOS ONE*, 7 (4). doi:10.1371/annotation/18f08a33-35e1-4bf9-8d21-476757dccbef

Almeida, C.F. & Teixeira, N. & Valente, M.J. & *et al*. (2023) Cannabidiol as a promising adjuvant therapy for estrogen receptor-positive breast tumors: Unveiling its benefits with aromatase inhibitors. *Cancers*, 15 (9): 2517. doi:10.3390/cancers15092517

Almogi-Hazan, O. & Or, R. (2020) Cannabis, the endocannabinoid system and immunity—the journey from the bedside to the bench and back. *International Journal of Molecular Sciences*, 21 (12): 4448. doi:10.3390/ijms21124448

Al-thoubaity, F.K. (2020) Molecular classification of breast cancer: A retrospective cohort study. *Annals of Medicine and Surgery*, 49: 44–48. doi: 10.1016/j.amsu.2019.11.021

Alzahrani, A.M. & Rajendran, P. (2020) The multifarious link between cytochrome p450s and cancer. Oxidative Medicine and Cellular Longevity, 2020: 1–18. doi:10.1155/2020/3028387

An, D. & Peigneur, S. & Hendrickx, L.A. & *et al*. (2020) Targeting cannabinoid receptors: Current status and prospects of natural products. *International Journal of Molecular Sciences*, 21 (14): 5064. doi:10.3390/ijms21145064

Armat, M. & Oghabi Bakhshaiesh, T. & Sabzichi, M. & et al. (2015) The role of six1 signaling in paclitaxel-dependent apoptosis in MCF-7 cell line. *Bosnian Journal of Basic Medical Sciences*,. doi:10.17305/bjbms.2016.674

Arnold, M. & Morgan, E. & Rumgay, H. & *et al*. (2022) Current and future burden of breast cancer: Global Statistics for 2020 and 2040. *The Breast*, 66: 15–23. doi: 10.1016/j.breast.2022.08.010

Atalay, S. & Jarocka-Karpowicz, I. & Skrzydlewska, E. (2019) Antioxidative and anti-inflammatory properties of Cannabidiol. *Antioxidants*, 9 (1): 21. doi:10.3390/antiox9010021

Atalay, S. & Jarocka-Karpowicz, I. & Skrzydlewska, E. (2019) Antioxidative and anti-inflammatory properties of Cannabidiol. *Antioxidants*, 9 (1): 21. doi:10.3390/antiox9010021

Ates, G. & Vanhaecke, T. & Rogiers, V. & *et al*. (2017) Assaying cellular viability using the neutral red uptake assay. *Methods in Molecular Biology*, 19–26. doi:10.1007/978-1-4939-6960-9_2

Azubuike, S.O. & Muirhead, C. & Hayes, L. & *et al*. (2018) Rising global burden of breast cancer: The case of sub-saharan africa (with emphasis on Nigeria) and implications for regional development: A Review. *World Journal of Surgical Oncology*, 16 (1). doi:10.1186/s12957-018-1345-2

Bathula, P.P. & Maciver, M.B. (2023) Cannabinoids in treating chemotherapy-induced nausea and vomiting, cancer-associated pain, and tumor growth. *International Journal of Molecular Sciences*, 25 (1): 74. doi:10.3390/ijms25010074

Bekele, R.T. & Venkatraman, G. & Liu, R.-Z. & *et al*. (2016) Oxidative stress contributes to the tamoxifen-induced killing of breast cancer cells: Implications for tamoxifen therapy and resistance. *Scientific Reports*, 6 (1). doi:10.1038/srep21164

Ben-David, U. & Siranosian, B. & Ha, G. & *et al*. (2018) Genetic and transcriptional evolution alters cancer cell line drug response. *Nature*, 560 (7718): 325–330. doi:10.1038/s41586-018-0409-3

Benz, C.C. & Scott, G.K. & Sarup, J.C. & *et al*. (1992) Estrogen-dependent, tamoxifen-resistant tumorigenic growth of MCF-7 cells transfected with HER2/neu. *Breast Cancer Research and Treatment*, 24 (2): 85–95. doi:10.1007/bf01961241

Bobadilla, A.V. & Arévalo, J. & Sarró, E. & *et al*. (2019) in vitro cell migration quantification method for scratch assays. *Journal of The Royal Society Interface*, 16 (151): 20180709. doi:10.1098/rsif.2018.0709

Borenfreund, E. & Puerner, J.A. (1985) Toxicity determined in vitro by morphological alterations and neutral red absorption. *Toxicology Letters*, 24 (2–3): 119–124. doi:10.1016/0378-4274(85)90046-3

Bosch, F. & Mulder, F. & Franken, L. & *et al*. (2023) Effect of the P-glycoprotein inhibitor tamoxifen on edoxaban plasma levels in women with breast cancer. *Thrombosis Research*, 228: 46–53. doi: 10.1016/j.thromres.2023.05.021

Brueggemeier, R.W. & Hackett, J.C. & Diaz-Cruz, E.S. (2005) Aromatase inhibitors in the treatment of breast cancer. *Endocrine Reviews*, 26 (3): 331–345. doi:10.1210/er.2004-0015

Caffarel, M.M. & Andradas, C. & Pérez-Gómez, E. & *et al*. (2012) Cannabinoids: A new hope for breast cancer therapy? *Cancer Treatment Reviews*, 38 (7): 911–918. doi: 10.1016/j.ctrv.2012.06.005

Callaghan, R. & Higgins, C. (1995) Interaction of tamoxifen with the multidrug resistance P-glycoprotein. *British Journal of Cancer*, 71 (2): 294–299. doi:10.1038/bjc.1995.59

Casbas-Hernandez, P. & Fleming, J.M. & Troester, M.A. (2011) Gene expression analysis ofin vitrococultures to study interactions between breast epithelium and stroma. *Journal of Biomedicine and Biotechnology*, 2011: 1–12. doi:10.1155/2011/520987

Chen, W. & Park, S. & Patel, C. & *et al*. (2021) The migration of metastatic breast cancer cells is regulated by matrix stiffness via yap signalling. *Heliyon*, 7 (2). doi: 10.1016/j.heliyon. 2021.e06252

Cho, N. (2016) Molecular subtypes and imaging phenotypes of breast cancer. *Ultrasonography*, 35 (4): 281–288. doi:10.14366/usg.16030

Cianchi, F. & Papucci, L. & Schiavone, N. & *et al*. (2008) Cannabinoid receptor activation induces apoptosis through tumor necrosis factor α–mediated ceramide de novo synthesis in colon cancer cells. *Clinical Cancer Research*, 14 (23): 7691–7700. doi: 10.1158/1078-0432.ccr-08-0799

Cronin-Fenton, D.P. & Damkier, P. & Lash, T.L. (2013) Metabolism and transport of tamoxifen in relation to its effectiveness: New Perspectives on an ongoing controversy. *Future Oncology*, 10 (1): 107–122. doi:10.2217/fon.13.168

Dalby, K. & Tekedereli, I. & Lopez-Berestein, G. & *et al*. (2010) Targeting the pro-death and pro-survival functions of autophagy as novel therapeutic strategies in cancer. *Autophagy*, 6 (3): 322–329. doi:10.4161/auto.6.3.11625

De Blander, H. & Morel, A.-P. & Senaratne, A.P. & *et al*. (2021) Cellular plasticity: A route to senescence exit and tumorigenesis. *Cancers*, 13 (18): 4561. doi:10.3390/cancers13184561

Deng, L. & Feng, J. & Broaddus, R.R. (2010) The novel estrogen-induced gene EIG121 regulates autophagy and promotes cell survival under stress. *Cell Death & Disease*, 1 (4). doi:10.1038/cddis.2010.9

Devinsky, O. & Cilio, M.R. & Cross, H. & *et al*. (2014) Cannabidiol: Pharmacology and potential therapeutic role in epilepsy and other neuropsychiatric disorders. *Epilepsia*, 55 (6): 791–802. doi:10.1111/epi.12631

Ding, L. & Liu, B. & Qi, L. & *et al*. (2009) Anti-proliferation, cell cycle arrest and apoptosis induced by a natural xanthone from Gentianopsis Paludosa Ma, in human promyelocytic leukemia cell line HL-60 cells. *Toxicology in Vitro*, 23 (3): 408–417. doi: 10.1016/j.tiv.2009.01.010

Djavaheri-Mergny, M. & Botti, J. & Codogno, P. (2007) Autophagy and Autophagic Cell Death. In: Apoptosis, Senescence and Cancer, 5. Totowa (New Jersey): *Humana Press*: 93–107. (essay).

Dobovišek, L. & Novak, M. & Krstanović, F. & *et al*. (2022) Effect of combining CBD with standard breast cancer therapeutics. *Advances in Cancer Biology - Metastasis*, 4: 100038. doi: 10.1016/j.adcanc.2022.100038

Donvito, G. & Nass, S.R. & Wilkerson, J.L. & *et al*. (2017) The Endogenous Cannabinoid System: A Budding Source of Targets for Treating Inflammatory and Neuropathic Pain. *Neuropsychopharmacology*, 43 (1): 52–79. doi:10.1038/npp.2017.204

DU, X. & KLASCHIK, K. & MALLMANN, P. & et al. (2018) An experimental model of breast cancer cells: Informative protocol for *in vitro* culture. *Anticancer Research*, 38 (11): 6237–6245. doi:10.21873/anticanres.12979

Ellsworth, R.E. & Blackburn, H.L. & Shriver, C.D. & *et al*. (2017) Molecular heterogeneity in breast cancer: State of the science and implications for patient care. *Seminars in Cell & Developmental Biology*, 64: 65–72. doi: 10.1016/j.semcdb.2016.08.025

Elmore, S. (2007) Apoptosis: A review of Programmed Cell Death. *Toxicologic Pathology*, 35 (4): 495–516. doi:10.1080/01926230701320337

Etienne, M. & Milano, G. & Fischel, J. & *et al*. (1989) Tamoxifen metabolism: *Pharmacokinetic and in vitro study. British Journal of Cancer*, 60 (1): 30–35. doi:10.1038/bjc.1989.214

Farrar, M.C. (2023) *Tamoxifen*. [online] Available from: https://www.ncbi.nlm.nih.gov/books/NBK532905/ (Accessed 03 May 2024).

Freundt-Revilla, J. & Kegler, K. & Baumgärtner, W. & *et al*. (2017) Spatial distribution of cannabinoid receptor type 1 (CB1) in normal canine central and peripheral nervous system. *PLOS ONE*, 12 (7). doi: 10.1371/journal.pone.0181064

Gan, L. & von Moltke, L.L. & Trepanier, L.A. & et al. (2008) Role of NADPH-cytochrome P450 reductase and cytochrome-*B*5/NADH-*B*5Reductase in variability of CYP3A activity in human liver microsomes. *Drug Metabolism and Disposition*, 37 (1): 90–96. doi:10.1124/dmd.108.023424

Gao, Y. & Li, X. & Zeng, C. & *et al*. (2020) CD63+ cancer-associated fibroblasts confer tamoxifen resistance to breast cancer cells through exosomal Mir-22. *Advanced Science*, 7 (21). doi:10.1002/advs.202002518

Gatica, D. & Hu, G. & Liu, X. & *et al*. (2019) The PAT1-LSM complex stabilizes ATG mrna during nitrogen starvation-induced autophagy. *Molecular Cell*, 73 (2). doi: 10.1016/j.molcel.2018.11.002

Gavilán, E. & Giráldez, S. & Sánchez-Aguayo, I. & *et al*. (2015) Breast Cancer Cell Line MCF7 escapes from G1/S arrest induced by proteasome inhibition through a gsk-3β dependent mechanism. *Scientific Reports*, 5 (1). doi:10.1038/srep10027

Gill, J.G. & Piskounova, E. & Morrison, S.J. (2016) Cancer, oxidative stress, and metastasis. *Cold Spring Harbor Symposia on Quantitative Biology*, 81: 163–175. doi:10.1101/sqb.2016.81.030791

Government notices, no43347 (2020) *Government Gazette of South Africa*. Available at: https://www.greengazette.co.za/documents/regulation-gazette-43347-of-22-may-2020-vol-659-no-11118_20200522-GGR-43347 (Accessed: 28 May 2023).

Grada, A. & Otero-Vinas, M. & Prieto-Castrillo, F. & *et al*. (2017) Research techniques made simple: Analysis of collective cell migration using the wound healing assay. *Journal of Investigative Dermatology*, 137 (2). doi: 10.1016/j.jid.2016.11.020

Granada, A.E. & Jiménez, A. & Stewart-Ornstein, J. & *et al*. (2020) The effects of proliferation status and cell cycle phase on the responses of single cells to chemotherapy. *Molecular Biology of the Cell*, 31 (8): 845–857. doi:10.1091/mbc. e19-09-0515

Guengerich, F.P. & Martin, M.V. & Sohl, C.D. & et al. (2009) Measurement of cytochrome P450 and NADPH–cytochrome P450 reductase. *Nature Protocols*, 4 (9): 1245–1251. doi:10.1038/nprot.2009.121

Gump, J.M. & Thorburn, A. (2011) Autophagy and apoptosis: What is the connection? *Trends in Cell Biology*, 21 (7): 387–392. doi: 10.1016/j.tcb.2011.03.007

Guo, L. & Kong, D. & Liu, J. & *et al*. (2023) Breast cancer heterogeneity and its implication in personalized precision therapy. *Experimental Hematology & Oncology*, 12 (1). doi:10.1186/s40164-022-00363-1

Gupta, S. (2001) Molecular steps of death receptor and mitochondrial pathways of apoptosis. *Life Sciences*, 69 (25–26): 2957–2964. doi:10.1016/s0024-3205(01)01404-7

Heery, APRN, AOCNS, CBCN, M. & Corbett, RPh, PharmD, P. & Zelkowitz, MD, R. (2018) Precautions for patients taking tamoxifen. Journal of the Advanced Practitioner in Oncology, 9 (1). doi:10.6004/jadpro.2018.9.1.6

Hellemans, J. & Mortier, G. & De Paepe, A. & *et al*. (2007) *Genome Biology*, 8 (2). doi:10.1186/gb-2007-8-2-r19

Holland, M.L. & Allen, J.D. & Arnold, J.C. (2008) Interaction of plant cannabinoids with the multidrug transporter ABCC1 (MRP1). *European Journal of Pharmacology*, 591 (1–3): 128–131. doi: 10.1016/j.ejphar.2008.06.079

Howell, A. & Howell, S.J. (2023) Tamoxifen evolution. *British Journal of Cancer*, 128 (3): 421–425. doi:10.1038/s41416-023-02158-5

Huestis, M.A. (2007) Human cannabinoid pharmacokinetics. *ChemInform*, 38 (47). doi:10.1002/chin.200747256

Hwang, H.J. & Ha, H. & Lee, B.S. & *et al*. (2022) LC3B is an RNA-binding protein to trigger rapid mrna degradation during autophagy. *Nature Communications*, 13 (1). doi:10.1038/s41467-022-29139-1

Jacobsson, S.O.P. & Rongård, E. & Stridh, M. & *et al*. (2000) Serum-dependent effects of tamoxifen and cannabinoids upon C6 glioma cell viability. *Biochemical Pharmacology*, 60 (12): 1807–1813. doi:10.1016/s0006-2952(00)00492-5

Jain, M.V. & Paczulla, A.M. & Klonisch, T. & *et al*. (2013) Interconnections between apoptotic, autophagic and necrotic pathways: Implications for cancer therapy development. *Journal of Cellular and Molecular Medicine*, 17 (1): 12–29. doi:10.1111/jcmm.12001

Jiang, R. & Yamaori, S. & Takeda, S. & *et al*. (2011) Identification of cytochrome P450 enzymes responsible for metabolism of cannabidiol by human liver microsomes. *Life Sciences*, 89 (5–6): 165–170. doi: 10.1016/j.lfs.2011.05.018

Johänning, J. & Kröner, P. & Thomas, M. & *et al*. (2017) The formation of estrogen-like tamoxifen metabolites and their influence on enzyme activity and gene expression of ADME genes. *Archives of Toxicology*, 92 (3): 1099–1112. doi:10.1007/s00204-017-2147-y

Jooste, J. & Laurens, J.B. & Jordaan, M. & *et al*. (2021) The implications of the use of cannabidiol-related products in a safety-sensitive drug testing environment: A Medical-Legal Perspective. South African Medical Journal, 111 (10): 942. doi:10.7196/samj. 2021.v111i10.15866

K, S. (2017) Tamoxifen: Pharmacokinetics and pharmacodynamics. *Open Access Journal of Pharmaceutical Research*, 1 (8). doi:10.23880/oajpr-16000143

Kamentsky, L. & Jones, T.R. & Fraser, A. & *et al*. (2011) Improved structure, function and compatibility for cellprofiler: Modular High-Throughput Image Analysis Software. *Bioinformatics*, 27 (8): 1179–1180. doi:10.1093/bioinformatics/btr095

Kendall, D.A. & Yudowski, G.A. (2017) Cannabinoid receptors in the central nervous system: Their signaling and roles in disease. *Frontiers in Cellular Neuroscience*, 10. doi:10.3389/fncel.2016.00294

Kitaeva, K.V. & Rutland, C.S. & Rizvanov, A.A. & *et al*. (2020) Cell culture based in vitro test systems for anticancer drug screening. *Frontiers in Bioengineering and Biotechnology*, 8. doi:10.3389/fbioe.2020.00322

Klein, D.J. & Thorn, C.F. & Desta, Z. & *et al*. (2013) Pharmgkb summary. *Pharmacogenetics and Genomics*, 23 (11): 643–647. doi: 10.1097/fpc.0b013e3283656bc1

Klein, T.W. & Newton, C.A. & Friedman, H. (2001) Cannabinoids and the immune system. *Pain Research and Management*, 6 (2): 95–101. doi:10.1155/2001/326867

Kudela, E. & Samec, M. & Koklesova, L. & *et al*. (2020) MIRNA expression profiles in luminal a breast cancer—implications in biology, prognosis, and prediction of response to hormonal treatment. *International Journal of Molecular Sciences*, 21 (20): 7691. doi:10.3390/ijms21207691

Kuhn, M.J. & Putman, A.K. & Sordillo, L.M. (2020) Widespread basal cytochrome P450 expression in extrahepatic bovine tissues and isolated cells. *Journal of Dairy Science*, 103 (1): 625–637. doi:10.3168/jds.2019-17071

Kumar, R.N. & Chambers, W.A. & Pertwee, R.G. (2001) Pharmacological actions and therapeutic uses of cannabis and cannabinoids. *Anaesthesia*, 56 (11): 1059–1068. doi:10.1111/j.1365-2044.2001. 02269.x

Kwiatkowska, M. & Parker, LindaA. & Burton, P. & *et al*. (2004) A comparative analysis of the potential of cannabinoids and Ondansetron to suppress cisplatin-induced emesis in the suncus murinus (House musk shrew). *Psychopharmacology*, 174 (2). doi:10.1007/s00213-003-1739-9

Lawson, D.A. & Kessenbrock, K. & Davis, R.T. & *et al*. (2018) Tumour heterogeneity and metastasis at single-cell resolution. *Nature Cell Biology*, 20 (12): 1349–1360. doi:10.1038/s41556-018-0236-7

Li, Z. & Hu, P. & Tu, J. & *et al*. (2016) Luminal B breast cancer: Patterns of recurrence and clinical outcome. *Oncotarget*, 7 (40): 65024–65033. doi:10.18632/oncotarget.11344

Liang, C.-C. & Park, A.Y. & Guan, J.-L. (2007) In vitro scratch assay: A convenient and inexpensive method for analysis of cell migration in vitro. *Nature Protocols*, 2 (2): 329–333. doi:10.1038/nprot.2007.30

Ligresti, A. & Moriello, A.S. & Starowicz, K. & *et al*. (2006) Antitumor activity of plant cannabinoids with emphasis on the effect of cannabidiol on human breast carcinoma. *Journal of Pharmacology and Experimental Therapeutics*, 318 (3): 1375–1387. doi:10.1124/jpet.106.105247

Lippai, M. & Lőw, P. (2014) The role of the selective adaptor P62 and ubiquitin-like proteins in autophagy. *BioMed Research International*, 2014: 1–11. doi:10.1155/2014/832704

Lorizio, W. & Wu, A.H. & Beattie, M.S. & *et al*. (2011) Clinical and biomarker predictors of side effects from tamoxifen. *Breast Cancer Research and Treatment*, 132 (3): 1107–1118. doi:10.1007/s10549-011-1893-4

Lu, H.-Y. & Zhu, J.-S. & Xie, J. & *et al*. (2020) Hydroxytyrosol and Oleuropein inhibit migration and invasion via induction of autophagy in ER-positive breast cancer cell lines (MCF7 and T47D). *Nutrition and Cancer*, 73 (2): 350–360. doi:10.1080/01635581.2020.1750661

Lukhele, S.T. & Motadi, L.R. (2016) Cannabidiol rather than cannabis sativa extracts inhibit cell growth and induce apoptosis in cervical cancer cells. *BMC Complementary and Alternative Medicine*, 16 (1). doi:10.1186/s12906-016-1280-0

Luo, B. & Yan, D. & Yan, H. & *et al*. (2021) Cytochrome P450: Implications for human breast cancer (review). *Oncology Letters*, 22 (1). doi:10.3892/ol.2021.12809

Luo, S. & Rubinsztein, D. (2009) Apoptosis blocks Beclin 1-dependent autophagosome synthesis: An effect rescued by Bcl-XL. *Cell Death & Differentiation*, 17 (2): 268–277. doi:10.1038/cdd.2009.121

Maiuri, M.C. & Tasdemir, E. & Criollo, A. & *et al*. (2008) Control of autophagy by oncogenes and tumor suppressor genes. *Cell Death & Differentiation*, 16 (1): 87–93. doi:10.1038/cdd.2008.131

Massi, P. & Solinas, M. & Cinquina, V. & *et al*. (2013) Cannabidiol as potential anticancer drug. *British Journal of Clinical Pharmacology*, 75 (2): 303–312. doi:10.1111/j.1365-2125.2012.04298.x

Maximov, P.Y. & McDaniel, R.E. & Fernandes, D.J. & *et al*. (2014) Simulation with cells *in vitro* of tamoxifen treatment in premenopausal breast cancer patients with different cyp2d6 genotypes. *British Journal of Pharmacology*, 171 (24): 5624–5635. doi:10.1111/bph.12864

McAllister, S.D. & Christian, R.T. & Horowitz, M.P. & *et al*. (2007) Cannabidiol as a novel inhibitor of ID-1 gene expression in aggressive breast cancer cells. *Molecular Cancer Therapeutics*, 6 (11): 2921–2927. doi: 10.1158/1535-7163.mct-07-0371

McCowan, C. & Shearer, J. & Donnan, P.T. & *et al*. (2008) Cohort study examining tamoxifen adherence and its relationship to mortality in women with breast cancer. *British Journal of Cancer*, 99 (11): 1763–1768. doi: 10.1038/sj.bjc.6604758

Millar, S.A. & Stone, N.L. & Yates, A.S. & *et al*. (2018) A systematic review on the pharmacokinetics of cannabidiol in humans. *Frontiers in Pharmacology*, 9. doi:10.3389/fphar.2018.01365

Mirabelli, P. & Coppola, L. & Salvatore, M. (2019) Cancer cell lines are useful model systems for Medical Research. *Cancers*, 11 (8): 1098. doi:10.3390/cancers11081098

Mokoena, D.R. & George, B.P. & Abrahamse, H. (2019) Enhancing breast cancer treatment using a combination of cannabidiol and gold nanoparticles for photodynamic therapy. *International Journal of Molecular Sciences*, 20 (19): 4771. doi:10.3390/ijms20194771

Moodley, J. & Cairncross, L. & Naiker, T. & *et al*. (2016) Understanding pathways to breast cancer diagnosis among women in the Western Cape Province, South Africa: A qualitative study. *BMJ Open*, 6 (1). doi:10.1136/bmjopen-2015-009905

Mortimer, J.E. & Flatt, S.W. & Parker, B.A. & *et al*. (2007) Tamoxifen, hot flashes and recurrence in breast cancer. *Breast Cancer Research and Treatment*, 108 (3): 421–426. doi:10.1007/s10549-007-9612-x

Muller, C. & Morales, P. & Reggio, P.H. (2019) Cannabinoid ligands targeting TRP channels. *Frontiers in Molecular Neuroscience*, 11. doi:10.3389/fnmol.2018.00487

Murray, G.I. & Patimalla, S. & Stewart, K.N. & *et al*. (2010) Profiling the expression of cytochrome P450 in breast cancer. *Histopathology*, 57 (2): 202–211. doi:10.1111/j.1365-2559.2010. 03606.x

Nasrin, S. & Watson, C.J.W. & Perez-Paramo, Y.X. & *et al*. (2021) Cannabinoid metabolites as inhibitors of major hepatic CYP450 enzymes, with implications for cannabis-drug interactions. *Drug Metabolism and Disposition*, 49 (12): 1070–1080. doi:10.1124/dmd.121.000442

Nazarali, S. & Narod, S. (2014) Tamoxifen for women at high risk of breast cancer. *Breast Cancer: Targets and Therapy*, 29. doi:10.2147/bctt. s43763

Nazarewicz, R.R. & Zenebe, W.J. & Parihar, A. & *et al*. (2007) Tamoxifen induces oxidative stress and mitochondrial apoptosis via stimulating mitochondrial nitric oxide synthase. *Cancer Research*, 67 (3): 1282–1290. doi: 10.1158/0008-5472.can-06-3099

Nihira, K. & Miki, Y. & Ono, K. & *et al*. (2014) An inhibition of P62/sqstm1 caused autophagic cell death of several human carcinoma cells. *Cancer Science*, 105 (5): 568–575. doi:10.1111/cas.12396

Ning, S. & Wang, L. (2019) The multifunctional protein P62 and its mechanistic roles in cancers. *Current Cancer Drug Targets*, 19 (6): 468–478. doi:10.2174/1568009618666181016164920

Niu, N. & Wang, L. (2015) *in vitro* human cell line models to predict clinical response to anticancer drugs. *Pharmacogenomics*, 16 (3): 273–285. doi:10.2217/pgs.14.170

Odieka, A.E. & Obuzor, G.U. & Oyedeji, O.O. & *et al*. (2022a) The medicinal natural products of Cannabis Sativa Linn.: A Review. *Molecules*, 27 (5): 1689. doi:10.3390/molecules27051689

Odieka, A.E. & Obuzor, G.U. & Oyedeji, O.O. & *et al*. (2022b) The medicinal natural products of Cannabis Sativa Linn.: A Review. *Molecules*, 27 (5): 1689. doi:10.3390/molecules27051689

Ofir, R. & Seidman, R. & Rabinski, T. & et al. (2002) Taxol-induced apoptosis in human SKOV3 ovarian and MCF7 breast carcinoma cells is caspase-3 and caspase-9 independent. *Cell Death & Differentiation*, 9 (6): 636–642. doi:10.1038/sj.cdd.4401012

Ortiz de Montellano, P.R. (2013) Cytochrome P450-activated prodrugs. *Future Medicinal Chemistry*, 5 (2): 213–228. doi:10.4155/fmc.12.197

Ouyang, L. & Shi, Z. & Zhao, S. & *et al*. (2012) Programmed cell death pathways in cancer: A review of apoptosis, autophagy and programmed necrosis. *Cell Proliferation*, 45 (6): 487–498. doi:10.1111/j.1365-2184.2012. 00845.x

Parzych, K.R. & Klionsky, D.J. (2014) An overview of autophagy: Morphology, mechanism, and regulation. *Antioxidants & Redox Signaling*, 20 (3): 460–473. doi:10.1089/ars.2013.5371

Pather, K. & Augustine, T.N. (2020) Tamoxifen induces hypercoagulation and alterations in ERA and ERB dependent on breast cancer sub-phenotype ex vivo. *Scientific Reports*, 10 (1). doi:10.1038/s41598-020-75779-y

Pather, K. & Dix-Peek, T. & Duarte, R. & *et al*. (2019) Breast cancer cell-induced platelet activation is compounded by tamoxifen and anastrozole in vitro. *Thrombosis Research*, 177: 51–58. doi: 10.1016/j.thromres.2019.02.027

Pather, K., 2019. Project Title: Cannabidiol & hormone - therapies in breast cancer - Modelling immunological and haematological mediation of tumour processes. PhD Thesis. University of the Witwatersrand. Available from: https://wiredspace.wits.ac.za/items/5f5a8687-f2bd-4dcd-85db-3d0992fcb751 (Accessed 14 January 2022)

Pertwee, R.G. (2005) Pharmacological actions of Cannabinoids. *Handbook of Experimental Pharmacology*, 1–51. doi:10.1007/3-540-26573-2_1

Pertwee, R.G. (2008) The diverse cb1 and CB2 receptor pharmacology of three plant cannabinoids: Δ9-tetrahydrocannabinol, cannabidiol and Δ9-tetrahydrocannabivarin. *British Journal of Pharmacology*, 153 (2): 199–215. doi: 10.1038/sj.bjp.0707442

Piszczatowska, K. & Przybylska, D. & Sikora, E. & et al. (2020) Inhibition of NADPH oxidases activity by diphenyleneiodonium chloride as a mechanism of senescence induction in human cancer cells. *Antioxidants*, 9 (12): 1248. doi:10.3390/antiox9121248

Prat, A. & Perou, C.M. (2011) Withdrawn: Deconstructing the molecular portraits of breast cancer. *Molecular Oncology*,. doi: 10.1016/j.molonc.2010.04.003

Pucci, B. & Kasten, M. & Giordano, A. (2000) Cell cycle and apoptosis. *Neoplasia*, 2 (4): 291–299. doi: 10.1038/sj.neo.7900101

Qi, J.-L. & He, J.-R. & Liu, C.-B. & *et al*. (2022) SQSTM1/P62 regulate breast cancer progression and metastasis by inducing cell cycle arrest and regulating immune cell infiltration. *Genes & Diseases*, 9 (5): 1332–1344. doi: 10.1016/j.gendis.2021.03.008

Radde, B.N. & Ivanova, M.M. & Mai, H.X. & et al. (2014) Bioenergetic differences between MCF-7 and T47D breast cancer cells and their regulation by oestradiol and Tamoxifen. *Biochemical Journal*, 465 (1): 49–61. doi:10.1042/bj20131608

Ramer, R. & Rohde, A. & Merkord, J. & *et al*. (2010) Decrease of plasminogen activator inhibitor-1 May contribute to the anti-invasive action of Cannabidiol on human lung cancer cells. *Pharmaceutical Research*, 27 (10): 2162–2174. doi:10.1007/s11095-010-0219-2

Ritchie, H. & Roser, M. (2018) *Causes of death*. [online] Available from: https://ourworldindata.org/causes-of-death (Accessed 28 May 2023).

Rothberg, A. (2017) Cannabidiol, a non-psychotropic component of cannabis, attenuates vomiting and nausea-like behaviour via indirect agonism of 5-HT1a somatodendritic autoreceptors in the dorsal raphe nucleus. *South African Journal of Child Health*, 11 (4): 153–153. doi:10.1111/j.1476-5381.2011. 01621.x

Ryan, D. & Drysdale, A.J. & Lafourcade, C. & *et al*. (2009) Cannabidiol targets mitochondria to regulate intracellular Ca2+levels. *The Journal of Neuroscience*, 29 (7): 2053–2063. doi:10.1523/jneurosci.4212-08.2009

Salati, N.A. & Ahmad, S.S. & Khwaja, K.J. (2013) Assessment of cytotoxicity in chemotherapeutic drugs—by Invitro methods. *IOSR Journal of Pharmacy and Biological Sciences*, 5 (5): 73–76. doi:10.9790/3008-0557376

Sánchez-Martín, P. & Komatsu, M. (2018) P62/SQSTM1 – steering the cell through health and disease. *Journal of Cell Science*, 131 (21). doi:10.1242/jcs.222836

Saunders, D.E. & Lawrence, W.D. & Christensen, C. & *et al*. (1997) Paclitaxel-induced apoptosis in MCF-7 breast-cancer cells. *International Journal of Cancer*, 70 (2): 214–220. doi:10.1002/(sici)1097-0215(19970117)70:2< 214::aid-ijc13>3.0.co;2-i

Schoeman, R. & Beukes, N. & Frost, C. (2020) Cannabinoid combination induces cytoplasmic vacuolation in MCF-7 breast cancer cells. *Molecules*, 25 (20): 4682. doi:10.3390/molecules25204682

Seltzer, E.S. & Watters, A.K. & MacKenzie, D. & *et al*. (2020) Cannabidiol (CBD) as a promising anti-cancer drug. *Cancers*, 12 (11): 3203. doi:10.3390/cancers12113203

Shahbazi, F. & Grandi, V. & Banerjee, A. & *et al*. (2020) Cannabinoids and cannabinoid receptors: The story so far. *iScience*, 23 (7): 101301. doi: 10.1016/j.isci.2020.101301

Shrivastava, A. & Kuzontkoski, P.M. & Groopman, J.E. & *et al*. (2011) Cannabidiol induces programmed cell death in breast cancer cells by coordinating the crosstalk between apoptosis and autophagy. *Molecular Cancer Therapeutics*, 10 (7): 1161–1172. doi: 10.1158/1535-7163.mct-10-1100

Singh, M.S. & Francis, P.A. & Michael, M. (2011) Tamoxifen, cytochrome P450 genes and breast cancer clinical outcomes. *The Breast*, 20 (2): 111–118. doi: 10.1016/j.breast.2010.11.003

Sirinian, C. & Peroukidis, S. & Kriegsmann, K. & *et al*. (2022) Cellular senescence in normal mammary gland and breast cancer. implications for cancer therapy. *Genes*, 13 (6): 994. doi:10.3390/genes13060994

Śledziński, P. & Zeyland, J. & Słomski, R. & *et al*. (2018) The current state and future perspectives of cannabinoids in cancer biology. *Cancer Medicine*, 7 (3): 765–775. doi:10.1002/cam4.1312

Smith, R.T. & Gruber, S.A. (2023) Contemplating cannabis? the complex relationship between cannabinoids and hepatic metabolism resulting in the potential for drug-drug interactions. *Frontiers in Psychiatry*, 13. doi:10.3389/fpsyt.2022.1055481

Smolarz, B. & Nowak, A.Z. & Romanowicz, H. (2022) Breast cancer—epidemiology, classification, pathogenesis and treatment (review of literature). *Cancers*, 14 (10): 2569. doi:10.3390/cancers14102569

Sneha, S. & Baker, S.C. & Green, A. & *et al*. (2021) Intratumoural cytochrome P450 expression in breast cancer: Impact on standard of care treatment and new efforts to develop tumour-selective therapies. *Biomedicines*, 9 (3): 290. doi:10.3390/biomedicines9030290

Sørlie, T. (2004) Molecular portraits of breast cancer: Tumour subtypes as distinct disease entities. *European Journal of Cancer*, 40 (18): 2667–2675. doi: 10.1016/j.ejca.2004.08.021

Spiller, K.J. & Bi, G. & He, Y. & *et al*. (2019) Cannabinoid CB1 and CB2 receptor mechanisms underlie cannabis reward and aversion in rats. *British Journal of Pharmacology*, 176 (9): 1268–1281. doi:10.1111/bph.14625

Sultan, A.S. & Marie, M.A. & Sheweita, S.A. (2018) Novel mechanism of cannabidiol-induced apoptosis in breast cancer cell lines. *The Breast*, 41: 34–41. doi: 10.1016/j.breast.2018.06.009

Sun, K. & Deng, W. & Zhang, S. & *et al*. (2013) Paradoxical roles of autophagy in different stages of tumorigenesis: Protector for normal or cancer cells. *Cell & Bioscience*, 3 (1). doi:10.1186/2045-3701-3-35

Surapaneni, S.K. & Patel, N. & Sun, L. & *et al*. (2022) Anticancer and chemosensitization effects of cannabidiol in 2D and 3D cultures of TNBC: Involvement of gadd45α, Integrin-α5, -B5, -β1, and autophagy. *Drug Delivery and Translational Research*, 12 (11): 2762–2777. doi:10.1007/s13346-022-01137-2

Tellez-Gabriel, M. & Ory, B. & Lamoureux, F. & *et al*. (2016) Tumour heterogeneity: The key advantages of single-cell analysis. *International Journal of Molecular Sciences*, 17 (12): 2142. doi:10.3390/ijms17122142

Tompkins, K.D. & Thorburn, A. (2019) Regulation of Apoptosis by Autophagy to Enhance Cancer Therapy. *Apoptosis*, 92 (4): 707–718. doi:10.1007/s10495-007-0154-9

Tu, S.-H. & Chang, C.-C. & Chen, C.-S. & *et al*. (2009) Increased expression of enolase α in human breast cancer confers tamoxifen resistance in human breast cancer cells. *Breast Cancer Research and Treatment*, 121 (3): 539–553. doi:10.1007/s10549-009-0492-0

Turashvili, G. & Brogi, E. (2017) Tumor heterogeneity in breast cancer. *Frontiers in Medicine*, 4. doi:10.3389/fmed.2017.00227

Ujváry, I. & Hanuš, L. (2016) Human metabolites of Cannabidiol: A review on their formation, biological activity, and relevance in therapy. *Cannabis and Cannabinoid Research*, 1 (1): 90–101. doi:10.1089/can.2015.0012

Venter, C. (2020) MCF-7 human breast cancer cells form differentiated microtissues in scaffold-free hydrogels. *African journals*, 6 (7): 28–29.

Vicente-Acosta, A. & Ceprian, M. & Sobrino, P. & *et al*. (2022) Cannabinoids as glial cell modulators in ischemic stroke: Implications for neuroprotection. *Frontiers in Pharmacology*, 13. doi:10.3389/fphar.2022.888222

Vinette, B. & Côté, J. & El-Akhras, A. & *et al*. (2022) Routes of administration, reasons for use, and approved indications of medical cannabis in oncology: A scoping review. *BMC Cancer*, 22 (1). doi:10.1186/s12885-022-09378-7

Wang, C.-W. & Klionsky, D.J. (2003) The molecular mechanism of autophagy. *Molecular Medicine*, 9 (3–4): 65–76. doi:10.1007/bf03402040

WHO (2024) *Breast cancer*, *World Health Organization*. Available at: https://www.who.int/news-room/fact-sheets/detail/breast-cancer (Accessed: 28 April 2024).

Widowati, W. & Murti, H. & Widyastuti, H. & *et al*. (2021) Decreased inhibition of proliferation and induction of apoptosis in breast cancer cell lines (T47D and MCF7) from treatment with conditioned medium derived from hypoxia-treated Wharton's jelly mscs compared with normoxia-treated mscs. *International Journal of Hematology-Oncology and Stem Cell Research*,. doi:10.18502/ijhoscr. v15i2.6038

Wirawan, E. & Berghe, T.V. & Lippens, S. & *et al*. (2011) Autophagy: For better or for worse. *Cell Research*, 22 (1): 43–61. doi:10.1038/cr.2011.152

Wiseman, H. & Lewis, D.F.V. (1996) The metabolism of tamoxifen by human cytochromes P450 is rationalized by molecular modelling of the enzyme-substrate interactions: Potential importance to its proposed anti-carcinogenic/carcinogenic actions. *Carcinogenesis*, 17 (6): 1357–1360. doi:10.1093/carcin/17.6.1357

Wright, R.H. & Vastolo, V. & Oliete, J.Q. & *et al*. (2022a) Global signalling network analysis of Luminal T47D breast cancer cells in response to progesterone. *Frontiers in Endocrinology*, 13. doi:10.3389/fendo.2022.888802

Wright, R.H. & Vastolo, V. & Oliete, J.Q. & *et al*. (2022b) Global signalling network analysis of Luminal T47D breast cancer cells in response to progesterone. *Frontiers in Endocrinology*, 13. doi:10.3389/fendo.2022.888802

Wu, J. (2019) Cannabis, cannabinoid receptors, and endocannabinoid system: Yesterday, today, and tomorrow. *Acta Pharmacologica Sinica*, 40 (3): 297–299. doi:10.1038/s41401-019-0210-3

Xulu, K. & Duarte, R. & Augustine, T. (2020) Combined anastrozole and antiplatelet therapy treatment differentially promotes breast cancer cell survival. *Microscopy and Microanalysis*, 26 (3): 497–508. doi:10.1017/s1431927620001324

Yim, S.-K. & Yun, C.-H. & Ahn, T.-H. & et al. (2005) A continuous spectrophotometric assay for NADPH-cytochrome P450 reductase activity using 3-(4,5-dimethylthiazol-2-YL)-2,5-diphenyltetrazolium bromide. *BMB Reports*, 38 (3): 366–369. doi:10.5483/bmbrep.2005.38.3.366

Yin, L. & Duan, J.-J. & Bian, X.-W. & *et al*. (2020) Triple-negative breast cancer molecular subtyping and treatment progress. *Breast Cancer Research*, 22 (1). doi:10.1186/s13058-020-01296-5

Yu, S. & Kim, T. & Yoo, K.H. & *et al*. (2017) The T47D cell line is an ideal experimental model to elucidate the progesterone-specific effects of a luminal a subtype of breast cancer. *Biochemical and Biophysical Research Communications*, 486 (3): 752–758. doi: 10.1016/j.bbrc.2017.03.114

Yue, P.Y.K. & Leung, E.P.Y. & Mak, N.K. & *et al*. (2010) A simplified method for quantifying cell migration/wound healing in 96-well plates. *SLAS Discovery*, 15 (4): 427–433. doi:10.1177/1087057110361772

Zhang, J. & Wang, X. & Vikash, V. & *et al*. (2016) Ros and Ros-mediated cellular signaling. *Oxidative Medicine and Cellular Longevity*, 2016: 1–18. doi:10.1155/2016/4350965

Zhao, M. & Ma, J. & Li, M. & *et al*. (2021) Cytochrome P450 enzymes and drug metabolism in humans. *International Journal of Molecular Sciences*, 22 (23): 12808. doi:10.3390/ijms222312808

Zheng, A. & Kallio, A. & Härkönen, P. (2007) Tamoxifen-induced rapid death of MCF-7 breast cancer cells is mediated via extracellularly signal-regulated kinase signaling and can be abrogated by estrogen. *Endocrinology*, 148 (6): 2764–2777. doi:10.1210/en.2006-1269

Zhu, H.-J. & Wang, J.-S. & Markowitz, J.S. & *et al*. (2006) Characterization of P-glycoprotein inhibition by major cannabinoids from marijuana. *Journal of Pharmacology and Experimental Therapeutics*, 317 (2): 850–857. doi:10.1124/jpet.105.098541

Zhu, W. & Qu, H. & Xu, K. & *et al*. (2017) Differences in the starvation-induced autophagy response in MDA-MB-231 and MCF-7 breast cancer cells. *Animal Cells and Systems*, 21 (3): 190–198. doi:10.1080/19768354.2017.133076

Appendix A-Drugs and reagents preparation and Tamoxifen pre-treatment.

Single dose-treatment (model 1) and daily-replacement treatment (model 2) per cell line

Tamoxifen

Making 2500µM Tamoxifen stock solution

Molecular weight: 371.51g/mol

Stock 1: make 1ml of 2500μM solution in ethanol

Find mass of Tamoxifen to weigh and dissolve in 1ml ethanol

$$c = \frac{n}{v}$$

$$n = c \times v = (2500 \times 10^{-6}M)(1 \times 10^{-3}L) = 2.5 \times 10^{-6}moles$$

$$n = \frac{m}{M}$$

$$m = n \times M = (2.5 \times 10^{-6}mol)\left(\frac{371.5g}{mol}\right) = 9.28755 \times 10^{-4}g = 0.0092875mg$$

Weigh 0.009mg of Tamoxifen and dissolve in 1ml ethanol and freeze down

Total Tamoxifen needed per run at 100µl per well for single treatments and combined treatments is 6400 µl for only one cell line so total volume per run for each concentration will be made to 6500µl per run.

From the initial stock of 2500µM tamoxifen make 4µM Tamoxifen:

$$C1V1 = C2V2$$

$$(2500\mu M)V1 = (4\mu M)(6500\mu l)$$

$$V1 = 10.4\mu l\ of\ stock\ 1\ solution\ dissolved\ in\ 6489.6\mu l\ culture\ media$$

CBD

CBD stock solution

Initial concentration in ethanol: 1mg/ml

Molarity of stock solution

$$\frac{1 \times 10^{-3} g/10^{-3} l}{314.5 g/mole} = 0.0032M = 3200\mu M$$

Total CBD needed per run at 100µl per well for the single and combined treatments is 4600 µl for only one cell line so total volume per run for each CBD concentration will be made to 5000µl per run.

Stock solution for the treatment with CBD concentration of 5µM made as 10 µM CBD

$$C1V1 = C2V2$$

$$(3200\mu M)V1 = (10\mu M)(5000\mu l)$$

$$V1 = 15.625\ \mu l\ of\ initial\ CBD\ stock\ solution\ dissolved\ in\ 4984.375\mu l\ of media$$

Stock solution for the treatment with CBD concentration of 7.5µM made as 15 µM CBD

$$C1V1 = C2V2$$

$$(3200\mu M)V1 = (15\mu M)(5000\mu l)$$

$$V1 = 23.4375 \cong 9.44\ \mu l\ of\ CBD\ stock\ solution\ dissolved\ in\ 4976.56\ \mu l\ of\ media$$

Stock solution for the treatment with CBD concentration of 10µM made as 20 µM CBD

$$C1V1 = C2V2$$

$$(3200\mu M)V1 = (20\mu M)(5000\mu l)$$

$$V1 = 31.25\ \mu l\ of CBD\ stock\ solution\ dissolved\ in\ 4968.75\ \mu l\ of\ media$$

Diluent

- **Total ethanol diluents needed per run at 200µl per is 6400µl for only one cell line so total volume per run will be made to 6500µl.**

$$C1V1 = C2V2$$

$$(100\ \%)V1 = (0.8\ \%)(5000\mu l)$$

$$V1 = 40\mu l\ of\ 100\ \%\ ethanol\ dissolved\ in\ 4960\ \mu l\ of\ media$$

1X PBS recipe

Reagent	Concentration
NaCl	8 g
Na2HPO4	1.44 g
KCl	0.2 g
KH_2PO	0.2 g

Dissolve the reagents in 800ml distilled water; adjust to pH to 7.4. Add 200ml distilled water to make up 1000ml.

1X EBSS

Reagent	Concentration
$CaCl_2$	0.2 g
$MgSO_4$-$7H_2O$	0.2 g
KCl	0.4 g
$NaHCO_3$	2.2 g
NaCl	6.8 g
$NaH_2PO_4H_2O$	0.14 g
D-Glucose	1 g
Phenol Red	0.01 g

Dissolve the salts in 800ml distilled water; adjust to pH to 7.4. Add 200ml distilled water to make up 1000ml.

Appendix B – Neutral red assay raw data and normality test

MCF7-Model 1

Run 1

24 h

Treatment	A	B
Media	0.188948	0.192427
Diluent	0.189798	0.20719
2µM TAM	0.161137	0.182172
5µM CBD	0.070378	0.076674
7.5µM CBD	0.087555	0.086278
10µM CBD	0.076289	0.085917
2 µM TAM+ 5µM CBD	0.080153	0.073031
2 µM TAM+ 7.5µM CBD	0.071601	0.076749
2 µM TAM+ 7.5µM CBD	0.081475	0.081611
Blank	0.028562	0.027701

48 h

Treatment	A	B
Media	0.1424897	0.1944681
Diluent	0.1817797	0.1709713
2µM TAM	0.138827	0.0832671
5µM CBD	0.0703777	0.0766738
7.5µM CBD	0.0690719	0.0677302
10µM CBD	0.064964	0.0698404
2 µM TAM+ 5µM CBD	0.0697443	0.0688799
2 µM TAM+ 7.5µM CBD	0.0659635	0.0707548
2 µM TAM+ 7.5µM CBD	0.0691679	0.0718644
Blank	0.0304334	0.0282873

72 h

Treatment	A	B
Media	0.1795869	0.1492799
Diluent	0.1691228	0.167757
2µM TAM	0.1873779	0.1918156
5µM CBD	0.0802756	0.0837615
7.5µM CBD	0.0870545	0.0934015
10µM CBD	0.109247	0.0952323
2 µM TAM+ 5µM CBD	0.0839448	0.0873608
2 µM TAM+ 7.5µM CBD	0.0892293	0.0859305
2 µM TAM+ 7.5µM CBD	0.1048961	0.0967509
Blank	0.0359444	0.0343515

Run 2

Treatment	A	B
Media	0.199948	0.1934272
Diluent	0.189798	0.2081904
2µM TAM	0.171137	0.1921723
5µM CBD	0.0803777	0.0776738
7.5µM CBD	0.0876551	0.0862782
10µM CBD	0.0772889	0.086917
2 µM TAM+ 5µM CBD	0.0811534	0.0740309
2 µM TAM+ 7.5µM CBD	0.0726013	0.0797485
2 µM TAM+ 7.5µM CBD	0.0804746	0.0826115
Blank	0.0295621	0.0287012

Treatment	A	B
Media	0.1542884	0.1378992
Diluent	0.1279082	0.1374647
2µM TAM	0.1421034	0.1204325
5µM CBD	0.0963709	0.0944493
7.5µM CBD	0.092634	0.0867017
10µM CBD	0.094892	0.0924871
2 µM TAM+ 5µM CBD	0.0957787	0.0940561
2 µM TAM+ 7.5µM CBD	0.0931239	0.0927319
2 µM TAM+ 7.5µM CBD	0.0985492	0.0992943
Blank	0.0384379	0.0375745

Treatment	A	B
Media	0.1705869	0.1482799
Diluent	0.1741228	0.164757
2µM TAM	0.1918156	0.1883779
5µM CBD	0.0802956	0.0832615
7.5µM CBD	0.0860545	0.0914015
10µM CBD	0.102247	0.0962213
2 µM TAM+ 5µM CBD	0.0849448	0.0873609
2 µM TAM+ 7.5µM CBD	0.0902293	0.0853305
2 µM TAM+ 7.5µM CBD	0.1018961	0.0987509
Blank	0.0389444	0.0363515

Run 3

Treatment	A	B
Media	0.3264199	0.1137506
Diluent	0.1064624	0.1373759
2µM TAM	0.1089994	0.0832438
5µM CBD	0.0873246	0.0845671
7.5µM CBD	0.0878684	0.0850582
10µM CBD	0.0838314	0.0849599
2 µM TAM+ 5µM CBD	0.0870283	0.0831948
2 µM TAM+ 7.5µM CBD	0.0891066	0.0883633
2 µM TAM+ 7.5µM CBD	0.0841746	0.0907466
Blank	0.0357748	0.0379738

Treatment	A	B
Media	0.1557705	0.1600433
Diluent	0.1295179	0.1290854
2µM TAM	0.1693688	0.1127541
5µM CBD	0.0923723	0.0893047
7.5µM CBD	0.0911328	0.0955118
10µM CBD	0.074331	0.1036395
2 µM TAM+ 5µM CBD	0.1050176	0.0936154
2 µM TAM+ 7.5µM CBD	0.0945127	0.0910833
2 µM TAM+ 7.5µM CBD	0.0948621	0.1074783
Blank	0.0368424	0.0342287

Treatment	A	B
Media	0.1087804	0.0935469
Diluent	0.0894112	0.0902551
2µM TAM	0.0827675	0.0806726
5µM CBD	0.0819381	0.0793623
7.5µM CBD	0.0771872	0.0877778
10µM CBD	0.088767	0.0844312
2 µM TAM+ 5µM CBD	0.088767	0.0844312
2 µM TAM+ 7.5µM CBD	0.0823282	0.0877778
2 µM TAM+ 7.5µM CBD	0.0869387	0.0842842
Blank	0.0356086	0.0336851

MCF7-Model 2

Run 1

24 h

Treatment	A	B
Media	0.097394	0.09083
Diluent	0.071977	0.08564
2µM TAM	0.05376	0.046763
5µM CBD	0.069979	0.042194
7.5µM CBD	0.032422	0.041602
10µM CBD	0.032289	0.030866
2 µM TAM+ 5µM CBD	0.065583	0.043334
2 µM TAM+ 7.5µM CBD	0.035999	0.034386
2 µM TAM+ 7.5µM CBD	0.039696	0.040603
Blank	0.004794	0.004193

48 h

Treatment	A	B
Media	0.089907	0.092919
Diluent	0.071888	0.089847
2µM TAM	0.045896	0.044856
5µM CBD	0.067127	0.048163
7.5µM CBD	0.048664	0.034818
10µM CBD	0.04418	0.033014
2 µM TAM+ 5µM CBD	0.063107	0.051863
2 µM TAM+ 7.5µM CBD	0.041484	0.038494
2 µM TAM+ 7.5µM CBD	0.037472	0.035171
Blank	0.004744	0.004175

72 h

Treatment	A	B
Media	0.098844	0.0768
Diluent	0.092688	0.053301
2µM TAM	0.046986	0.027682
5µM CBD	0.059069	0.032054
7.5µM CBD	0.037494	0.027987
10µM CBD	0.025642	0.026509
2 µM TAM+ 5µM CBD	0.056691	0.039367
2 µM TAM+ 7.5µM CBD	0.028902	0.031659
2 µM TAM+ 7.5µM CBD	0.029295	0.026509
Blank	0.003589	0.003298

Run 2

Treatment	A	B
Media	0.060409	0.16494
Diluent	0.090611	0.084535
2µM TAM	0.072365	0.065743
5µM CBD	0.064707	0.04115
7.5µM CBD	0.034236	0.044037
10µM CBD	0.037345	0.036632
2 µM TAM+ 5µM CBD	0.077423	0.04626
2 µM TAM+ 7.5µM CBD	0.059752	0.042726
2 µM TAM+ 7.5µM CBD	0.039758	0.043675
Blank	0.003743	0.003886

Treatment	A	B
Media	0.099023	0.097276
Diluent	0.087083	0.093345
2µM TAM	0.046353	0.068649
5µM CBD	0.058617	0.039831
7.5µM CBD	0.044531	0.039966
10µM CBD	0.033273	0.051309
2 µM TAM+ 5µM CBD	0.07085	0.051678
2 µM TAM+ 7.5µM CBD	0.041859	0.037366
2 µM TAM+ 7.5µM CBD	0.033229	0.03314
Blank	0.003866	0.003336

Treatment	A	B
Media	0.058204	0.036799
Diluent	0.029194	0.047165
2µM TAM	0.031422	0.045307
5µM CBD	0.038799	0.025592
7.5µM CBD	0.03353	0.033618
10µM CBD	0.027324	0.029848
2 µM TAM+ 5µM CBD	0.048712	0.031816
2 µM TAM+ 7.5µM CBD	0.032036	0.024729
2 µM TAM+ 7.5µM CBD	0.035294	0.03671
Blank	0.004467	0.004117

Run 3

Treatment	A	B
Media	0.103651	0.096717
Diluent	0.088405	0.097537
2µM TAM	0.069618	0.07908
5µM CBD	0.057843	0.035023
7.5µM CBD	0.031576	0.039842
10µM CBD	0.054721	0.034181
2 µM TAM+ 5µM CBD	0.065201	0.028899
2 µM TAM+ 7.5µM CBD	0.027152	0.029205
2 µM TAM+ 7.5µM CBD	0.037203	0.030301
Blank	0.005379	0.005153

Treatment	A	B
Media	0.093157	0.096712
Diluent	0.077551	0.096214
2µM TAM	0.045715	0.063551
5µM CBD	0.066998	0.052341
7.5µM CBD	0.030256	0.031308
10µM CBD	0.030388	0.025209
2 µM TAM+ 5µM CBD	0.058695	0.035274
2 µM TAM+ 7.5µM CBD	0.029994	0.032758
2 µM TAM+ 7.5µM CBD	0.035983	0.03523
Blank	0.003843	0.004058

Treatment	A	B
Media	0.079494	0.099935
Diluent	0.078836	0.089768
2µM TAM	0.032718	0.035741
5µM CBD	0.061567	0.042213
7.5µM CBD	0.034449	0.03525
10µM CBD	0.034004	0.029144
2 µM TAM+ 5µM CBD	0.052431	0.040676
2 µM TAM+ 7.5µM CBD	0.029715	0.027784
2 µM TAM+ 7.5µM CBD	0.028485	0.028397
Blank	0.003897	0.003802

T47D-Model 1

Run 1

Treatment	24 h A	24 h B	Treatment	48 h A	48 h B	Treatment	72 h A	72 h B
Media	0.304182	0.231751	Media	0.257905	0.301218	Media	0.755501	0.650785
Diluent	0.195413	0.189155	Diluent	0.389129	0.270589	Diluent	0.590081	0.55691
2µM TAM	0.130477	0.130921	2µM TAM	0.114633	0.113138	2µM TAM	0.439028	0.430546
5µM CBD	0.208139	0.218663	5µM CBD	0.303526	0.310022	5µM CBD	0.489401	0.577498
2 µM TAM+ 5µM CBD	0.135603	0.13281	2 µM TAM+ 5µM CBD	0.130377	0.120179	2 µM TAM+ 5µM CBD	0.485119	0.514408
Blank	0.056276	0.058523	Blank	0.063418	0.063941	Blank	0.062104	0.064382

Run 2

Treatment	A	B	Treatment	A	B	Treatment	A	B
Media	0.341817	0.271751	Media	0.327276	0.490723	Media	0.360797	0.450045
Diluent	0.185413	0.188155	Diluent	0.329395	0.288392	Diluent	0.273619	0.464039
2µM TAM	0.250487	0.260921	2µM TAM	0.122357	0.125499	2µM TAM	0.157523	0.153142
5µM CBD	0.208139	0.218663	5µM CBD	0.347554	0.31495	5µM CBD	0.509082	0.392117
2 µM TAM+ 5µM CBD	0.135603	0.13281	2 µM TAM+ 5µM CBD	0.220279	0.19417	2 µM TAM+ 5µM CBD	0.141059	0.13328
Blank	0.059276	0.057523	Blank	0.058517	0.059561	Blank	0.061213	0.056661

Run 3

Treatment	A	B	Treatment	A	B	Treatment	A	B
Media	0.060409	0.16494	Media	0.27836	0.284884	Media	0.060409	0.16494
Diluent	0.090611	0.084535	Diluent	0.237753	0.224159	Diluent	0.090611	0.084535
2µM TAM	0.072365	0.065743	2µM TAM	0.228855	0.163677	2µM TAM	0.072365	0.065743
5µM CBD	0.064707	0.04115	5µM CBD	0.310815	0.258902	5µM CBD	0.064707	0.04115
2 µM TAM+ 5µM CBD	0.077423	0.04626	2 µM TAM+ 5µM CBD	0.135332	0.144809	2 µM TAM+ 5µM CBD	0.077423	0.04626
Blank	0.003743	0.003886	Blank	0.057425	0.058233	Blank	0.003743	0.003886

T47D-Model 2

Run 1

Treatment	24 h A	24 h B	48 h A	48 h B	72 h A	72 h B
Media	0.224626	0.233935	0.310628	0.410292	0.642181	0.681511
Diluent	0.198425	0.20091	0.360266	0.310795	0.54957	0.65113
2µM TAM	0.151154	0.13842	0.11176	0.112235	0.34272	0.361632
5µM CBD	0.215783	0.187227	0.338549	0.351192	0.507823	0.509818
2 µM TAM+ 5µM CBD	0.136946	0.140583	0.10469	0.108341	0.262894	0.338118
Blank	0.060314	0.061311	0.06179	0.061132	0.05901	0.066821

Run 2

Treatment	24 h A	24 h B	48 h A	48 h B	72 h A	72 h B
Media	0.378342	0.307984	0.465767	0.455326	0.731165	0.60597
Diluent	0.359773	0.349923	0.294865	0.287712	0.851477	0.863135
2µM TAM	0.29915	0.282732	0.248652	0.214925	0.229052	0.285234
5µM CBD	0.312655	0.307256	0.429432	0.408176	0.440591	0.584872
2 µM TAM+ 5µM CBD	0.366266	0.313493	0.323925	0.241998	0.289499	0.155625
Blank	0.059276	0.057523	0.062328	0.060795	0.063367	0.060255

Run 3

Treatment	24 h A	24 h B	48 h A	48 h B	72 h A	72 h B
Media	0.308342	0.327984	0.223867	0.231117	0.42782	0.448606
Diluent	0.329773	0.322923	0.209721	0.226433	0.38324	0.389627
2µM TAM	0.303504	0.292832	0.204798	0.228524	0.304652	0.327763
5µM CBD	0.322658	0.308256	0.239707	0.263051	0.404482	0.413021
2 µM TAM+ 5µM CBD	0.316266	0.313493	0.135479	0.132668	0.159037	0.159218
Blank	0.060413	0.056716	0.060172	0.06542	0.052428	0.055776

Shapiro-Wilk Test for normality

MCF7

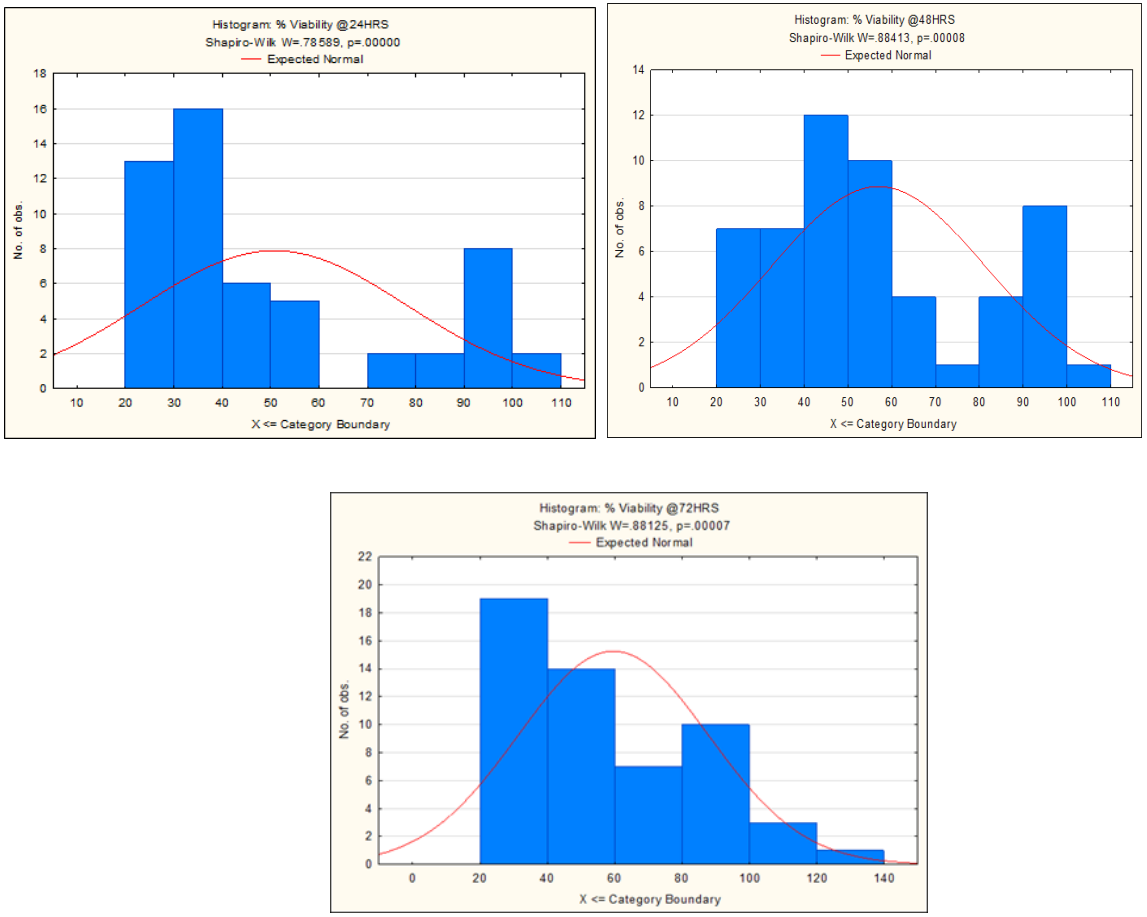


Figure 1: Histograms showing MCF7 data distribution from the Shapiro-Wilk normality test.

T47D

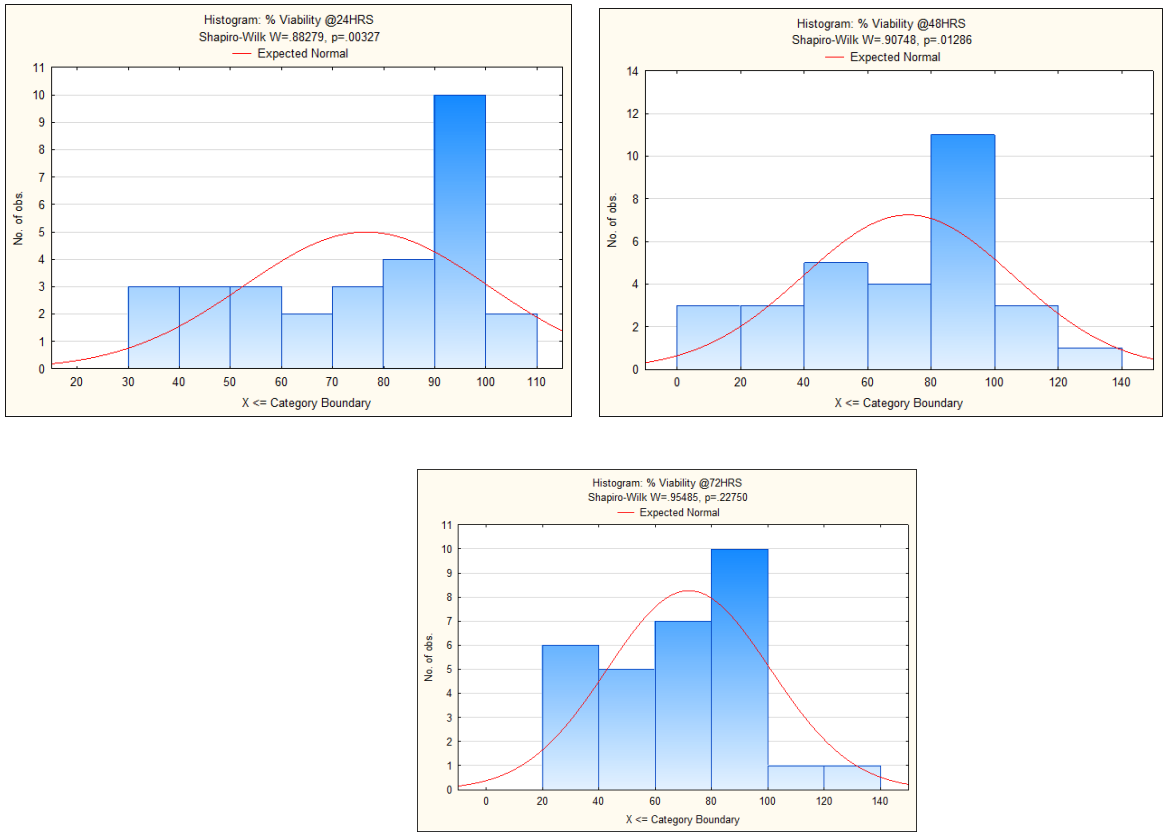
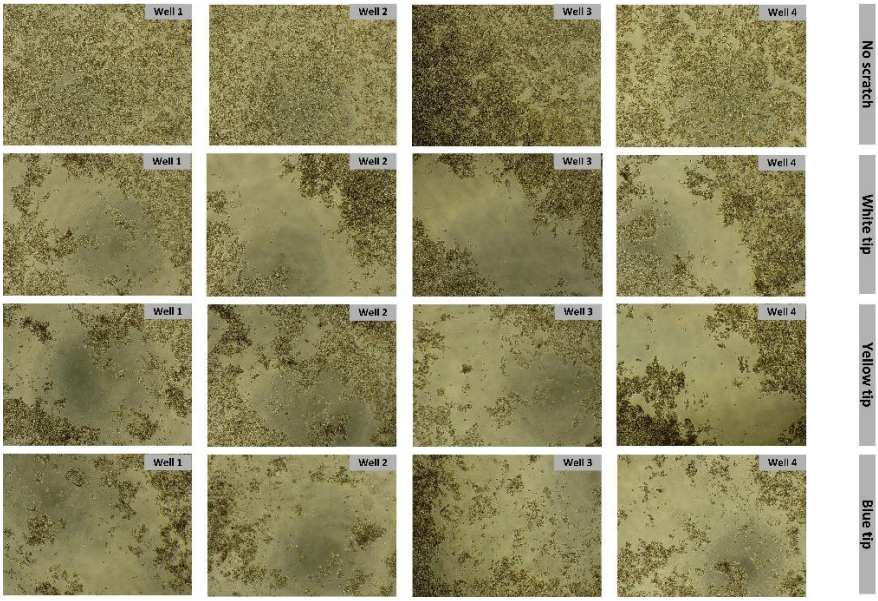


Figure 2: Histograms showing T47D data distribution from the Shapiro-Wilk normality test.

Appendix C – Scratch assay optimization results

Scratch assay optimization results

96 well plate



24 well plate

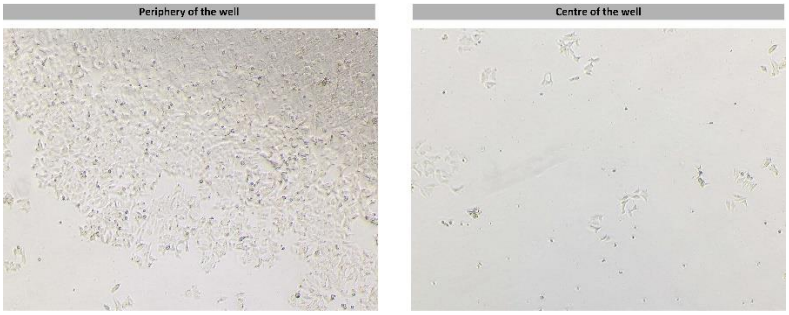


Figure 2 : Photomicrographs showing the optimization for the scratch assay with the 96 well plate and the 24 well plate. 96 well plate: Cells reached confluency and the centre of the well plate had enough cells adhered and allowed visualization of the scratch area and the periphery. 24 well plate: Cells were adhered to the periphery only and therefore no scratch could be made in the centre due to lack of cells.

Appendix D- CYP450 reductase assay reagents' preparation

Table 1: CYP reagents dilutions and preparation.

Reagent	**Preparation method**
CPR assay buffer	Ready to use
G6P standard	Reconstituted in 300 µl of double distilled water (ddH_2O) to acquire a 100Mm solution
inhibitor (10mMDiphenyleneiodium chloride)	900 µl of CPR buffer was added to make 1mM Diphenyleneodium chloride
NADPH substrate mix	Reconstituted in 600 µl of CPR buffer
G6P standard developer	Dissolved in 600 µl of distilled water (dH_2O)
Human CPR positive control	Reconstituted in 50 µl of CPR buffer
20mM G6P	**Making 20mM G6P from 100mM G6P** $$C1V1 = C2V2$$ $$(100mM)V1 = (20mM)(640\mu l)$$ $$V1 = 132\mu l\ of\ 100mM\ G6P\ dissolved\ in\ 528\ \mu l\ of\ CPR\ assay\ buffer$$

Table 2: CYP450 assay' reaction mix.

	1rxn (µl)	90rxn (µl)
NADPH substrate	5	450
CPR assay buffer	25	2250
Total	30	2700

Appendix E-ICC primary antibody optimization

Plate layout

LC3B 1/100 AF594 1/1000(With 10 % DMSO)	LC3B 1/250 No 2(With 10 % DMSO)	p62 2.5µg No 2(With 10 % DMSO)	BECN1 1/50 AF647 1/1000 (Media only)	BECN1 1/50 AF647 1/1000 (With 10 % DMSO)	
LC3B 1/250 AF594 1/1000(With 10 % DMSO)	p62 1µg AF488 1/1000(With 10 % DMSO)	DAPI (With 10 % DMSO)	BECN1 1/100 AF647 1/1000(Media only)	BECN1 1/100 AF647 1/1000(With 10 % DMSO)	
LC3B 1/500 AF594 1/1000(With 10 % DMSO)	p62 2.5µg AF488 1/1000(With 10 % DMSO)		BECN1 1/50 No 2(Media only)	BECN1 1/50 No 2(With 10 % DMSO)	
No 1 AF594 1/1000(With 10 % DMSO)	p62 5µg AF488 1/1000(With 10 % DMSO)		No 1 AF488 1/1000 (Media only)	No 1 AF488 1/1000(With 10 % DMSO)	

Controls:

1. No primary (each dilution)
2. No Secondary (each dilution)
1. No primary and secondary
2. DAPI cell control
3. Positive Control Cells – Induced Autophagy (with 10 % DMSO)

Primary antibody dilution for 40 wells at 50 µl per well

LC3B ; $\frac{1}{500} \times 2000\ \mu\text{l} = 4\mu\text{l}$ of antibody dissolved in 1996 µl of PBS/Tween/BSA

BECN1 ; $\frac{1}{50} \times 2000\ \mu\text{l} = 40\mu\text{l}$ of antibody dissolved in 1960 µl of PBS/ Tween /BSA

P62 ; $C1V1 = C2V2$

$$(1\mu\text{g/ml})V1 = (430\mu\text{g/ml})(2000\mu l)$$

$V1 = 4.65\mu l$ of primary antibody dissolved in 1995.35µl of PBS/ Tween /BSA

C2. Secondary antibody dilution for 40 wells at 50 µl per well

AF594 (LC3B) ; $\frac{1}{1000} \times 2000\ \mu l = 2\ \mu l$ of antibody dissolved in 1998 µl of PBS/Tween

AF488 (P62) ; $\frac{1}{1000} \times 2000\ \mu l = 2\ \mu l$ of antibody dissolved in 1998 µl of PBS/ Tween

AF647 (BECN1) ; $\frac{1}{1000} \times 2000\ \mu l = 2\ \mu l$ of antibody dissolved in 1998 µl of PBS/ Tween

Appendix F-qPCR nanodrop results

Table 1: MCF7 single-dose treatment (model 1) RNA concentrations and purity ratios.

Code	RNA concentration(ng/µl)	260/280	260/230
M1m1a	293.4	2.11	1.86
M1m1b	120.8	2.12	1.79
M1m1c	252.8	2.09	1.79
M2m1a	189.5	2.09	1.92
M2m1b	382.1	2.1	1.83
M2m1c	23.4	2.09	1.93
M3m1a	193.5	2.1	1.93
M3m1b	269.7	2.09	2.05
M3m1c	239.7	2.08	1.15
M4m1a	150.3	2.1	2.08
M4m1b	101.3	2.09	0.95
M4m1c	309.2	2.09	2.29
M5m1a	133.6	2.1	2.08
M5m1b	203.6	2.09	1.75
M5m1c	295.1	2.09	1.72
M6m1a	269.5	2.1	2.19
M6m1b	200.2	2.09	1.82
M6m1c	155.5	2.09	2.03
M7m1a	289.2	2.1	1.99
M7m1b	275.8	2.11	0.62
M7m1c	190	2.1	1.69

Table 2: MCF7 daily-replacement treatment (model 2) RNA concentrations and purity ratios.

Code	RNA concentration(ng/µl)	260/280	260/230
M1m2a	277.5	2.1	1.65
M1m2b	228.7	2.1	1.92
M1m2c	259.3	2.11	1.4
M2m2a	269.1	2.12	1.56
M2m2b	299.4	2.11	0.56
M2m2c	197.2	2.11	1.35
M3m2a	481.4	2.08	1.9
M3m2b	493.9	2.06	2.04
M3m2c	364.2	2.08	2.16
M4m2a	356	2.09	2.18
M4m2b	401.2	2.09	1.75
M4m2c	321.1	2.1	1.86
M5m2a	354	2.07	1.93
M5m2b	355.2	2.09	2.08
M5m2c	343.3	2.08	1.86
M6m2a	300.9	2.09	2.15
M6m2b	195.8	2.1	1.74
M6m2c	220.8	2.1	1.01
M7m2a	149.7	2.08	2.14
M7m2b	262.2	2.1	2.04
M7m2c	228.6	2.6	1.6

Table 3: T47D single-dose treatment (model 1) RNA concentrations and purity ratios**.**

Code	RNA concentration(ng/µl)	260/280	260/230
T1m1a	197	2.07	1.93
T1m1b	401	2.1	2.12
T1m1c	222.7	2.07	1.33
T2m1a	81.3	2.12	2.15
T2m1b	293.8	2.14	1.07
T2m1c	111.7	2.16	0.89
T3m1a	293.8	2.1	2.13
T3m1b	350.9	2.12	0.72
T3m1c	492.1	2.08	1.92
T4m1a	326.3	2.11	1.73
T4m1b	550.9	2.1	2.17
T4m1c	67.7	2.11	0.66
T5m1a	293.9	2.12	2
T5m1b	258.7	2.12	1.32
T5m1c	568.2	2.12	2.12
T6m1a	564.8	2.1	2.2
T6m1b	378.8	2.09	2.15
T6m1c	100.6	2.19	0.81
T7m1a	248.1	2.09	1.48
T7m1b	204.4	2.1	2.2
T7m1c	645.5	2.14	2.03

Table 4: T47D daily-replacement treatment (model 2) RNA concentrations and purity ratios.

Code	RNA concentration(ng/µl)	260/280	260/230
T1m2a	373	2.1	1.06
T1m2b	390.6	2.1	1.97
T1m2c	157.9	2.23	1.75
T2m2a	248.2	2.12	1.5
T2m2b	446.5	2.1	0.8
T2m2c	201.2	2.2	1.37
T3m2a	567.6	2.11	1.79
T3m2b	616.2	2.11	2.22
T3m2c	644.2	2.13	2.15
T4m2a	529.5	2.1	2.22
T4m2b	540.2	2.11	2.07
T4m2c	208.9	2.15	1.73
T5m2a	395.8	2.1	2.06
T5m2b	547.5	2.09	0.88
T5m2c	502.1	2.07	1.92
T6m2a	224.8	2.11	1.95
T6m2b	191.1	2.11	2.27
T6m2c	82.7	2.34	0.54
T7m2a	354.4	2.13	2.24
T7m2b	384.8	2.1	213
T7m2c	170.6	2.41	1.28

Table 5: cDNA synthesis master mix

	1X rxn	X rxns
10X buffer	**2ul**	
25X dNTP Mix (100mM)	**0.8ul**	
10X RT Random Primers	**2ul**	
Nuclease free H20	**4.2ul**	
MultiScribe Reverse Transcriptase	**1ul**	
Total	**10ul**	

Appendix G-MTT statistical output

Model 1

Absolute Differences between Mean Rank Approx. significant if highlighted at .05 significance level

	MCF7 MC	T47D MC	MCF7 DC	T47D DC	MCF7 2TAM	T47D 2TAM	MCF7 5CBD	T47D 5CBD	MCF7 2TAM +5CBD	T47D 2TAM +5CBD	MCF7 PAC	T47D PAC	MCF7 EBSS	T47D EBSS
MCF7 MC	---	0	1,5	5,5	2,5	11,5	1,5	9,5	6,5	4,5	7,5	8,5	3,5	10,5
T47D MC	0	---	1,5	5,5	2,5	11,5	1,5	9,5	6,5	4,5	7,5	8,5	3,5	10,5
MCF7 DC	1,5	1,5	---	7	4	13	3	11	8	6	9	10	5	12
T47D DC	5,5	5,5	7	---	3	6	4	4	1	1	2	3	2	5
MCF7 2TAM	2,5	2,5	4	3	---	9	1	7	4	2	5	6	1	8
T47D 2TAM	11,5	11,5	13	6	9	---	10	2	5	7	4	3	8	1
MCF7 5CBD	1,5	1,5	3	4	1	10	---	8	5	3	6	7	2	9
T47D 5CBD	9,5	9,5	11	4	7	2	8	---	3	5	2	1	6	1
MCF7 2TAM +5CBD	6,5	6,5	8	1	4	5	5	3	---	2	1	2	3	4
T47D 2TAM +5CBD	4,5	4,5	6	1	2	7	3	5	2	---	3	4	1	6
MCF7 PAC	7,5	7,5	9	2	5	4	6	2	1	3	---	1	4	3
T47D PAC	8,5	8,5	10	3	6	3	7	1	2	4	1	---	5	2
MCF7 EBSS	3,5	3,5	5	2	1	8	2	6	3	1	4	5	---	7
T47D EBSS	10,5	10,5	12	5	8	1	9	1	4	6	3	2	7	---

Model 2

Absolute Differences between Mean Rank Approx. significant if highlighted at .05 significance level

	MCF7 MC	T47D MC	MCF7 DC	T47D DC	MCF7 2TAM	T47D 2TAM	MCF7 5CBD	T47D 5CBD	MCF7 2TAM +5CBD	T47D 2TAM +5CBD	MCF7 PAC	T47D PAC	MCF7 EBSS	T47D EBSS
MCF7 MC	---	0	2,5	4,5	6,5	12,5	3,5	9,5	5,5	1,5	8,5	10,5	7,5	11,5
T47D MC	0	---	2,5	4,5	6,5	12,5	3,5	9,5	5,5	1,5	8,5	10,5	7,5	11,5
MCF7 DC	2,5	2,5	---	2	4	10	1	7	3	1	6	8	5	9
T47D DC	4,5	4,5	2	---	2	8	1	5	1	3	4	6	3	7
MCF7 2TAM	6,5	6,5	4	2	---	6	3	3	1	5	2	4	1	5
T47D 2TAM	12,5	12,5	10	8	6	---	9	3	7	11	4	2	5	1
MCF7 5CBD	3,5	3,5	1	1	3	9	---	6	2	2	5	7	4	8
T47D 5CBD	9,5	9,5	7	5	3	3	6	---	4	8	1	1	2	2
MCF7 2TAM +5CBD	5,5	5,5	3	1	1	7	2	4	---	4	3	5	2	6
T47D 2TAM +5CBD	1,5	1,5	1	3	5	11	2	8	4	---	7	9	6	10
MCF7 PAC	8,5	8,5	6	4	2	4	5	1	3	7	---	2	1	3
T47D PAC	10,5	10,5	8	6	4	2	7	1	5	9	2	---	3	1
MCF7 EBSS	7,5	7,5	5	3	1	5	4	2	2	6	1	3	---	4
T47D EBSS	11,5	11,5	9	7	5	1	8	2	6	10	3	1	4	---

Figure 1: MTT assay Kruskal Wallis post hoc- test outputs for both Model 1 and Model 2 using Statistica v.14.0

Appendix H- CYP450 reductase assay statistical output

MCF7 MODEL 1 @ 15 min

	Absolute Differences between Mean Rank Approx. significant if highlighted						
	MC	DC	2TAM	5CBD	2TAM +5CBD	PAC	EBSS
MC	---	1	4	2	2	1	3
DC	1	---	3	3	1	2	2
2TAM	4	3	---	6	2	5	1
5CBD	2	3	6	---	4	1	5
2TAM +5CBD	2	1	2	4	---	3	1
PAC	1	2	5	1	3	---	4
EBSS	3	2	1	5	1	4	---

MCF7 MODEL 1 @ 30 min

	Absolute Differences between Mean Rank Approx. significant if highlighted						
	MC	DC	2TAM	5CBD	2TAM +5CBD	PAC	EBSS
MC	---	1	4	2	6	5	3
DC	1	---	3	1	5	4	2
2TAM	4	3	---	2	2	1	1
5CBD	2	1	2	---	4	3	1
2TAM +5CBD	6	5	2	4	---	1	3
PAC	5	4	1	3	1	---	2
EBSS	3	2	1	1	3	2	---

T47D MODEL 1 @ 15 min

	Absolute Differences between Mean Rank Approx. significant if highlighted						
	MC	DC	2TAM	5CBD	2TAM +5CBD	PAC	EBSS
MC	---	1	4	2	6	5	3
DC	1	---	3	1	5	4	2
2TAM	4	3	---	2	2	1	1
5CBD	2	1	2	---	4	3	1
2TAM +5CBD	6	5	2	4	---	1	3
PAC	5	4	1	3	1	---	2
EBSS	3	2	1	1	3	2	---

T47D MODEL 1 @ 30 min

	Absolute Differences between Mean Rank Approx. significant if highlighted						
	MC	DC	2TAM	5CBD	2TAM +5CBD	PAC	EBSS
MC	---	1	4	2	6	5	3
DC	1	---	3	1	5	4	2
2TAM	4	3	---	2	2	1	1
5CBD	2	1	2	---	4	3	1
2TAM +5CBD	6	5	2	4	---	1	3
PAC	5	4	1	3	1	---	2
EBSS	3	2	1	1	3	2	---

Figure 1: CYP450 enzyme activity assay Kruskal Wallis post hoc- test outputs for both Model 1 MCF7 and T47D cells using Statistica v14.0

MCF7 MODEL 2 @ 15 min

	Absolute Differences between Mean Rank Approx. significant if highlighted at						
	MC	DC	2TAM	5CBD	2TAM +5CBD	PAC	EBSS
MC	---	1	4	2	6	5	3
DC	1	---	3	1	5	4	2
2TAM	4	3	---	2	2	1	1
5CBD	2	1	2	---	4	3	1
2TAM +5CBD	6	5	2	4	---	1	3
PAC	5	4	1	3	1	---	2
EBSS	3	2	1	1	3	2	---

MCF7 MODEL 2 @ 30 min

	Absolute Differences between Mean Rank Approx. significant if highlighted at						
	MC	DC	2TAM	5CBD	2TAM +5CBD	PAC	EBSS
MC	---	1	4	2	6	5	3
DC	1	---	3	1	5	4	2
2TAM	4	3	---	2	2	1	1
5CBD	2	1	2	---	4	3	1
2TAM +5CBD	6	5	2	4	---	1	3
PAC	5	4	1	3	1	---	2
EBSS	3	2	1	1	3	2	---

T47D MODEL 2 @ 15 min

	Absolute Differences between Mean Rank Approx. significant if highlighted at						
	MC	DC	2TAM	5CBD	2TAM +5CBD	PAC	EBSS
MC	---	1	4	2	6	5	3
DC	1	---	3	1	5	4	2
2TAM	4	3	---	2	2	1	1
5CBD	2	1	2	---	4	3	1
2TAM +5CBD	6	5	2	4	---	1	3
PAC	5	4	1	3	1	---	2
EBSS	3	2	1	1	3	2	---

T47D MODEL 2 @ 30 min

	Absolute Differences between Mean Rank Approx. significant if highlighted at						
	MC	DC	2TAM	5CBD	2TAM +5CBD	PAC	EBSS
MC	---	1	4	2	6	5	3
DC	1	---	3	1	5	4	2
2TAM	4	3	---	2	2	1	1
5CBD	2	1	2	---	4	3	1
2TAM +5CBD	6	5	2	4	---	1	3
PAC	5	4	1	3	1	---	2
EBSS	3	2	1	1	3	2	---

Figure 2: CYP450 enzyme activity assay Kruskal Wallis post hoc- test outputs for both Model 2 MCF7 and T47D cells using Statistica v14.0

Appendix I- ICC results and statistical ouput

1. **ICC primary antibody optimization results**

Chosen concentrations :

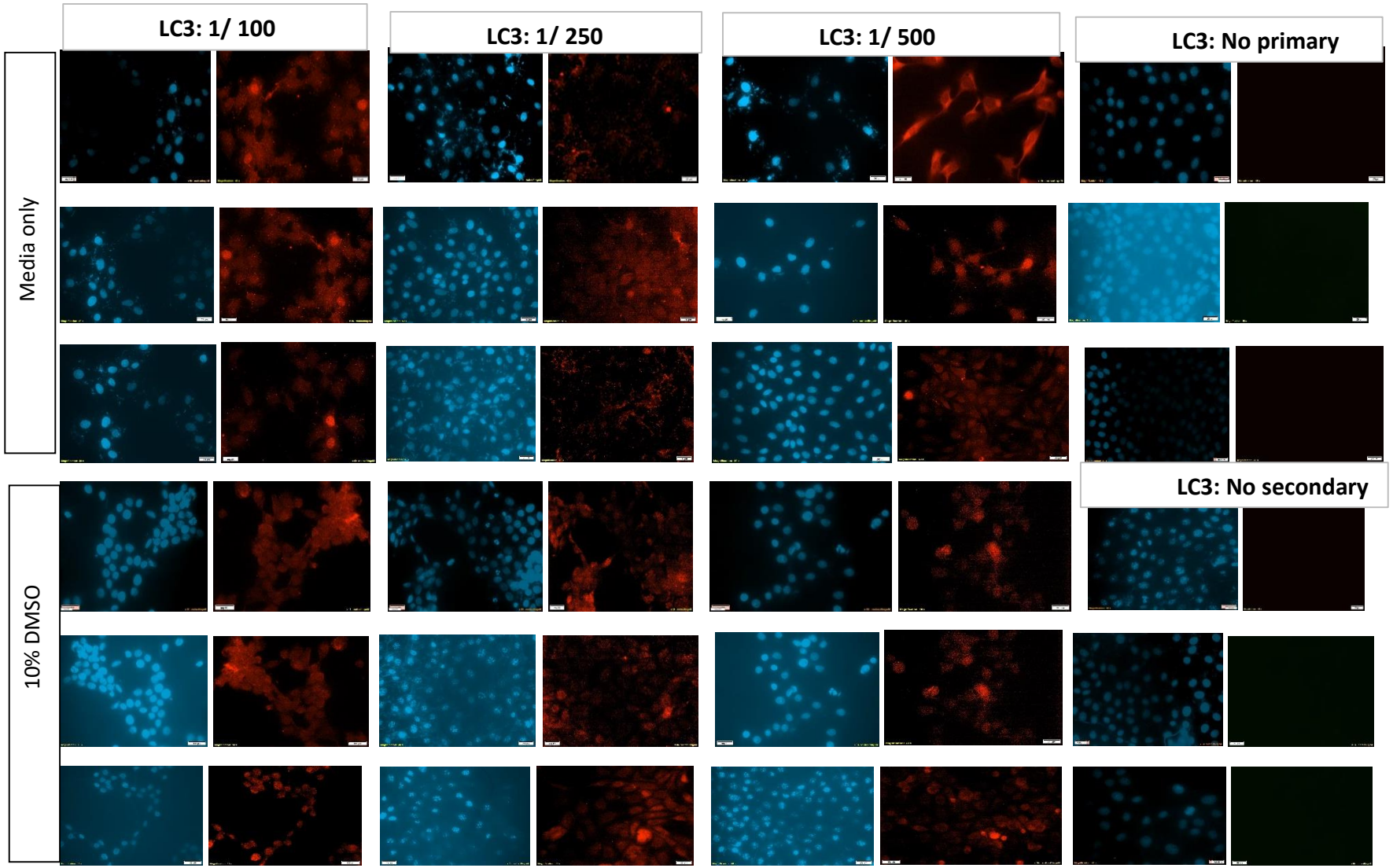
LC3B (Abcam,ab243506): 1/500

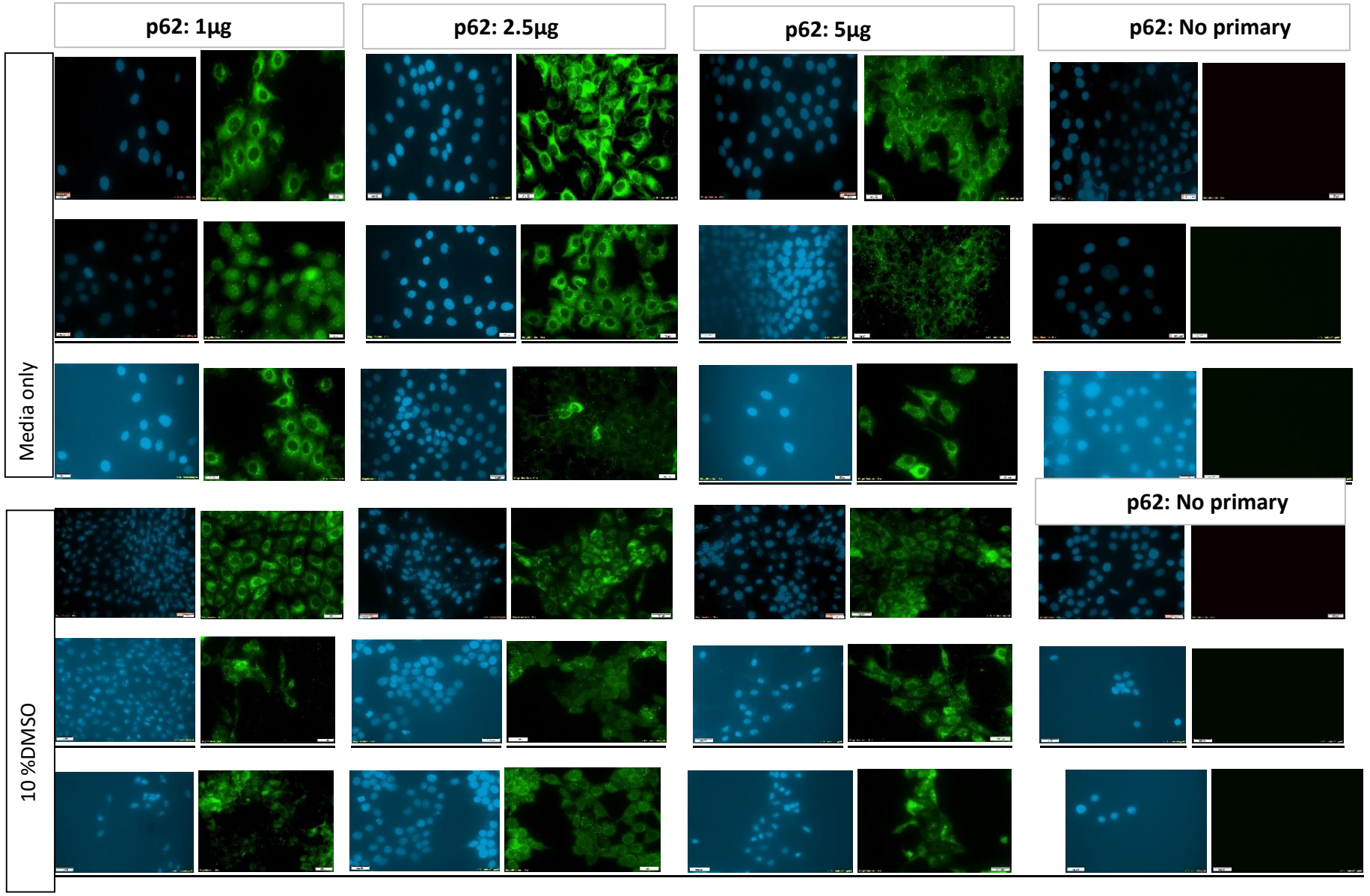
P62 (Abcam,ab240635): 2.5 µg/ml

BECN1 (Abcam,ab217179) : 1/50

All secondary antibodies[Alexa flour-594(Abcam,ab150116), Alexa flour-488 (Abcam,ab150077) and Alexa flour-647 (Abcam,ab175471] were diluted at 1/1000.

2. ICC antibody optimization images




p62: 1µg
p62: 2.5µg
p62: 5µg
p62: No primary
Media only
10 %DMSO
p62: No primary

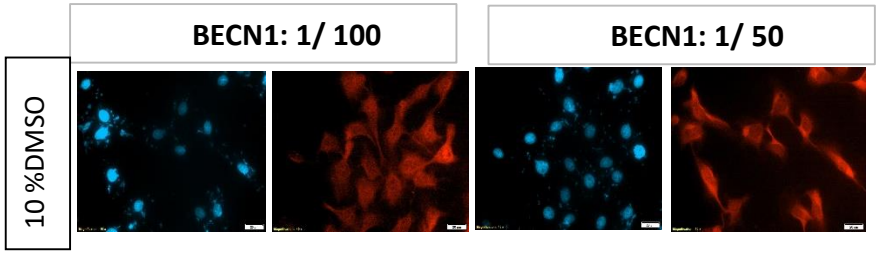


Figure1: ICC antibody optimization MCF7 cells' images showing the different antibody concentrations tested. The images show the dapi stained nuclei and the flourecence under the 594nm filter for LC3B and BECN1 antibody stains and 488nm filter for p62 antibody stains (both the primary and secondary antibodies). The images on the last column show results for samples stained with only the primary antibodies and those strained with only the secondary antibody.

3. Immunolocalization of LC3B in MCF7 and T47D cells

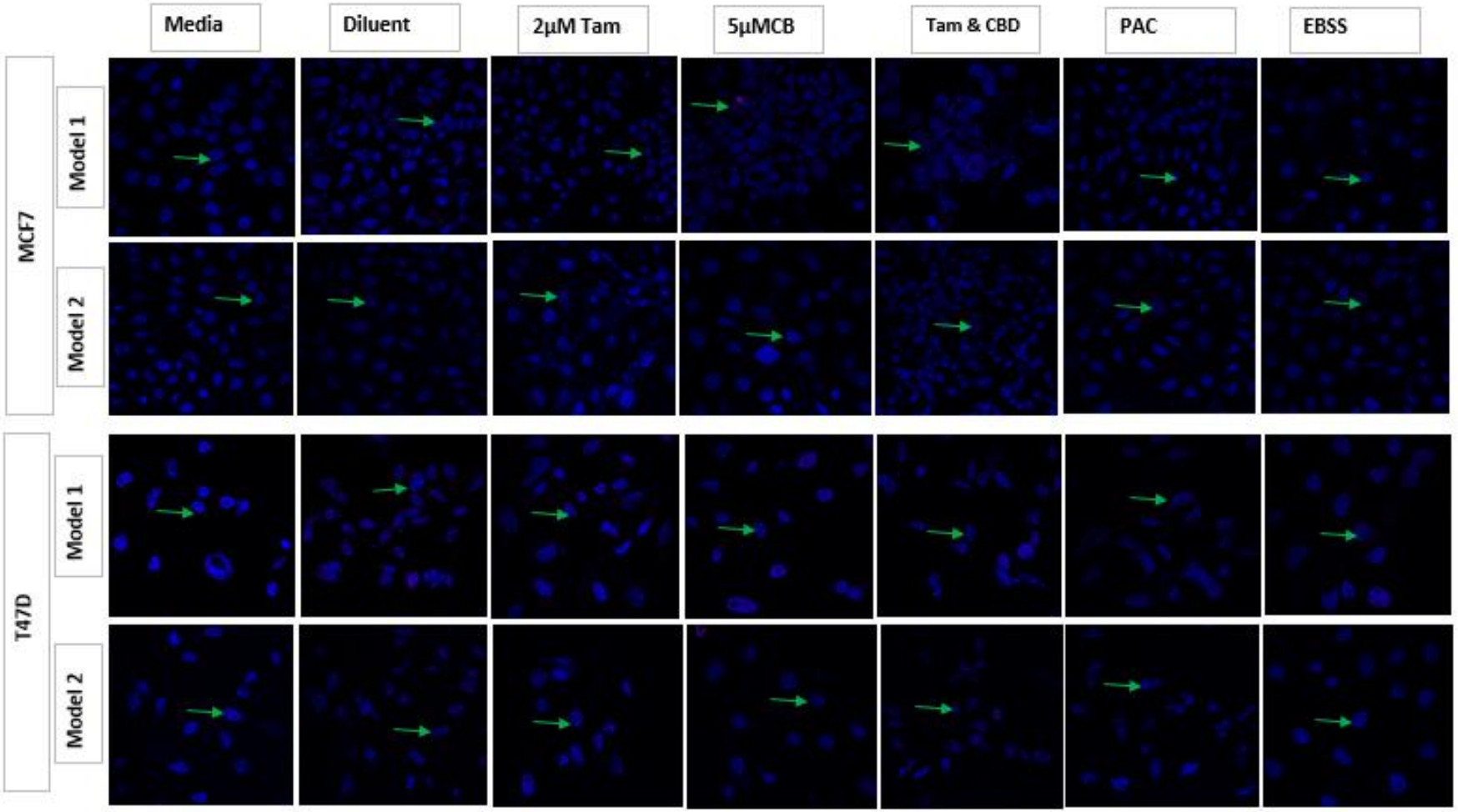


Figure 2. Photomicrographs showing LC3B stained cells (red fluorescence) which is not expressed in MCF7, and T47D breast cancer cells treated with media, diluent, tamoxifen, CBD, combined CBD and Tamoxifen, Paclitaxel and EBSS. Green arrow (Dapi stained nuclei).

MCF7 Model 1 Kruskal post hoc							
	Absolute Differences between Mean Rank Approx. significant if highlighted at						
	Media	Diluent	2TAM	5CBD	2TAM +5CBD	PAC	EBSS
Media	---	510.6764	16.72028	222.1111	327.4765	406.9127	581.9722
Diluent	510.6764	---	527.3967	288.5652	183.1999	917.589	1092.649
2TAM	16.72028	527.3967	---	238.8314	344.1968	390.1924	565.252
5CBD	222.1111	288.5652	238.8314	---	105.3654	629.0238	804.0834
2TAM +5C	327.4765	183.1999	344.1968	105.3654	---	734.3892	909.4487
PAC	406.9127	917.589	390.1924	629.0238	734.3892	---	175.0596
EBSS	581.9722	1092.649	565.252	804.0834	909.4487	175.0596	---
MCF7 Model 2 Kruskal post hoc							
	Absolute Differences between Mean Rank Approx. significant if highlighted at						
	Media	Diluent	2TAM	5CBD	2TAM +5CBD	PAC	EBSS
Media	---	803.8322	519.8382	69.90459	213.4002	492.2524	121.468
Diluent	803.8322	---	1323.67	733.9276	1017.232	311.5798	682.3642
2TAM	519.8382	1323.67	---	589.7428	306.438	1012.091	641.3062
5CBD	69.90459	733.9276	589.7428	---	283.3048	422.3478	51.56339
2TAM +5C	213.4002	1017.232	306.438	283.3048	---	705.6526	334.8682
PAC	492.2524	311.5798	1012.091	422.3478	705.6526	---	370.7844
EBSS	121.468	682.3642	641.3062	51.56339	334.8682	370.7844	---

Table 1: Immunochytochemistry-P62 expression Kruskal Wallis post hoc- test outputs for both Model 1 and Model 2 in MCF7 cells using Statistica v14.0.

T47D Model 1 Kruskal post hoc							
	Absolute Differences between Mean Rank Approx. significant if highlighted at						
	Media	Diluent	2TAM	5CBD	2TAM +5CBD	EBSS	PAC
Media	---	127.9097	83.37903	137.8255	105.6624	164.4511	97.46356
Diluent	127.9097	---	44.5307	9.915727	22.24737	36.54133	225.3733
2TAM	83.37903	44.5307	---	54.44643	22.28333	81.07203	180.8426
5CBD	137.8255	9.915727	54.44643	---	32.1631	26.62561	235.289
2TAM +5C	105.6624	22.24737	22.28333	32.1631	---	58.7887	203.1259
EBSS	164.4511	36.54133	81.07203	26.62561	58.7887	---	261.9146
PAC	97.46356	225.3733	180.8426	235.289	203.1259	261.9146	---
T47D Model 2 Kruskal post hoc							
	Absolute Differences between Mean Rank Approx. significant if highlighted at						
	Media	Diluent	2TAM	5CBD	2TAM +5CBD	EBSS	PAC
Media	---	40.68671	43.54802	211.4733	117.3412	17.25682	104.5662
Diluent	40.68671	---	2.861305	170.7866	76.65449	23.42989	63.87949
2TAM	43.54802	2.861305	---	167.9253	73.79318	26.29119	61.01818
5CBD	211.4733	170.7866	167.9253	---	94.13214	194.2165	106.9071
2TAM +5C	117.3412	76.65449	73.79318	94.13214	---	100.0844	12.775
EBSS	17.25682	23.42989	26.29119	194.2165	100.0844	---	87.30938
PAC	104.5662	63.87949	61.01818	106.9071	12.775	87.30938	---

Table 1: Immunochytochemistry-P62 expression Kruskal Wallis post hoc- test outputs for both Model 1 and Model 2 in T47D cells using Statistica v14.0.

Appendix J-Gene amplification graphs, fold change data and qPCR statistical outputs

1. Gene amplification graphs

MCF7 Model 1

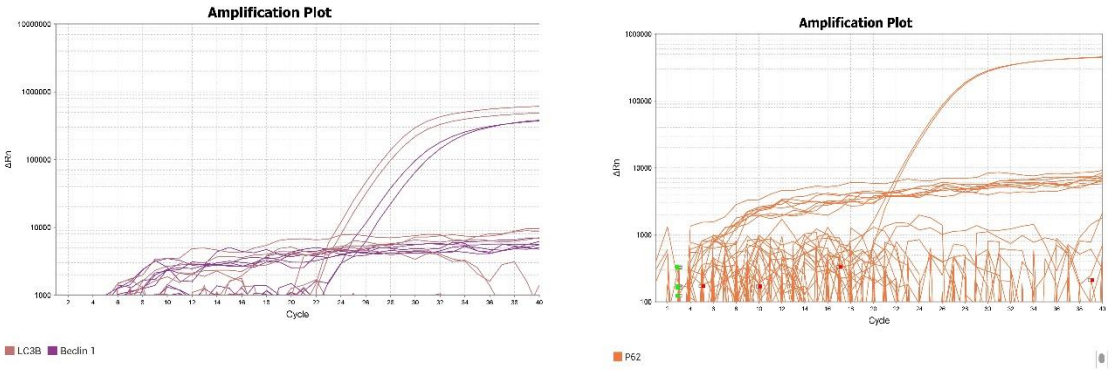


Figure 1: Gene application graphs depicting LC3B(brown), Beclin-1(purple) and P62(orange) gene amplification in MCF7 cells which were undetermined with the IPC control determined.

MCF7 Model 2

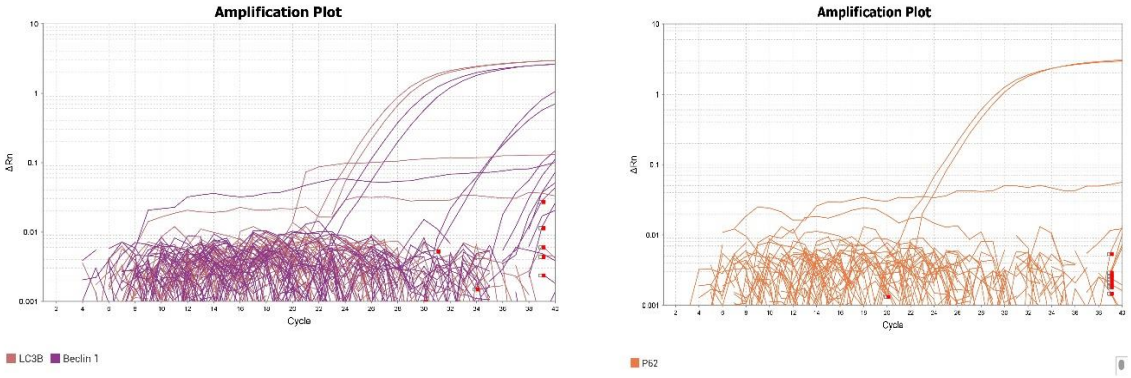


Figure 2: Gene application graphs depicting LC3B(brown), Beclin-1(purple) and P62(orange) gene amplification in MCF7 cells which were undetermined with the IPC control determined.

T47D model 1and Model 2

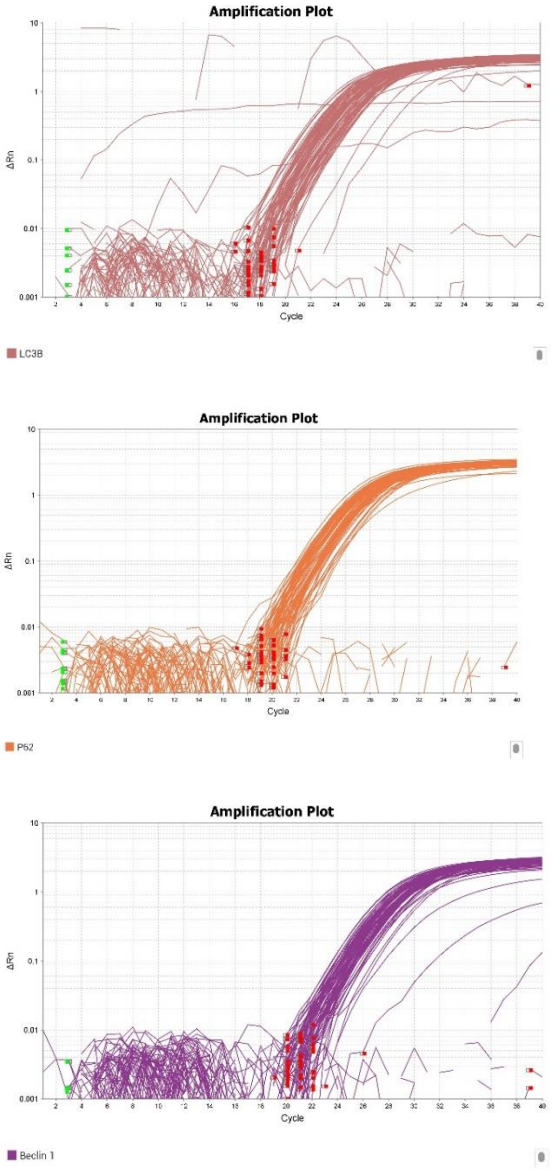


Figure 2: Gene application graphs depicting LC3B(brown), Beclin-1(purple) and P62(orange) gene amplification in T47D cells which were determined for both models.

Table 1: Showing the fold changes in gene expression for LC3B, P62 and BECN1 in MCF7 treated according to the single-dose treatment model (model 1) and daily-replacement treatment model (model 2).

MCF7 Fold change			
Model 1			
Treatment	***LC3B***	***P62***	***BECN1***
Media	Undetermined	Undetermined	Undetermined
Diluent	Undetermined	Undetermined	Undetermined
2 µM Tam	Undetermined	Undetermined	Undetermined
5 µM CBD	Undetermined	Undetermined	Undetermined
2 µM Tam +5 µM CBD	Undetermined	Undetermined	Undetermined
Paclitaxel	Undetermined	Undetermined	Undetermined
1X EBSS	Undetermined	Undetermined	Undetermined
Model 2			
Treatment	***LC3B***	***P62***	***BECN1***
Media	Undetermined	Undetermined	Undetermined
Diluent	Undetermined	Undetermined	Undetermined
2 µM Tam	Undetermined	Undetermined	Undetermined
5 µM CBD	Undetermined	Undetermined	Undetermined
2 µM Tam +5 µM CBD	Undetermined	Undetermined	Undetermined
Paclitaxel	Undetermined	Undetermined	Undetermined
1X EBSS	Undetermined	Undetermined	Undetermined

2. qPCR Statistica outputs

LC3B

LC3B M1

	Absolute Differences between Mean Rank Approx. significant if highlighte						
	Media control	Diluent control	2μM Tamoxifen	5μM CBD	2 μm Tamoxifen+ 5 μM CBD	0.1μM Paclitaxel	EBSS
Media control	---	9	6	2	2	6.33333	1.33333
Diluent control	9	---	3	7	7	15.3333	7.66667
2μM Tamoxifen	6	3	---	4	4	12.3333	4.66667
5μM CBD	2	7	4	---	0	8.33333	0.66667
2 μm Tamoxifen+ 5 μM CB	2	7	4	0	---	8.33333	0.66667
0.1μM Paclitaxel	6.33333	15.3333	12.3333	8.33333	8.33333	---	7.66667
EBSS	1.33333	7.66667	4.66667	0.66667	0.66667	7.66667	---

LC3B M2

	Absolute Differences between Mean Rank Approx. significant if highlighted at .05 significance level						
	Media control	Diluent control	2μM Tamoxifen	5μM CBD	2 μm Tamoxifen+ 5 μM CBD	0.1μM Paclitaxel	EBSS
Media cor	---	2	5	2	8.66667	0.66667	3
Diluent co	2	---	3	0	6.66667	2.66667	5
2μM Tamo	5	3	---	3	3.66667	5.66667	8
5μM CBD	2	0	3	---	6.66667	2.66667	5
2 μm Tam	8.66667	6.66667	3.66667	6.66667	---	9.33333	11.6667
0.1μM Pac	0.66667	2.66667	5.66667	2.66667	9.33333	---	2.33333
EBSS	3	5	8	5	11.6667	2.33333	---

P62

P62 M1

	Absolute Differences between Mean Rank Approx. significant if highlighte						
	Media control	Diluent control	2μM Tamoxifen	5μM CBD	2 μm Tamoxifen+ 5 μM CBD	0.1μM Paclitaxel	EBSS
Media control	---	3	9.33333	2.33333	0	1.33333	0.66667
Diluent control	3	---	6.33333	0.66667	3	4.33333	2.33333
2μM Tamoxifen	9.33333	6.33333	---	7	9.33333	10.6667	8.66667
5μM CBD	2.33333	0.66667	7	---	2.33333	3.66667	1.66667
2 μm Tamoxifen+ 5 μM CB	0	3	9.33333	2.33333	---	1.33333	0.66667
0.1μM Paclitaxel	1.33333	4.33333	10.6667	3.66667	1.33333	---	2
EBSS	0.66667	2.33333	8.66667	1.66667	0.66667	2	---

P62 M2

	Absolute Differences between Mean Rank Approx. significant if highlighted at .05 significance level						
	Media control	Diluent control	2μM Tamoxifen	5μM CBD	2 μm Tamoxifen+ 5 μM CBD	0.1μM Paclitaxel	EBSS
Media cor	---	1	1	1.66667	1	1.33333	3
Diluent co	1	---	2	2.66667	2	2.33333	4
2μM Tamo	1	2	---	0.66667	0	0.33333	2
5μM CBD	1.66667	2.66667	0.66667	---	0.66667	0.33333	1.33333
2 μm Tam	1	2	0	0.66667	---	0.33333	2
0.1μM Pac	1.33333	2.33333	0.33333	0.33333	0.33333	---	1.66667
EBSS	3	4	2	1.33333	2	1.66667	---

BECN1

BECN1 M1

	Absolute Differences between Mean Rank Approx. significant if highlighte						
	Media control	Diluent control	2μM Tamoxifen	5μM CBD	2 μm Tamoxifen+ 5 μM CBD	0.1μM Paclitaxel	EBSS
Media control	---	3	9.33333	3.33333	5.33333	3	4
Diluent control	3	---	6.33333	0.33333	2.33333	0	1
2μM Tamoxifen	9.33333	6.33333	---	6	4	6.33333	5.33333
5μM CBD	3.33333	0.33333	6	---	2	0.33333	0.66667
2 μm Tamoxifen+ 5 μM CB	5.33333	2.33333	4	2	---	2.33333	1.33333
0.1μM Paclitaxel	3	0	6.33333	0.33333	2.33333	---	1
EBSS	4	1	5.33333	0.66667	1.33333	1	---

BECN1 M2

	Absolute Differences between Mean Rank Approx. significant if highlighted at .05 significance level						
	Media control	Diluent control	2μM Tamoxifen	5μM CBD	2 μm Tamoxifen+ 5 μM CBD	0.1μM Paclitaxel	EBSS
Media cor	---	5.66667	6	1.66667	0.66667	1.33333	1.33333
Diluent co	5.66667	---	0.33333	4	5	4.33333	7
2μM Tamo	6	0.33333	---	4.33333	5.33333	4.66667	7.33333
5μM CBD	1.66667	4	4.33333	---	1	0.33333	3
2 μm Tam	0.66667	5	5.33333	1	---	0.66667	2
0.1μM Pac	1.33333	4.33333	4.66667	0.33333	0.66667	---	2.66667
EBSS	1.33333	7	7.33333	3	2	2.66667	---

Table 2: qPCR-LC3B, P62a and BECN1 expression Kruskal Wallis post hoc- test outputs for both Model 1 and Model 2 in T47D cells using Statistica v14.0 checking for significant differences between treatment groups within each model.

LC3B

LC3B M1 vs M2											
	Absolute Differences between Mean Rank Approx. significant if highlighted at .05 significance level										
	T47D DC-M1	T47D DC-M2	T47D 2TAM-M1	T47D 2TAM-M2	T47D 5CBD-M1	T47D 5CBD-M2	T47D 2TAM +5CBD-M2	T47D EBSS-M1	T47D EBSS-M2	T47D PAC-M1	T47D PAC-M2
T47D DC-M1	---	14	3	19.3333	10.8333	14.6667	24.6667	24.6667	10.3333	11.3333	6.33333
T47D DC-M2	14	---	11	5.33333	3.16667	0.66667	10.6667	10.6667	3.66667	2.66667	7.66667
T47D 2TAM-M1	3	11	---	16.3333	7.83333	11.6667	21.6667	21.6667	7.33333	8.33333	3.33333
T47D 2TAM-M2	19.3333	5.33333	16.3333	---	8.5	4.66667	5.33333	5.33333	9	8	13
T47D 5CBD-M1	10.8333	3.16667	7.83333	8.5	---	3.83333	13.8333	13.8333	0.5	0.5	4.5
T47D 5CBD-M2	14.6667	0.66667	11.6667	4.66667	3.83333	---	10	10	4.33333	3.33333	8.33333
T47D 2TAM +5CBD-M2	24.6667	10.6667	21.6667	5.33333	13.8333	10	---	0	14.3333	13.3333	18.3333
T47D EBSS-M1	24.6667	10.6667	21.6667	5.33333	13.8333	10	0	---	14.3333	13.3333	18.3333
T47D EBSS-M2	10.3333	3.66667	7.33333	9	0.5	4.33333	14.3333	14.3333	---	1	4
T47D PAC-M1	11.3333	2.66667	8.33333	8	0.5	3.33333	13.3333	13.3333	1	---	5
T47D PAC-M2	6.33333	7.66667	3.33333	13	4.5	8.33333	18.3333	18.3333	4	5	---

BECN1 M1 vs M2											
	Absolute Differences between Mean Rank Approx. significant if highlighted at .05 significance level										
	T47D DC-M1	T47D DC-M2	T47D 2TAM-M1	T47D 2TAM-M2	T47D 5CBD-M1	T47D 5CBD-M2	T47D 2TAM +5CBD-M2	T47D EBSS-M1	T47D EBSS-M2	T47D PAC-M1	T47D PAC-M2

P62

P62 M1 and M2											
	Absolute Differences between Mean Rank Approx. significant if highlighted at .05 significance level										
	T47D DC-M1	T47D DC-M2	T47D 2TAM-M1	T47D 2TAM-M2	T47D 5CBD-M1	T47D 5CBD-M2	T47D 2TAM +5CBD-M2	T47D EBSS-M1	T47D EBSS-M2	T47D PAC-M1	T47D PAC-M2
T47D DC-M1	---	10	10	6.66667	2.83333	8	7.33333	7.66667	8.33333	4.66667	5.66667
T47D DC-M2	10	---	20	3.33333	7.16667	2	2.66667	2.33333	1.66667	5.33333	4.33333
T47D 2TAM-M1	10	20	---	16.6667	12.8333	18	17.3333	17.6667	18.3333	14.6667	15.6667
T47D 2TAM-M2	6.66667	3.33333	16.6667	---	3.83333	1.33333	0.66667	1	1.66667	2	1
T47D 5CBD-M1	2.83333	7.16667	12.8333	3.83333	---	5.16667	4.5	4.83333	5.5	1.83333	2.83333
T47D 5CBD-M2	8	2	18	1.33333	5.16667	---	0.66667	0.33333	0.33333	3.33333	2.33333
T47D 2TAM +5CBD-M2	7.33333	2.66667	17.3333	0.66667	4.5	0.66667	---	0.33333	1	2.66667	1.66667
T47D EBSS-M1	7.66667	2.33333	17.6667	1	4.83333	0.33333	0.33333	---	0.66667	3	2
T47D EBSS-M2	8.33333	1.66667	18.3333	1.66667	5.5	0.33333	1	0.66667	---	3.66667	2.66667
T47D PAC-M1	4.66667	5.33333	14.6667	2	1.83333	3.33333	2.66667	3	3.66667	---	1
T47D PAC-M2	5.66667	4.33333	15.6667	1	2.83333	2.33333	1.66667	2	2.66667	1	---

BECN1

BECN1 M1 vs M2											
	Absolute Differences between Mean Rank Approx. significant if highlighted at .05 significance level										
	T47D DC-M1	T47D DC-M2	T47D 2TAM-M1	T47D 2TAM-M2	T47D 5CBD-M1	T47D 5CBD-M2	T47D 2TAM +5CBD-M2	T47D EBSS-M1	T47D EBSS-M2	T47D PAC-M1	T47D PAC-M2
T47D DC-M1	---	12.6667	8.66667	13	0	5.33333	4.33333	0	6.33333	1	2
T47D DC-M2	12.6667	---	21.3333	0.33333	12.6667	7.33333	8.33333	12.6667	6.33333	13.6667	10.6667
T47D 2TAM-M1	8.66667	21.3333	---	21.6667	8.66667	14	13	8.66667	15	7.66667	10.6667
T47D 2TAM-M2	13	0.33333	21.6667	---	13	7.66667	8.66667	13	6.66667	14	11
T47D 5CBD-M1	0	12.6667	8.66667	13	---	5.33333	4.33333	0	6.33333	1	2
T47D 5CBD-M2	5.33333	7.33333	14	7.66667	5.33333	---	1	5.33333	1	6.33333	3.33333
T47D 2TAM +5CBD-M2	4.33333	8.33333	13	8.66667	4.33333	1	---	4.33333	2	5.33333	2.33333
T47D EBSS-M1	0	12.6667	8.66667	13	0	5.33333	4.33333	---	6.33333	1	2
T47D EBSS-M2	6.33333	6.33333	15	6.66667	6.33333	1	2	6.33333	---	7.33333	4.33333
T47D PAC-M1	1	13.6667	7.66667	14	1	6.33333	5.33333	1	7.33333	---	3
T47D PAC-M2	2	10.6667	10.6667	11	2	3.33333	2.33333	2	4.33333	3	---

Table 2 :qPCR-LC3B, P62a and BECN1 expression Kruskal Wallis post hoc- test outputs for both Model 1 and Model 2 in T47D cells using Statistica v14.0 checking for significant differences between treatment models at matched treatment groups .

Appendix K- Proof of ethical clearance

UNIVERSITY OF THE WITWATERSRAND, JOHANNESBURG	HUMAN RESEARCH ETHICS COMMITTEE (MEDICAL)

Office of the Deputy Vice-Chancellor (Research & Post Graduate Affairs)

TO: Ms MF Mahasha
School: Anatomical Sciences
Department:
Medical School
University
E-mail: 1411488@students.wits.ac.za

CC: Supervisor: Dr T Augustine <Tanya.Augustine@wits.ac.za>
and <HREC-Medical.ResearchOffice@wits.ac.za>

FROM: Iain Burns
Human Research Ethics Committee (Medical)
Tel: 011 717 1252

E-mail: Iain.Burns@wits.ac.za

DATE: 03/11/2020

REF: *R14/49*

PROTOCOL NO: W-CBP-201103-01 (This is your ethics application study reference number. Please quote this reference number in all correspondence relating to this study)

PROJECT TITLE: *Impact of CBD and Tamoxifen treatment on cell death and cell survival in breast cancer: 2D and 3D in vitro models*

Please find attached the Ethics Waiver Certificate for the above project. I hope it goes well and that an article in a recognized publication comes out of it. This will reflect well on your professional standing and contribute to the Government funding of the University.

MSWorks2000/Iain0007/ClearScanWaiver.wps

UNIVERSITY OF THE
WITWATERSRAND
JOHANNESBURG

HUMAN RESEARCH ETHICS COMMITTEE (MEDICAL)

03/11/2020

Ref: W-CBP-201103-01

TO WHOM IT MAY CONCERN:

Waiver: This certifies that the following research does not require clearance from the Human Research Ethics Committee (Medical).

Investigator: Ms MF Mahasha
Student No. (if appropriate): 1411488
Staff No. (if appropriate):

Supervisor: Dr T Augustine

School: Anatomical Sciences
Department:
Medical School
University

Project title: *Impact of CBD and Tamoxifen treatment on cell death and cell survival in breast cancer: 2D and 3D in vitro models*

Reason: In vitro laboratory study.
No human participants will be involved in the study.

Dr CB Penny
Co-Chairperson: Human Research Ethics Committee (Medical)

Appendix L- Turnitin report

1411488 Mahlatse Mahasha MSc dissertation.docx

ORIGINALITY REPORT

9%	7%	8%	4%
SIMILARITY INDEX	INTERNET SOURCES	PUBLICATIONS	STUDENT PAPERS

PRIMARY SOURCES

1	Submitted to University of Witwatersrand Student Paper	1%
2	www.mdpi.com Internet Source	1%
3	Jang, S.Y.. "Celastrol inhibits the growth of estrogen positive human breast cancer cells through modulation of estrogen receptor @a", Cancer Letters, 20110101 Publication	<1%
4	vital.seals.ac.za:8080 Internet Source	<1%
5	Submitted to University of Nottingham Student Paper	<1%
6	Submitted to University of Pittsburgh Student Paper	<1%
7	dokumen.pub Internet Source	<1%
8	academic.oup.com Internet Source	<1%

9	www.frankysfarm.de Internet Source	<1 %
10	www.nature.com Internet Source	<1 %
11	www.ncbi.nlm.nih.gov Internet Source	<1 %
12	researchonline.ljmu.ac.uk Internet Source	<1 %
13	kuscholarworks.ku.edu Internet Source	<1 %
14	J Jooste, J B Laurens, M Jordaan, A A S Marais, L G Curlewis. "The implications of the use of cannabidiol-related products in a safety-sensitive drug testing environment: A medical-legal perspective", South African Medical Journal, 2021 Publication	<1 %
15	rgu-repository.worktribe.com Internet Source	<1 %
16	Murielle Mimeault, Ganesh Venkatraman, Sonny L. Johansson, Erik Moore et al. "Novel combination therapy against metastatic and androgen-independent prostate cancer by using gefitinib, tamoxifen and etoposide", International Journal of Cancer, 2007 Publication	<1 %